

AWARD NUMBER: W81XWH-13-1-0400

TITLE: Targeting Epigenetics Therapy for Estrogen Receptor-Negative Breast Cancers

PRINCIPAL INVESTIGATOR: Dewey G. McCafferty, Ph.D.

CONTRACTING ORGANIZATION: Duke University  
Duke University  
Durham, NC 27708

REPORT DATE: October 2015

TYPE OF REPORT: Other

PREPARED FOR: U.S. Army Medical Research and Materiel Command  
Fort Detrick, Maryland 21702-5012

DISTRIBUTION STATEMENT: Approved for Public Release;  
Distribution Unlimited

The views, opinions and/or findings contained in this report are those of the author(s) and should not be construed as an official Department of the Army position, policy or decision unless so designated by other documentation.

# REPORT DOCUMENTATION PAGE

Form Approved  
OMB No. 0704-0188

Public reporting burden for this collection of information is estimated to average 1 hour per response, including the time for reviewing instructions, searching existing data sources, gathering and maintaining the data needed, and completing and reviewing this collection of information. Send comments regarding this burden estimate or any other aspect of this collection of information, including suggestions for reducing this burden to Department of Defense, Washington Headquarters Services, Directorate for Information Operations and Reports (0704-0188), 1215 Jefferson Davis Highway, Suite 1204, Arlington, VA 22202-4302. Respondents should be aware that notwithstanding any other provision of law, no person shall be subject to any penalty for failing to comply with a collection of information if it does not display a currently valid OMB control number. **PLEASE DO NOT RETURN YOUR FORM TO THE ABOVE ADDRESS.**

<b>1. REPORT DATE</b> October 2015		<b>2. REPORT TYPE</b> Annual		<b>3. DATES COVERED</b> 30 Sep 2014 - 29 Sep 2015	
<b>4. TITLE AND SUBTITLE</b>  Targeting Epigenetics Therapy for Estrogen Receptor-Negative Breast Cancers				<b>5a. CONTRACT NUMBER</b>	
				<b>5b. GRANT NUMBER</b> W81XWH-13-1-0400	
				<b>5c. PROGRAM ELEMENT NUMBER</b>	
<b>6. AUTHOR(S)</b> Dewey G. McCafferty, Ph.D.  E-Mail:dewey@duke.edu				<b>5d. PROJECT NUMBER</b>	
				<b>5e. TASK NUMBER</b>	
				<b>5f. WORK UNIT NUMBER</b>	
<b>7. PERFORMING ORGANIZATION NAME(S) AND ADDRESS(ES)</b> Duke University 220 W. Main Street Durham, NC 27708-4640				<b>8. PERFORMING ORGANIZATION REPORT NUMBER</b>	
<b>9. SPONSORING / MONITORING AGENCY NAME(S) AND ADDRESS(ES)</b>  U.S. Army Medical Research and Materiel Command Fort Detrick, Maryland 21702-5012				<b>10. SPONSOR/MONITOR'S ACRONYM(S)</b>	
				<b>11. SPONSOR/MONITOR'S REPORT NUMBER(S)</b>	
<b>12. DISTRIBUTION / AVAILABILITY STATEMENT</b>  Approved for Public Release; Distribution Unlimited					
<b>13. SUPPLEMENTARY NOTES</b>					
<b>14. ABSTRACT</b> Our goals for this project are to explore LSD1 inhibition of protein-protein interactions as a potential therapy for ER $\alpha$ <sup>-</sup> breast cancer, ameliorating iLCC for <i>in vivo</i> use, and using novel proteomics approaches to identify coregulatory proteins interacting with ER $\alpha$ and LSD1 in ER $\alpha$ <sup>+</sup> cells and deduce how the complement of LSD1 associating proteins change in ER $\alpha$ <sup>-</sup> cancers. We have made significant progress on the aims this project, specifically by examining the effects of small molecule, LSD1-selective and broad-spectrum histone demethylase inhibitors on breast cancer tumor growth as compared to iLCC. Using protein engineering, and H/D exchange MS, we identified the LSD1 alpha helical coiled-coil as a central mediator of ER signaling and coregulatory protein recruitment. Using siRNA knockdown and a newly identified highly selective inhibitor of the LSD1 demethylase active site chemistry, we showed that loss of LSD1 or inhibition of the LSD1-CoREST complex by iLCC inhibits breast cancer proliferation, but the antiproliferative effects of tranylcyproline or pargyline exhibit antiproliferative effects in ER <sup>+</sup> and ER <sup>-</sup> breast cancers by a secondary mechanism requiring LSD1 as a scaffolding element.					
<b>15. SUBJECT TERMS</b>					
<b>16. SECURITY CLASSIFICATION OF:</b>			<b>17. LIMITATION OF ABSTRACT</b>  Unclassified	<b>18. NUMBER OF PAGES</b>  95	<b>19a. NAME OF RESPONSIBLE PERSON</b> USAMRMC
<b>a. REPORT</b>  Unclassified	<b>b. ABSTRACT</b>  Unclassified	<b>c. THIS PAGE</b>  Unclassified			<b>19b. TELEPHONE NUMBER</b> (include area code)

## Introduction

Our goals for this project are to explore LSD1 inhibition of protein-protein interactions as a potential therapy for ER $\alpha$  breast cancer, ameliorating iLCC for *in vivo* use, and using novel proteomics approaches to identify coregulatory proteins interacting with ER $\alpha$  and LSD1 in ER $\alpha$ <sup>+</sup> cells and deduce how the complement of LSD1 associating proteins change in ER $\alpha$ <sup>-</sup> cancers. We have made significant progress on the aims of this project. There are no changes we wish to make to the Statement of Work.

## Key Words

histone demethylase, estrogen receptor, CoREST, corepressor, estrogen-receptor positive breast cancer, estrogen receptor negative breast cancer, epigenetics, nuclear hormone receptor, estrogen

## Overall Project Summary

Flavin-dependent, lysine-specific protein demethylases (KDM1s) are a subfamily of amine oxidases that catalyze the selective posttranslational oxidative demethylation of methyllysine side chains within protein and peptide substrates, a process that generates chemical cues for the regulation of gene transcription. KDM1 family human demethylases utilize a FAD cofactor to oxidize C-N bonds with subsequent production of a demethylated lysine residue and formaldehyde byproduct. The most well characterized KDM1-family demethylase, LSD1/KDM1A, is an 852 amino acid (aa) polypeptide composed of three domains: an amine oxidase catalytic domain (AOD) (residues 272-415 and 515-852), an ~100aa insert known as the 'tower' domain (residues 415-515), and a SWIRM domain (residues 172-272) (Figure 1). The three-dimensional structure of LSD1 has been solved by X-ray crystallographic methods in the unliganded form and in complex with varying ligands, including peptides and inhibitors.

The LSD1 demethylase typically associates with biomolecules and enzymes that link its catalytic activity to distinctive biological occupations in normal and disease states. Such interactions among members of transcriptional regulatory complexes have been shown to influence the degree of catalytic activity, substrate specificity, and/or localization of these enzymes within chromatin. CoREST is one of the earliest identified interaction partners of LSD1 and this protein complex assembly (i.e. LSD1/CoREST complex) is frequently found within several distinct, larger multi-protein complexes. Most likely due to this early association, the structural and functional characterization of this particular interaction far outstrips that available for any other LSD1 interaction.

LSD1 regulates the expression of many genes important in breast cancer progression and proliferation. Present various transcriptional complexes paired with tightly-associated nucleosome targeting protein CoREST and the histone deacetylases HDACs 1 and 2, the LSD1/CoREST/HDAC complex is the core enzymatic machinery responsible for removing methyl marks on histone H3. The context to which the LSD1 complex acts is controlled by its interaction with partnering co-regulatory proteins that may direct access to specific methylation sites or influence LSD1 specificity.

By mechanisms that are far from well understood, estrogen binding to the estrogen receptor alpha (ER) undergoes conformational changes to facilitate co-regulatory protein association, then is recruited by components of the LSD1 multi-protein complex to translate nuclear hormone signaling into productive transcriptional activation of estrogen-responsive genes (Figure 2). In hormone-responsive breast cancers, ER activity is a proven target for pharmacological inhibition, as ER controls many cancer-associated proliferation genes. However in highly aggressive breast cancers, ER production is abrogated, and thus by comparison there are limited therapeutic options for these aggressive cancers. In both breast cancers, LSD1 is highly expressed and activated and we have validated in cell culture that LSD1 is a potential target for both ER-positive and ER-negative cancers. In this proposal we wish to examine the molecular contributors that govern signal transmission between the ER complex and the LSD1/CoREST/HDAC1/2 complex to initiate transcriptional programs at ER target genes, to validate that LSD1 as a breast cancer target in both ER- and ER+ cancers target by examining the ability of our recently developed potent and selective inhibitor the LSD1-CoREST interaction to reduce tumor growth in a murine xenograft models of breast cancer.

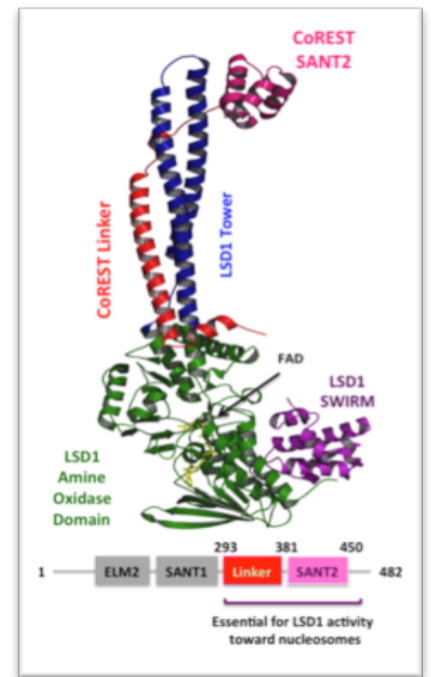


**Figure 1.** LSD1/KDM1A bound to residues 293-480 of CoREST

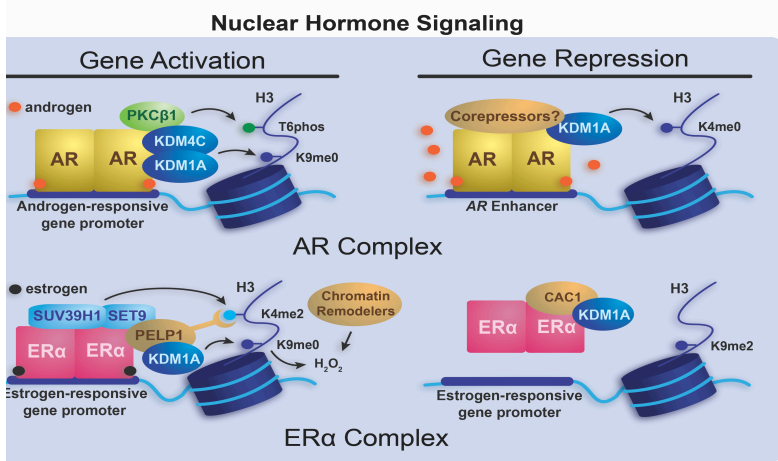


**Figure 2.** Epigenetic transcriptional complexes that recruit LSD1 via interactions with estrogen and androgen nuclear hormone receptor transcription factors.

**Aim 1 Progress-** We wish to unequivocally confirm that iLCC functions as an inhibitor of both ERα+ and ERα breast cancers *in vivo* in a clinically-relevant xenograft animal model of breast cancer.

**Evaluation of LSD1 Inhibition on Nuclear Hormone Transcription Factor Signaling** We initially turned to the estrogen-inducible ERα transcription factor to probe the involvement of the catalytic activity of the LSD1/CoREST, and later protein-protein interaction inhibitors. Using a combination of siRNA knockdown and LSD1 chemical inhibition by designed arylcyclopropylamine small molecule LSD1 inhibitors, we showed that LSD1 enzymatic activity is required for ER function (Figure 3). We also determined that inhibition of LSD1 demethylation prevents ER recruitment to estrogen-responsive elements (EREs) within promoters for target genes. LSD1 inhibition by small molecules showed strong antiproliferative effects on breast cancer cells and anticipated effects on H3K4 and H3K9 histone demethylation patterns. In ERα-negative cancers, LSD1 is highly overexpressed and presumably constitutively activated by stimulatory effects from coregulatory molecules. We recently also showed that in a dose-dependent manner, small molecule inhibitors of LSD1 exhibited marked antiproliferative effects in ER-negative cancer cell lines and disrupted transcriptional activation of ER target genes.

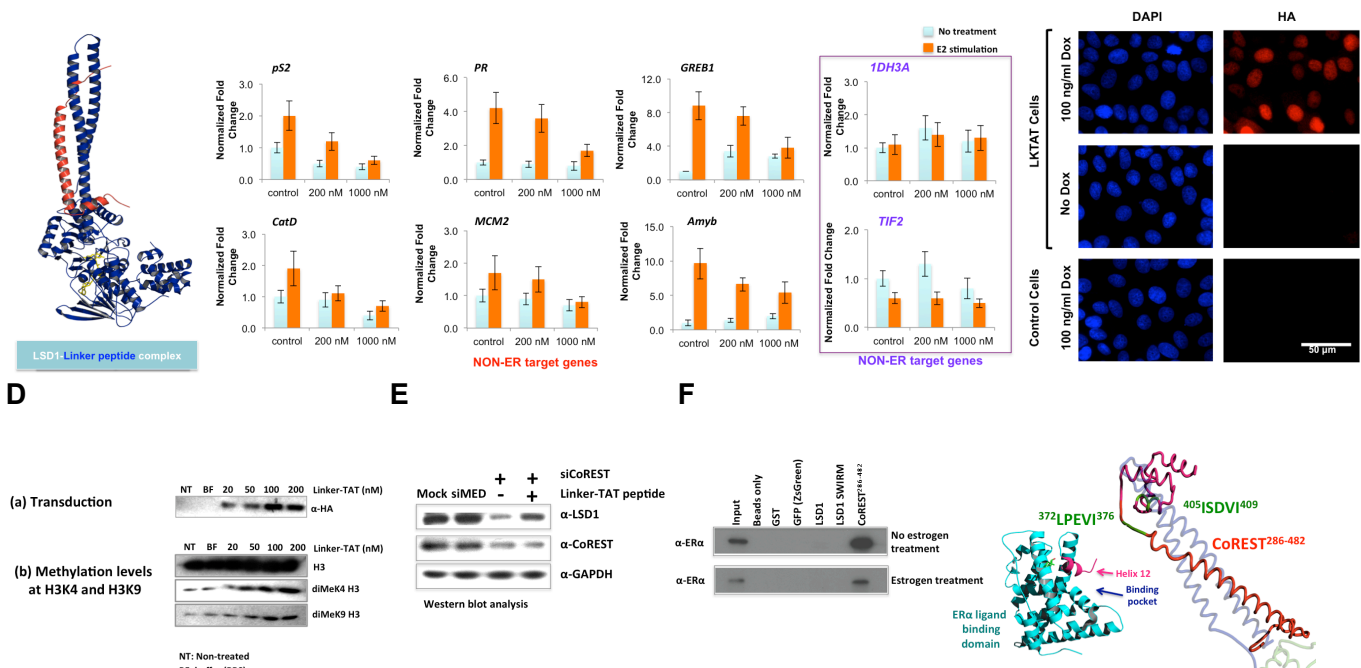


**Figure 4.** (A) Model of the CoREST-derived linker structure adapted from the structure of the LSD1-CoREST crystal structure; (B) LSD1 inhibitor iLCC (derived from the Linter region of CoREST) caused the dose-dependent inhibition of transcription at ER target genes in MCF7 cells when added exogenously; (C) Localization of iLCC to the nucleus of MCF7 cells following doxycycline induction; (D) Doxycycline mediated expression of iLCC causes a dose-dependent abrogation of methylation of histone H3; (E) iLCC stabilizes LSD1 during siRNA knockdown of CoREST; (F) Western blot indicating that CoREST Linker-Sant2 domain directly interacts with full length ER in an estrogen-dependent manner, but does not interact directly with LSD1.

**Analysis of the Interaction of LSD1 with a CoREST Fragment** We subsequently probed the interaction of CoREST with LSD1 using a combination of mutagenesis, activity assays, epitope mapping, and biophysical methods including isothermal titration calorimetry, surface plasmon resonance and hydrogen/deuterium exchange mass spectrometry. We discovered that CoREST residues 293-380, form a central isolated helix that interacts very strongly (16 nM  $K_D$ ) with the LSD1 coiled-coil tower domain to create an unusual offset dual triple-helical bundle interaction interface. To validate that this CoREST and LSD1 interacted only through this helix-helix interface, we used structure-driven design to produce a fully active deletion mutant of LSD1 lacking the tower domain, produced full length CoREST and confirmed that no additional sites of interaction exists between these two proteins.

In collaboration with Prof. Donald McDonnell (collaborator), we determined that a GST-CoREST<sup>293-380</sup> fusion expressed in both HeLa and MCF7 breast cancer cells was capable of pulling down endogenous LSD1 and partially depleting the pool of the LSD1-CoREST complex. We subsequently created a cell permeable HIV-Tat-HA tagged version of the truncated CoREST linker (iLCC) and evaluated its effectiveness at inhibiting the LSD1-CoREST interaction *in vitro* and *in vivo* and its capacity to prevent ER $\alpha$  recruitment and to inhibit cell proliferation in ER-positive and ER-negative cancers cell lines. iLCC proved to be *highly cell permeable and unusually stable* for over 20h in cell culture (and >8 days with daily dosing). We subsequently attributed this stability to protection by LSD1 binding, since in a CoREST siRNA knockdown normally LSD1 is unstable and rapidly degrades, but addition of iLCC rescued LSD1 protein levels, confirming that the helix-helix interactions of CoREST with LSD1 are required for stability. At 100 nM, iLCC marginally increased global histone demethylation levels at but significantly increased methylation at H3K4 within the promoter of ER target genes. In the absence of iLCC, we used ChIP/qPCR recruitment analysis to determine that CoREST and LSD1 associated with the proximal ERE binding site of ER $\alpha$ -promoter targets such as pS2 and PR in MCF7 cells. Treatment of the MCF7 cells with iLCC at 100 nM disrupted the binding interaction between LSD1 and CoREST, leading to the decreased recruitment of ER $\alpha$ , CoREST, and LSD1 to those promoter binding sites.

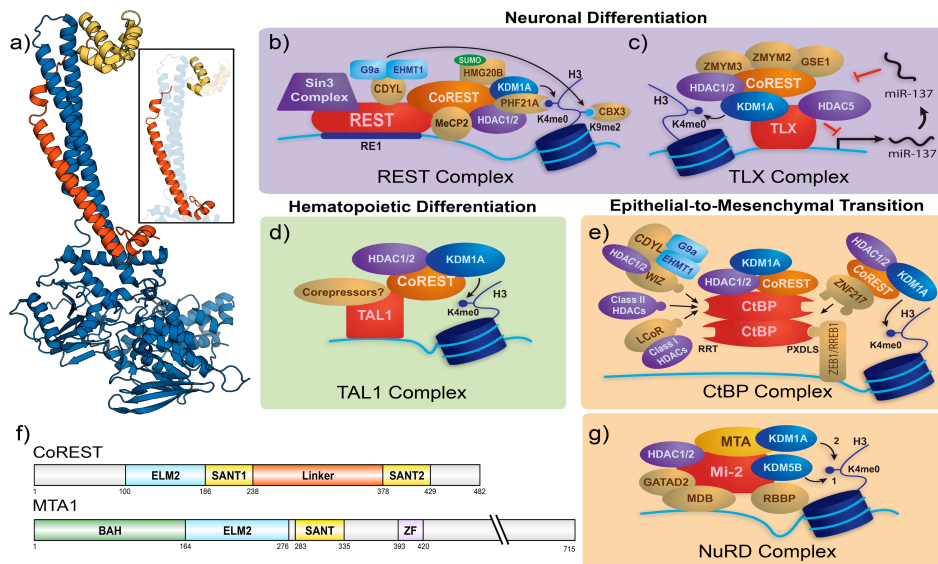


**Figure 4.** Epigenetic transcriptional complexes that recruit LSD1 via interactions with CoRESTs (RCoRs 1-3) or MTAs (MTAs 1-3). a) Ribbon representation of LSD1 (blue) in complex with the linker (orange) and SANT2 (yellow) domains of CoREST (PDB 2IW5). Insert highlights the regions of contact between CoREST and the LSD1 tower domain. b) CoREST recruits a LSD1 complex to suppress neuronal genes through its interaction with REST, which also recruits the Sin3 complex. c) The CoREST core complex is recruited by a direct interaction between TLX and LSD1. d) The transcription factor TAL1 recruits the CoREST complex, and potentially other coregulators, to repress gene transcription as an effector of hematopoietic differentiation. e) The CtBP proteins associate with DNA-binding proteins for genomic localization and recruit chromatin remodelers, including LSD1, to regulate the EMT. f) Domain maps of CoREST (RCoR1) and MTA1 are representative of their respective isoforms and show a similar ELM2/SANT domain organization. g) LSD1 is recruited by MTA1 subunit of the NuRD complex, and in this context suppresses the EMT in breast cancer.

In addition, iLCC treatment decreased transcriptional levels of ER $\alpha$ <sup>+</sup> target genes (e.g. pS2, PR, CatD, GREB1, AmyB, and MCM2), but not 1DH3A or TIF2 which are not targets of ER-positive and reduced cellular proliferation in a dosage-dependent manner. Lastly, moving to the ER-negative cancer cell line MDA-MB-231, as was seen when LSD1 activity was chemically inhibited or the protein levels knocked down by siRNA interference, we showed that siRNA knockdown of CoREST protein levels decreased the expression of proliferation-associated genes like pS2 and PR and inhibited growth proliferation. However, viability of the cells was preserved and no toxic effects have been observed at these inhibitor concentrations.

*Induction of the EMT in Murine Breast Cancer Xenografts with iLCC Treatment* Recently, we have conducted initial evaluation of iLCC in a xenograft nude mouse model of ER+ breast cancer. In preparation for this, we prepared a doxycycline-inducible retroviral expression system for iLCC and after selection for iLCC-expressing clones, evaluated the ability of iLCC to be expressed proportional to Dox dosing. We validated that Dox-induced iLCC exhibited nearly identical behavior as exogenously administered iLCC, creating antiproliferative effects, loss of ER, LSD1 and CoREST at ER target promoters, increased methylation at these sites, and we confirmed its nuclear localization using immunofluorescence. Transplantation of Dox-inducible iLCC-expressing cells into nude mice resulted in marked phenotypic changes to the palpable tumors, in some cases producing satellite tumors, a possible sign of stimulation of the EMT in these mice, which is negatively regulated by LSD1.

*MS and Biophysical Analyses of LSD1 Complexation by CoREST and ER* In year 2 of this proposal period, progress toward examining molecular contributors to these protein-protein interactions has also been made. We also examined the role of the LSD1 tower domain in CoREST recruitment and ER capture. In addition, isoform-selective potent small molecule inactivators of LSD1 were synthesized and used to examine the contribution of coregulatory molecule interactions to demethylase catalysis and its effect on ER+ and ER- breast cancer cellular proliferation. We have also successfully expressed full length CoREST to provide a physiologically-relevant template to examine ER binding and LSD1 recruitment, and how these events are required for proliferation versus demethylation chemistry in preparation of follow up murine xenograft implantation proliferation experiments that are scheduled.

LSD1 contains domains known to mediate interactions with other biomolecules. LSD1 contains an  $\alpha$ -helical, antiparallel coiled-coil 'tower' domain composed of two  $\alpha$ -helices (termed T $\alpha$ A and T $\alpha$ B) bridged by a tight turn formed by a KPPRD sequence. This domain projects almost 100 Å from the AOD and functionally contributes to the association with the corepressor CoREST (aka RCOR1/KIAA0071) by binding to a subdomain within its sequence. CoREST consists of an N-terminal ELM2 domain followed by dual SANT domains (SANT1 and SANT2) with an intervening region colloquially known as the linker domain (Figure 4). The N-terminal region spanning the ELM2 domain and first SANT domain have been mapped as a binding region for HDAC1, and a crystal structure of HDAC1 bound to a similar ELM2/SANT region in the CoREST-related protein, MTA1, has recently been reported. Although known to associate with the MTAs 1-3 and SMRT, it is not clear if these interactions are strictly tower domain mediated, nor is it clear where the LSD1 binding site is within these co-repressors since they only share a single SANT domain with CoREST.

Shi and colleagues initially investigated the interaction of LSD1 with domains within CoREST, and concluded that CoREST may act as a scaffolding protein that joins deacetylase and demethylase activities into a single catalytic sub-complex. The CoREST SANT2 domain, and possibly the SANT1 domain, has been shown to facilitate demethylation of nucleosomes, presumably by acting as a bridge between LSD1 and its substrate. A similar mechanism is observed in the SMRT protein, where the C-terminal SANT2 domain stabilizes the protein complex on chromatin by interacting with histone tails. In the first crystal structure of LSD1 in complex with the linker and SANT2 domains of CoREST, the CoREST linker domain forms an L-shaped helical conformation, with the short helix contacting the base of the LSD1 tower domain, the longer helix extending up the T $\alpha$ B helix, and the SANT2 domain contacting the top turn of the tower (Figure 4). These interactions are mainly hydrophobic in nature, although a few electrostatic interactions may facilitate proper alignment of the CoREST linker with the LSD1 tower domain. A second crystal structure of LSD1 and CoREST with a histone substrate-like peptide bound (pK4M) showed little overall conformational change as compared to the non-peptide-bound structure. However, the model does illustrate that the L-shaped short arm formed by the CoREST linker may have an indirect effect on substrate binding by stabilizing the helix formed from LSD1 residues 372-395.

As noted above, although the CoREST SANT2 domain contacts the LSD1 tower in reported crystal structures, our laboratory recently demonstrated that the CoREST linker domain is chiefly responsible for high affinity binding with LSD1. Specifically, a CoREST fragment consisting of the linker domain (residues 293-380) exhibits low nanomolar binding affinity towards LSD1 ( $K_d = 7.78$  nM), while inclusion of the SANT2 domain does not substantially alter binding affinity and in isolation lacks significant affinity towards LSD1. Our group also used mutagenesis and isothermal titration calorimetry to reveal that the energy of binding along the CoREST/LSD1 helix-helix interface is not concentrated into 'hotspots,' but *is instead distributed almost uniformly along the interaction interface*. As CoREST is required for nucleosomal demethylation, this argues that inhibitors of the CoREST linker/LSD1 tower interaction may inhibit LSD1 functionality in the cell.

**Aim 2 Progress-** Although iLCC is remarkably resistant to degradation *in cellulo*, we wish to also ameliorate its structure and develop formulations to that will reduce susceptibility to hydrolysis.

**Transcriptional Regulation by LSD1 Small Molecule Inhibition** Motivated by the relationship between the AOD of KDM1A to that of MAO-A/B and PAO, the first KDM1A small molecule inhibitors were discovered by our group in collaboration with R. Sheikhattar. Through screening a focused group of irreversible and reversible amine oxidase inhibitors, tranlycypromine (*trans*-2-phenylcyclopropylamine, 2-PCPA, Parnate™) was found to exhibit the highest KDM1A inhibitory activity towards methylated bulk histones as well as methylated nucleosomal substrates *in vitro*. Treatment of P19 embryonal carcinoma cells with parnate resulted in the global increase of H3K4 methylation as well as transcriptional derepression of two KDM1A target genes, *Egr1* and the pluripotent stem cell marker *Oct4*. This was the first example of inhibition of histone demethylation and interruption of transcriptional programs regulated by KDM1A using small molecules. In a subsequent study, our group determined that tranlycypromine was a mechanism-based inactivator of KDM1A, forming a covalent adduct with the FAD cofactor and demonstrating inactivation kinetic parameters of  $K_i = 242 \mu\text{M}$  and a  $k_{inact} = 0.0106 \text{ s}^{-1}$ . Soon after, the laboratories of Cole, Yokohama, and Mattevi provided additional support for this inhibitory mechanism, including defining the structure of the tranlycypromine-KDM1A adduct using X-ray methods, which revealed the N5 of the FAD isoalloxazine ring as the site of covalent attachment of the inhibitor.

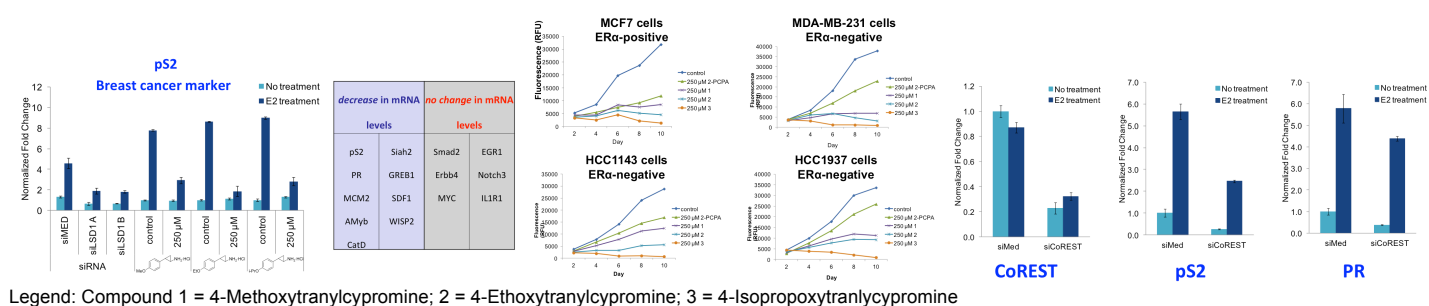


**Figure 5.** (A) siRNA and arylcyclopropylamines inhibit transcription of ER target genes; (B) Effect of arylcyclopropylamines inhibitors on cell proliferation of ER-positive and ER-negative breast cancer cell lines; (C) Knockdown of CoREST impacts the transcription of representative ER targets pS2 and PR.

**Antiproliferative Effects of iLCC compared to LSD1-Selective Inhibitors** In Aim 2 we sought investigate the activity of KDM1A inhibitors on MCF7 proliferation versus monoamine oxidase inhibitors previously used in the literature to help evaluate whether LSD1 demethylase activity, or the interactions with coregulatory proteins like CoREST are contributing to the antiproliferative activity of LSD1-CoREST antagonists or siRNA knockdown of ER, CoREST, and/or LSD1 (Figures 5 and 6). First, we treated MCF7 breast cancer cells with a gradient of GSK-LSD1 to test its ability to alter histone methylation state in a dose-dependent manner. Cells were treated with 0, 0.05, 0.25, 0.5, 1, or 10 μM GSK-LSD1 and incubated for 24 h. Cells were then collected and histones extracted. Each sample was analyzed by immunoblot such that each contained the same amount of total protein. Total histone H3 was analyzed as a loading control, while H3K4me2 was detected as a readout of KDM1A activity (Figure).

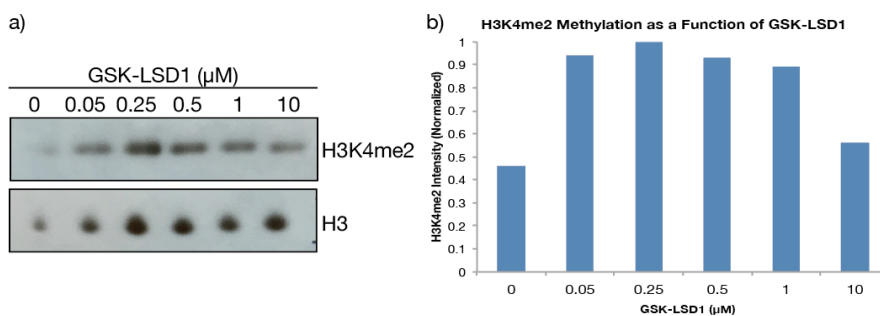


**Figure 6.** Histone methylation as a function of GSK-LSD1 concentration. (a) An immunoblot of MCF7 cells treated with the designated concentrations of GSK-LSD1. The top pane represents H3K4me2 modification, while the bottom pane represents total H3 as a loading control. (b) Quantification of H3K4me2 modification. The relative intensities of H3K4me2 bands were normalized by H3 total protein loading.

H3K4me2 methylation appears to be significantly increased between the no treatment control and most other samples, although a decrease in methylation is also observed at the highest concentration of 10 μM. Although a dose-dependent response it not observed, this may be due to the concentration range chosen. It is

possible that the lowest concentration tested (50 nM) gave the maximum effect detectable. A lower concentration range may in fact demonstrate a dose-dependent response similar to that observed by Kruger *et al.* in a small cell lung carcinoma model (*Cancer Cell*, 2015). To test this, 96-well plates of MCF7 cells were treated with a five-fold dilution series of GSK2879552 (abbrev. GSK-LSD1), Parnate, and ICI182,780 (ICI). The KDM1A inhibitor GSK-LSD1 and monoamine oxidase inhibitor Parnate dilutions series began at 10  $\mu$ M, while the ICI gradient began at 100 nM. Plates were treated with fresh media and compound every 2 days. On the final day, cell proliferation was measured and normalized to the initial seeding density. Proliferation curves were generated for each compound gradient (a-c). Additionally, a plot of the highest doses of each compound was generated for direct comparison (d). The proliferation assay indicated that both Parnate and ICI had a dose-dependent affect on MCF7 cell proliferation. Alternately, GSK-LSD1 did not appear to alter proliferation versus the control. At the highest doses, GSK-LSD1 and control cells reached nearly the same cell density, while ICI and Parnate both exhibited approximately 65% growth inhibition. This difference suggests that Parnate may be working through a mechanism other than KDM1A inhibition to slow breast cancer cell proliferation and throws into question recent reports that use the inhibitor to assign functionality to KDM1A. However, our results with iLCC and siRNA knockdown of LSD1 and CoREST support a clear relationship where LSD1 is required for proliferation, as such it suggests that LSD1 when in complex with the ER may be playing a scaffolding role in facilitating transcription.

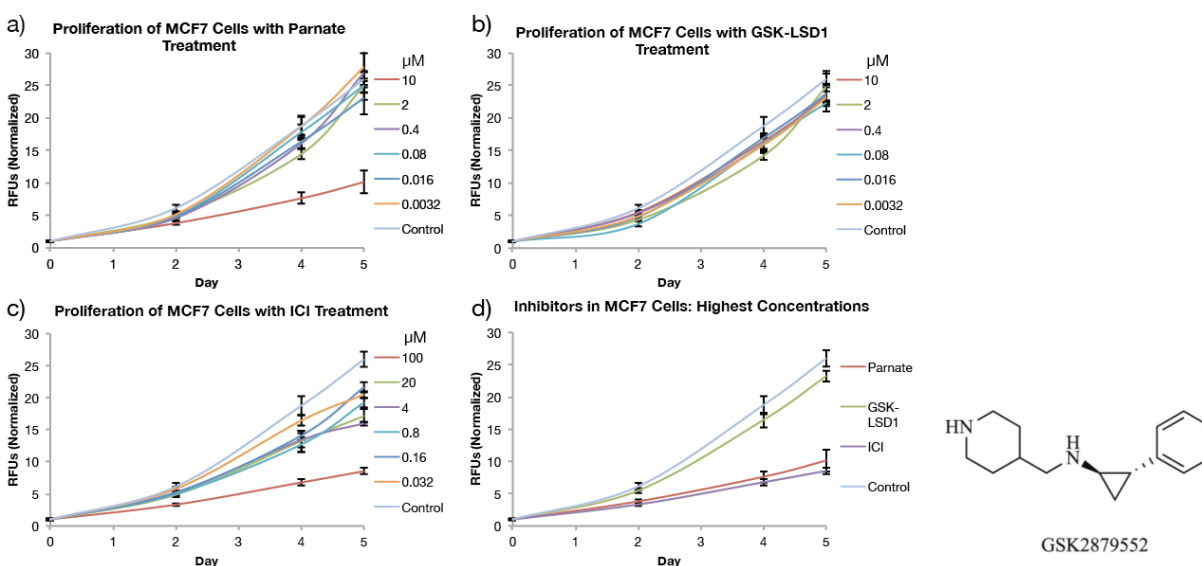
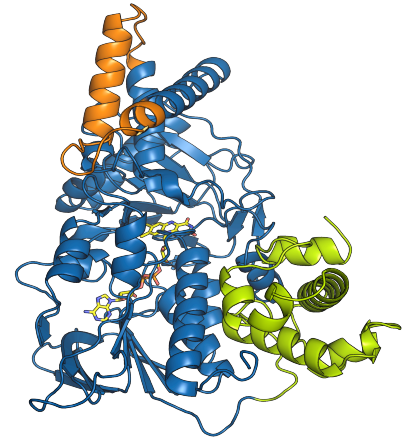


**Figure 7.** Proliferation of MCF7 cells as a function of inhibitor. (a) Proliferation as a function of monoamine oxidase inhibitor Parnate concentration. (b) Proliferation as a function of KDM1A inhibitor GSK2879552 (i.e. *GSK-LSD1*) concentration. (c) Proliferation as a function of estrogen receptor alpha antagonist ICI concentration. (d) Summary of the highest concentrations of each treatment.

**Aim 3-** To assist in understanding LSD1 function in breast cancer, we wish to provide an innovative solution to identify ER targets involved in communication with LSD1 within complex protein mixtures by combining SPROX shotgun proteomics with chemical genetic probes of ER communication with the LSD1 complex (developed by the PI).

*Interface Mapping by MS Methods* Mass spectrometry experiments to identify the physical basis for communication between the ER and LSD1 complex have been initiated. Unfortunately, because of the poor degree of fragmentation LSD1 exhibited using bottom up proteomics, insufficient coverage was achieved in initial MS analyses to facilitate SPROX studies with the ER. However, we have recently turned to using H/D exchange using high resolution ESI/MS methods which overcame the fragmentation issues. Based upon our preliminary analyses of LSD1 using binding to histone H3 and CoREST as probes, we have been able to easily visualize specific conformational changes within LSD1 and the LSD1 CoREST complex upon substrate binding. We are now pursuing similar analyses with LSD1 and CoREST fragments with the ligand binding domain of the ER $\alpha$ , aided as well by newly produced recombinant full length CoREST which serves as a template for these interactions.

*Molecular Interactions Underlying LSD1 Communication with Coregulatory Proteins* Lysine-specific demethylase 1A (KDM1A/LSD1) removes mono- and dimethyl post-translational modifications on lysine residues of histones leading to both repression and activation of associated genes. Interestingly, KDM1A activity and its substrate specificity are regulated by both active site recognition and association with a number of coregulatory proteins and inclusion into multiprotein complexes through protein-protein interactions. CoREST is one such binding partner of KDM1A that facilitates nucleosomal demethylation through interacting with its unprecedented tower domain. Besides CoREST and paralogs, there are many homologous binding partners that utilize this domain as an oligomerization motif. As the interaction with the tower domain is a central theme in the elaborate control of KDM1A and direction of its activity, over the past year, we conducted analysis of the binding interface between KDM1A and CoREST in order to provide insight into their collaborative mechanism. Toward this end, initial steps have been taken to define the key regions implicated in the binding interaction. Using this information along with structure-aided protein engineering, we developed an LSD1 enzyme that possessed full demethylase enzymatic activity, yet was devoid of the tower domain and subsequently lost all affinity for CoREST (see the structure of the 'towerless LSD1 in the inset).



*Interfacial Binding Kinetics Govern Histone H3 Recognition and Specificity* Lysine-specific demethylase 1A (KDM1A/LSD1) is an FAD-dependent enzyme that catalyzes the oxidative demethylation of histone H3K4me1/2 and H3K9me1/2 repressing and activating transcription, respectively. Although the active site is expanded compared to the greater amine oxidase superfamily, it is too sterically restricted to encompass the minimal 21-mer peptide substrate footprint. The remainder of the substrate/product is therefore expected to extend along the surface of KDM1A. We show that full-length histone H3 which lacks any posttranslational modifications is a tight-binding, competitive inhibitor of KDM1A demethylation activity with a  $K_i$  of  $18.9 \pm 1.2$  nM; a value that is approximately 100-fold higher than the 21-mer peptide product (i.e. H3<sup>1-21</sup>). The relative H3 affinity is independent of preincubation time suggesting that H3 rapidly reaches equilibrium with KDM1A. Rapid dilution experiments confirmed the increased binding affinity of full-length H3 was at least partially due to a slow off-rate ( $k_{off}$ ) of  $1.2 \times 10^{-3} \text{ s}^{-1}$ , a half-life ( $t_{1/2}$ ) of 9.63 min, and residence time ( $t$ ) of 13.9 min. Independent affinity capture surface plasmon resonance experiments confirmed the tight-binding nature of the H3/KDM1A interaction, revealing a  $K_d$  of  $9.02 \pm 2.27$  nM, a  $k_{on}$  of  $9.26 \times 10^4 \pm 1.5 \times 10^4 \text{ M}^{-1}\text{s}^{-1}$  and a  $k_{off}$  of  $8.35 \times 10^{-4} \pm 3.4 \times 10^{-5} \text{ s}^{-1}$ . Additionally, no other core histones exhibited inhibition of KDM1A demethylation activity, which is consistent with H3 being the preferred histone substrate of KDM1A. Together these data suggest that KDM1A likely contains a histone H3 secondary specificity recognition element on the enzyme surface.

### Key Research Accomplishments:

- Characterization of iLCC vs. the LSD1-selective inhibitor GSK2879552
- Validation of iLCC inhibition of LSD1 function in vivo and in vitro
- Identification of CoREST knockdown as a target for iLCC competition for LSD1
- Successful identification of LSD1-dependent protein-protein interactions with coregulatory molecules using H/D exchange MS methods and deletion mutagenesis (e.g. tower domain deletion mutant)
- Observation of mechanistic differences between iLCC, parnate the small molecule LSD1-selective inhibitor GSK2879552 that suggest a scaffolding function for LSD1 or additional target coregulatory molecules influence breast cancer proliferation

### Conclusion

In short we have made substantial progress on the project and are excited to complete the experiments outlined in the statement of work for the remaining period of this proposal period. Thank you for your generous support of this research project.

**Publications, Abstracts and Presentations**

Published or in press manuscripts are attached as supporting information. Two additional manuscripts not included in this update are under review.

This work was presented as a research talk by Prof. McCafferty at the Enzymes Gordon Research Conference, UCSF, UNC-Chapel Hill and a GSK-sponsored research symposium in the Research Triangle Park.

Jennifer Link will present this work in an invited talk in San Diego for the ACS National Meeting in March 2016 (abstract accepted Nov 2015)

**Inventions, Patents, and Licenses**

Nothing to report

**Reportable Outcomes**

Nothing to report

**Other Achievements**

Nothing to report

**References**

Nothing to report

**Appendices**

Nothing to report

## Review

# KDM1 Class Flavin-Dependent Protein Lysine Demethylases

Jonathan M. Burg, Jennifer E. Link, Brittany S. Morgan, Frederick J. Heller, Amanda E. Hargrove, Dewey G. McCafferty

Department of Chemistry, Duke University, Durham, NC 27708

Received 7 January 2015; revised 2 March 2015; accepted 7 March 2015

Published online 18 March 2015 in Wiley Online Library (wileyonlinelibrary.com). DOI 10.1002/bip.22643

### ABSTRACT:

Flavin-dependent, lysine-specific protein demethylases (KDM1s) are a subfamily of amine oxidases that catalyze the selective posttranslational oxidative demethylation of methyllysine side chains within protein and peptide substrates. KDM1s participate in the widespread epigenetic regulation of both normal and disease state transcriptional programs. Their activities are central to various cellular functions, such as hematopoietic and neuronal differentiation, cancer proliferation and metastasis, and viral lytic replication and establishment of latency. Interestingly, KDM1s function as catalytic subunits within complexes with coregulatory molecules that modulate enzymatic activity of the demethylases and coordinate their access to specific substrates at distinct sites within the cell and chromatin. Although several classes of KDM1-selective small molecule inhibitors have been recently developed, these pan-active site inhibition strategies lack the ability to selectively discriminate between KDM1 activity in specific, and occasionally opposing, functional contexts within these

complexes. Here we review the discovery of this class of demethylases, their structures, chemical mechanisms, and specificity. Additionally, we review inhibition of this class of enzymes as well as emerging interactions with coregulatory molecules that regulate demethylase activity in highly specific functional contexts of biological and potential therapeutic importance. © 2015 Wiley Periodicals, Inc. *Biopolymers (Pept Sci)* 104: 213–246, 2015.

**Keywords:** KDM1A; KDM1B; Epigenetic; LSD1; LSD2

This article was originally published online as an accepted preprint. The “Published Online” date corresponds to the preprint version. You can request a copy of any preprints from the past two calendar years by emailing the Biopolymers editorial office at [biopolymers@wiley.com](mailto:biopolymers@wiley.com).

### INTRODUCTION

The functional capacity of genetically encoded proteins can be powerfully expanded by reversible posttranslational modifications (PTMs). Protein side chain covalent modifications such as methylation, phosphorylation, acetylation, glycosylation, ubiquitination, sumoylation, ADP-ribosylation, nitrosylation, carboxylation, and sulfonation, among others, can potentiate local and global protein architecture and generate novel reactive functional groups for binding and catalysis. Additionally, these modifications can generate signals for cellular compartmentalization and confer alterations to physiochemical properties such as stability, solubility, and resistance to proteolytic degradation. Such modifications are intimately integrated into all aspects of modulating cellular proliferation and biological recognition.

Correspondence to: Dewey G. McCafferty, Department of Chemistry, Duke University, B120 Levine Science Research Center, Box 90346, 450 Research Drive, Durham, NC 27708-0346; e-mail: [dewey.mccafferty@duke.edu](mailto:dewey.mccafferty@duke.edu)

Contract grant sponsors: U.S. Department of Defense Office of Congressionally Directed Medical Research Programs for Breast Cancer Research Grant W81XWH-13-1-0400 (to D.G.M.), by the U.S. National Institutes of Health (NIH) for Research Grants R01-GM65539 (to D.G.M.), by the NIH Predoctoral Science Training Grant T32-GM 7105-39 in Pharmacological Sciences (to J.E.L.), and by the NIH Predoctoral Training Grant T32-GM 8487-19 in Structural Biology and Biophysics (to J.M.B. and B.S.M.), and by Duke University.

This manuscript is dedicated to Professor William F. DeGrado on the occasion of his 60th birthday.

Burg and Link contributed equally to this work.

© 2015 Wiley Periodicals, Inc.

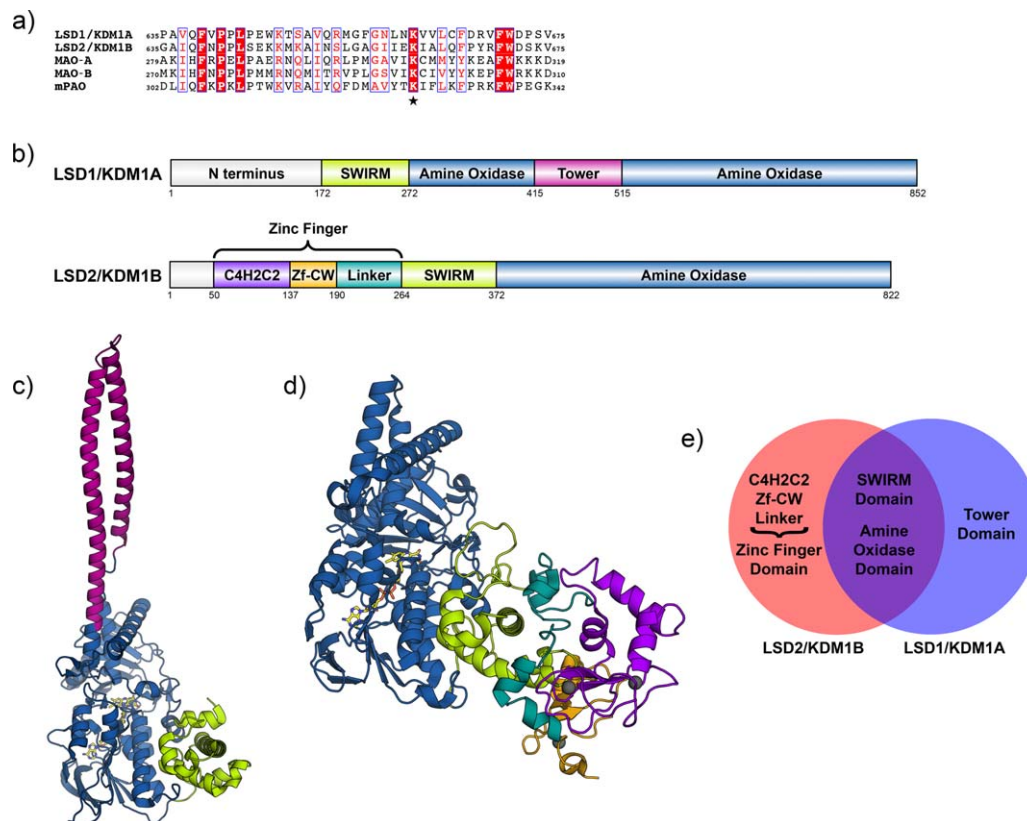


**FIGURE 1** Structural overview of KDM1 demethylases. (a) Sequence alignment of a portion of the amine oxidase domains of KDM1A, KDM1B, MAO-A, MAO-B, and maize polyamine oxidase (mPAO). Sequence conserved active site Lys residue is starred. (b) Domain maps of KDM1A and KDM1B. SWI3p, Rsc8p, and Moira (SWIRM) domains shown in green, amine oxidase domains shown in blue, tower domain shown in lavender, linker domain shown in teal, C4H2C2 domain shown in purple, and Zf-CW domain shown in orange. (c) Ribbon representation of the structure of KDM1A. Domains follow same color scheme as outlined above (PDB 2IW5). (d) Ribbon representation of the structure of KDM1B. Domains follow same color scheme as outlined above (PDB 4HSU). (e) Venn diagram of domain conservation between KDM1A and KDM1B.

Allfrey first linked histone acetylation and methylation to the control of RNA synthesis in 1964.<sup>1,2</sup> Since that time, it has become clear that protein and histone methylation is a pervasive cellular regulatory mechanism. Specifically, protein lysine methylation status plays a critical role in biology and pathobiology by influencing transcriptional activation and repression, chromatin remodeling, normal and oncogenic signaling, viral pathogenesis, and protein and transcription factor recruitment, among other functions. S-adenosylmethionine-dependent methyltransferases (SAM-dependent MTases) catalyze the installation of lysine methyl marks, forming mono-, di-, and tri-methylated side chain PTMs. These marks are removed by two mechanistically-distinct classes of lysine-specific demethylases (KDMs) that utilize either a flavin adenine dinucleotide (FAD) cofactor (KDM subfamily 1) or iron(II) and  $\alpha$ -ketoglutarate cofactors (KDM subfamily 2–6) to catalyze the oxidative demethylation of protein side chains.<sup>3–5</sup>

For decades, methylation marks on proteins like histones were presumed to be immutable, reversed only through protein turnover and degradation. The first hints of a candidate histone demethylase enzyme emerged in 1998 and again in 2001, when several histone deacetylase (HDAC)-containing complexes were discovered to associate with KIAA0601 (aka KDM1A/LSD1/BHC110/AOF2), a protein with homology to human FAD-dependent oxidoreductases (MAO-A/B) and maize polyamine oxidase (mPAO) (Figure 1a), enzymes that catalyze the oxidative cleavage of C-N bonds.<sup>6–8</sup> In 2003, Shiekhhattar reported that BHC110/KIAA0601 formed a stable complex with several proteins, including HDACs 1 and 2, CoREST, BRCA2-associated factor, BCH80, TFII-1, KIAA0182/GSE-1, ZNF217, ZNF198/FIM and ZNF261/X-FIM.<sup>9</sup>

In 2003 Amasino and coworkers independently discovered that the gene FLOWERING LOCUS D (FLD) encoded a plant homolog of KIAA0601.<sup>10</sup> FLD is one of six genes in the

*Arabidopsis thaliana* autonomous floral-promotion pathway that initiates the transition from a vegetative to reproductive state by repression of the MADS-box transcription factor FLOWERING LOCUS C (FLC). FLD not only contains a KIAA0601-like amine oxidase domain, but also possesses an N-terminal SWI3p, Rsc8p, and Moira (SWIRM) domain similar to that associated with a range of proteins involved in chromatin remodeling, including KIAA0601.<sup>11,12</sup> Deletion of FLD in *A. thaliana* results in hyperacetylation of histones in the FLC locus, upregulation of FLC expression, and extremely delayed flowering, suggesting that the autonomous pathway involves regulation of histone deacetylase activity by FLD.<sup>10</sup> Deletion of FLD also resulted in increased histone methylation levels (R. Amasino, personal communication), implicating FLD (and by analogy KIAA0601) as the elusive human histone demethylase enzyme.

In early 2004, Shi and coworkers provided the first direct evidence that KIAA0601 (from here on referred to as KDM1A) functions as a histone demethylase and transcriptional corepressor.<sup>13</sup> The authors reveal that KDM1A specifically demethylates mono- and di-methylated histone H3 lysine 4 (H3K4me1/2), a histone mark linked to active transcription, and that lysine demethylation occurs via an oxidative reaction that generates formaldehyde. In addition, loss of KDM1A through siRNA knockdown results in increased H3K4 methylation and concomitant derepression of several neuronal-associated target genes. Shi's discovery of KDM1A activity implied that lysine methylation might be dynamically controlled.

The second human flavin-dependent histone demethylase, KDM1B (aka LSD2/AOF1) was identified by Shi and coworkers in 2004 through a domain homology search of genomic databases.<sup>13</sup> Mattevi and coworkers first isolated and confirmed the flavin-dependent demethylation activity of KDM1B, noting specificity for H3K4me1/2, despite the relatively low sequence identity (<25%) with KDM1A.<sup>14</sup> Unlike KDM1A, KDM1B does not form a biochemically-stable complex with the C-terminal domain of the corepressor CoREST, but does possess both CW-type and C4H2C2-type zinc finger motifs. This suggests that KDM1B may interact with different targets or coregulatory molecules and may be involved in transcriptional programs distinct from those of KDM1A.

Herein we review the biological function, biochemical characterization, and inhibition of this enzyme class to date. First, we briefly discuss the biological importance and therapeutic potential of KDM1s. This is followed by the structural organization, chemical mechanism, and substrate specificity of the KDM1 enzymes. We then outline the various inhibitor classes that have been developed for these demethylases, specifically highlighting the utility of peptide-based inhibitors. Finally, we describe the known interactions between the KDM1s and regu-

latory biomolecules, which direct their activity toward specific cellular pathways. Given the wide-ranging and ubiquitous functions of this enzyme class, probes with the ability to target KDM1 activity in a manner that is pathway-specific would be of heuristic and therapeutic value. We see these coregulatory molecules as a valuable starting point for the development of such probes, as underscored by the recent development of peptide inhibitors of this enzyme class.

## KDM1A AND KDM1B BIOLOGY AND THERAPEUTIC POTENTIAL

KDM1A is involved in a wide variety of cellular processes and pathologies, including signal transduction, chromatin remodeling, transcriptional regulation, development, differentiation, viral pathogenesis, and cancer proliferation and metastasis.<sup>3,15-23</sup> As such, KDM1 demethylases have emerged as potential therapeutic targets. Although their clinical value is only beginning to be explored, at the time of this review's publication, five clinical trials involving KDM1A were either planned or currently recruiting subjects. Three trials will investigate KDM1A inhibition as a therapeutic strategy in acute myeloid leukemia (AML), one will evaluate the same strategy in small cell lung cancer, and one seeks to correlate the status of KDM1A with cardiovascular responses to changes in sodium intake (see <http://clinicaltrials.gov>). We expect the scope of clinical trials to expand with our growing knowledge of KDM1A function.

### Cellular Differentiation

Epigenetic modifications are critical for the maintenance of pluripotent stem cells and their subsequent differentiation into specialized tissues.<sup>24-26</sup> Specifically, KDM1A is an integral part of the cellular machinery that governs differentiation processes in various cell types, including embryonic,<sup>27,28</sup> hematopoietic,<sup>23,29-33</sup> neuronal,<sup>34-38</sup> pituitary,<sup>39</sup> and osteogenic.<sup>40</sup> While KDM1A activity is critical for proper development, aberrant regulation can contribute to tissue-specific disease states. For example, KDM1A activity has been linked to neuronal cell proliferation and survival<sup>41,42</sup> and long-term memory formation,<sup>43</sup> and is therefore an emerging therapeutic target for some neurological and cognitive disorders. Similarly, recent work has also identified KDM1A as a key regulator of leukemia stem cells,<sup>44</sup> sparking interest in its potential as a therapeutic target in AML (see below), among other hematopoietic-related diseases.<sup>45</sup>

### Cancer Development and Progression

KDM1A has also been widely implicated in the development and progression of cancer. In addition to the malignancies

described in detail below, KDM1A is emerging as a potential therapeutic target in various other cancer types.<sup>46–56</sup>

**Neuroblastoma.** Overexpression of KDM1A in neuroblastic tumors correlates with poor prognosis<sup>57</sup> and may be related to the aberrant downregulation of KDM1A-silencing micro-RNAs.<sup>58,59</sup> Schulte and coworkers first noted in 2009 that KDM1A inhibition in neuroblastoma cells leads to increased H3K4 methylation, decreased proliferation in cell culture, and reduced tumor growth in a xenograft model.<sup>57</sup> Similarly, KDM1A inhibitors synergize with retinoic acid, a currently approved treatment for neuroblastoma.<sup>60</sup> A later report demonstrated similar results in the closely-related medulloblastoma tumor type, where KDM1A inhibition decreases proliferation and initiates apoptosis.<sup>61</sup>

**Colorectal Cancer.** KDM1A is also an emerging target in colorectal cancers, where it is markedly overexpressed in tumor samples compared to matched normal tissue<sup>62</sup> and exhibits a positive correlation with metastatic potential.<sup>63,64</sup> Although genetic deletion of KDM1A does not result in a global increase of H3K4me2, it does alter gene expression programs and reduces proliferation in cell culture and *in vivo*.<sup>62,65</sup> KDM1A may also promote colorectal cancer progression by derepressing the Wnt/ $\beta$ -catenin signaling pathway, a known regulator of tumorigenesis.<sup>62</sup>

**Leukemia.** KDM1A is also a promising target for pharmacological intervention in leukemia. For example, KDM1A inhibition alone provokes cytotoxic effects in AML cell lines,<sup>66</sup> and when used in conjunction with HDAC inhibitors, reduces tumor engraftment and improves survival in mice.<sup>67</sup> KDM1A inhibition also unlocks the anti-leukemic effects of all-trans-retinoic acid (ATRA), a differentiation-inducing agent that otherwise is ineffective for the treatment of AML.<sup>68</sup> KDM1A has been implicated in other leukemia subtypes as well. In a model of MLL-AF9 leukemia cells, KDM1A cooperates with the MLL MTase fusion protein to maintain an oncogenic transcription program, and KDM1A inhibitors preferentially reduce the repopulation potential of MLL-AF9 cells over normal hematopoietic cells.<sup>44</sup> Interestingly, Sprüssel and coworkers evaluated the potential side effects of KDM1A inhibition in leukemia and found that while a conditional KDM1A knockdown significantly alters existing pools of normal hematopoietic tissues, these effects are largely reversible following reinstatement of the demethylase.<sup>31</sup> For a more detailed discussion of KDM1A's function and therapeutic potential in leukemia, we refer readers to a recent review by Mould and colleagues.<sup>69</sup>

**Breast Cancer.** KDM1A has also been implicated as a regulator of breast cancer development and progression. The majority of the breast tumors are estrogen-dependent, making estrogen antagonists one of the most commonly employed therapies. However, circumvention of estrogen signaling, such as through loss of estrogen-receptor alpha (ER $\alpha$ ), can lead to hormone-resistant tumors, reduced treatment options, and worse prognosis. KDM1A is generally associated with a more aggressive breast cancer phenotype and may be overexpressed in both ER $\alpha$ -positive and -negative cells,<sup>70–73</sup> possibly due to aberrant stabilization of the demethylase.<sup>74</sup> Correspondingly, several groups have reported that KDM1A inhibition decreases proliferation of breast cancer cells.<sup>70,72,75</sup> Notably, at least two groups have reported contradicting results that suggest KDM1A may be downregulated in breast cancer tissue and that inhibition affects metastasis with no observable effects on proliferation.<sup>76,77</sup> KDM1A inhibition may also have therapeutic effects when used in conjunction with anti-estrogen treatment<sup>78</sup> and HDAC inhibitors.<sup>79,80</sup>

**Prostate Cancer.** A similarly vague relationship exists between KDM1A and prostate cancer. One study reported a correlation between KDM1A expression and risk of recurrence,<sup>81</sup> while at least two other studies have noted little to no overexpression of KDM1A in prostate cancer cell lines and tumor samples.<sup>82,83</sup> However, Metzger and coworkers have linked KDM1A activity to transcriptional regulation with the androgen receptor (AR), a nuclear hormone receptor closely linked with prostate cancer.<sup>84</sup> Likewise, KDM1A inhibition appears to impede AR-mediated transcription and prostate cancer proliferation.<sup>84–87</sup> A review detailing further the roles of demethylases in prostate cancer has recently been published.<sup>88</sup>

### The Epithelial-to-Mesenchymal Transition

In addition to these roles in specific cancer types, KDM1A is also intimately linked with the epithelial-to-mesenchymal transition (EMT), the process by which a polarized, adhesive epithelial cell transitions into a motile, invasive mesenchymal phenotype. The importance of epigenetic mechanisms during the EMT is only beginning to be appreciated.<sup>89</sup> KDM1A is an established functional partner of the EMT master regulator SNAIL and cooperates to silence epithelial genes.<sup>90</sup> KDM1A also regulates upstream inducers of the EMT,<sup>91</sup> including TGF $\beta$ ,<sup>76,92,93</sup> Wnt,<sup>62,94</sup> NF- $\kappa$ B,<sup>80</sup> and Notch.<sup>95,96</sup> Through these and potentially other mechanisms, KDM1A participates in large-scale chromatin remodeling events that accompany the EMT.<sup>92</sup>

The EMT is a hallmark of aggressive cancers with a high risk of metastasis, potentially implicating KDM1A as a

therapeutic target.<sup>89</sup> Accordingly, KDM1A inhibition in AML models produces morphological features of differentiation in primary and cultured cells,<sup>67</sup> derepresses differentiation-associated genes,<sup>66,68</sup> and reduces engraftment of primary cells in a mouse model.<sup>68</sup> Similar effects are observed in MLL-AP9 leukemia and neuroblastoma models.<sup>44,57</sup> Furthermore, KDM1A activity is associated with increased metastatic potential and its inhibition or knockdown decreases migration and invasion in several cancer types,<sup>48,49,63,64</sup> with again conflicting reports concerning breast cancer.<sup>76,97,98</sup>

### Viral Pathogenesis

Lastly, KDM1A is associated with herpes simplex virus (HSV) infection and replication, as HSV hijacks KDM1A-containing machinery required for human neuronal gene repression during host infection. Cooption of KDM1A demethylase activity helps promote early stage ( $\alpha$ ) viral gene activation, regulates late stage ( $\beta/\gamma$ ) viral gene repression, and has been linked to gene repression during the development of HSV latency, the process by which viruses enter and emerge from dormancy in infected host cells.<sup>99</sup> Kristie and coworkers recently demonstrated that interruption of KDM1A activity potently represses HSV immediate-early (IE) gene expression and genome replication, resulting in suppression of primary infections and subsequent reactivation from latency in murine infection models.<sup>100–102</sup> In addition, KDM1A activity may play a similar role in the infection processes of several other viruses.<sup>101,103,104</sup> Collectively, these studies underscore the emerging importance of KDM1A as an antiviral target.

### Emerging Biological Roles for KDM1B

The biological roles of KDM1B are beginning to emerge; however, our current understanding of this enzyme lags far behind that of KDM1A. In general, KDM1B is believed to function as an enhancer of gene transcription that functions in highly transcribed coding regions of chromatin.<sup>105</sup> Although mechanistic data is not yet available, KDM1B has been linked to genomic imprinting,<sup>106</sup> liver development,<sup>107</sup> somatic cell reprogramming,<sup>108,109</sup> and NF- $\kappa$ B signaling.<sup>110</sup> Future research will likely reveal a broader set of KDM1B-dependent biological processes.

## DOMAIN ORGANIZATION AND STRUCTURAL FEATURES OF KDM1 DEMETHYLASES

### KDM1A Demethylase

KDM1A is an 852 amino acid (aa) polypeptide composed of three domains: an amine oxidase catalytic domain (AOD) (res-

idues 272–415 and 515–852), an  $\sim$ 100 aa insert known as the “tower” domain (residues 415–515), and a SWIRM domain (residues 172–272) (Figure 1b,c).<sup>11,111,112</sup> The N-terminal region of the enzyme ( $\sim$ 170 aa) has no predicted conserved structural elements, but does contain a nuclear localization signal (RRKRAK; residues 112–117) for nuclear import via importin- $\alpha$  translocases.<sup>113,114</sup> The three-dimensional structure of KDM1A has been solved by X-ray crystallographic methods in the unliganded form and in complex with varying ligands, including peptides and inhibitors.<sup>111,112,115–126</sup> The AOD of the enzyme contains a single non-covalently bound FAD molecule and bears similarity to human MAO-A/B and mPAO (17.6%, 17.6%, and 22.4% sequence identity, respectively; Figure 1a).<sup>127</sup> Consistent with other flavin-dependent amine oxidases,<sup>128,129</sup> the AOD can be further subdivided into two separate lobes, where residues 357–415, 515–558, and 658–769 are involved in substrate binding and residues 272–356, 559–657, and 770–852 form an expanded Rossmann fold used to bind FAD.<sup>112,115</sup>

The tower domain of KDM1A is an antiparallel coiled-coil composed of two  $\alpha$ -helices (termed T $\alpha$ A and T $\alpha$ B) bridged by a tight turn formed by a KPPRD sequence.<sup>112</sup> This domain projects almost 100 Å from the AOD and functionally is the site of association with corepressor CoREST (aka RCOR1/KIAA0071), among other proteins.<sup>112,115,130</sup> The SWIRM domain of KDM1A is predominantly a bundle of  $\alpha$ -helices, with a long central  $\alpha$ -helix that separates two smaller helix-turn-helix motifs (Figure 1c).<sup>111</sup> This domain also engages the C-terminal tail of the AOD with a highly hydrophobic interface that buries a surface area of  $\sim$ 1,700 Å<sup>2</sup>.<sup>111</sup> Mutations of conserved residues along this interface have been shown to reduce the catalytic activity of KDMA1 and its stability.<sup>111</sup>

Although SWIRM domains are highly conserved amongst chromatin associating proteins and have been shown to bind DNA,<sup>12,131</sup> this is not the case in KDM1A. The residues that compose the typical DNA-binding interface ( $\alpha$ 6; residues 247–259) are not conserved and are partially blocked by their interaction with the AOD.<sup>111,115</sup> Accordingly, neither KDM1A nor the isolated SWIRM domain binds DNA.<sup>115,132</sup>

In addition, Luka and coworkers showed that KDM1A binds to the small molecule tetrahydrofolate with a  $K_d$  of 2.8  $\mu$ M, and recently reported the crystal structure of the KDM1A-CoREST-tetrahydrofolate complex.<sup>126,133</sup> In this complex, the folate binds in the active site in close proximity to the FAD cofactor, and overlaps with the peptide-binding site observed by Forneris.<sup>117</sup> Luka and coworkers also detected the production of 5,10-methylene-tetrahydrofolate by mass spectrometry following incubation of KDM1A with a H3K4-derived methylated peptide substrate and tetrahydrofolate. From this data, it was postulated that tetrahydrofolate binding

might protect the cell from potentially toxic formaldehyde or regulate access of the substrate to the FAD within the active site. It is not known at this time if KDM1B exhibits a similar ability to bind tetrahydrofolate.

### KDM1B Demethylase

The closely related KDM1B is an 822 aa flavoenzyme amine oxidase that contains a predicted unordered N-terminus and a nuclear localization signal (~50 aa) responsible for its residence within the nucleus of human cells.<sup>106</sup> KDM1B is organized into three domains: an N-terminal dual zinc finger domain (residues 50–264), a SWIRM domain (residues 264–372), and a C-terminal catalytic AOD (residues 372–822; Figure 1b,d).<sup>134–136</sup> In the substrate-free structure of KDM1B, the zinc fingers and catalytic AOD are packed closely against a central SWIRM domain (Figure 1d), collectively resembling a boot.<sup>134</sup> Comparison of the AOD between KDM1A and KDM1B (33% sequence identity) shows that many secondary structural elements are conserved, including strong conservation of the catalytic architecture around the FAD-binding site.<sup>134</sup> However, when comparing the AODs through structural alignment, there is a 2.0 Å RMSD difference in the overall polypeptide backbone conformation. These structural differences are mostly attributed to the length and conformation of solvent exposed loops within the domain.<sup>134</sup> Despite these differences, the similarity of the AODs of KDM1A and KDM1B argues for a common chemical mechanism for catalysis.

### Structural Differences Between KDM1A and KDM1B

Despite catalyzing identical chemical reactions and sharing significant AOD structural similarity, KDM1A and KDM1B have several structurally important differences. For example, the SWIRM domains of both enzymes only share 24% sequence identity. Although helices within this domain are qualitatively positioned, significant differences have been observed at both solvent exposed interfaces along the helical termini. Since the entrance to the AOD active site lies at the interface of the AOD and SWIRM domains, structural and sequence differences at this interface are suspected to impact substrate specificity of each isoform.<sup>134</sup>

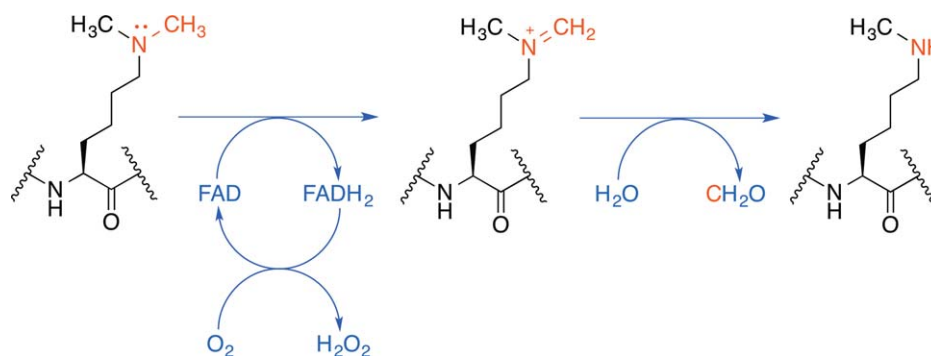
Indeed, at this interface the SWIRM-AOD subdomain interactions differ in several aspects when comparing KDM1A to KDM1B. Notably, the SWIRM domain of KDM1B closely packs against the N-terminal zinc finger domain, burying a surface area of 1,872 Å<sup>2</sup>.<sup>134</sup> As compared to KDM1A, the SWIRM domain of KDM1B lacks a C-terminal helix (KDM1A; residues 171–181), but is replaced by an extended, coiled loop (KDM1B; residues 271–281).<sup>136</sup> This substitution in KDM1B leads to the formation of two additional hydrogen

bonds (E452 with N266, and Y268 with D571) and one electrostatic interaction (E323 with K323) that may influence the degree of association among these domains.<sup>136</sup> Not only does this loop provide additional intramolecular interactions, but also forms a second binding site for the N-terminal tail of histone H3.<sup>135</sup>

The most striking structural difference between KDM1A and KDM1B is the inclusion of distinct domains that mediate interactions with other biomolecules (Figures 1b,e). KDM1A contains an  $\alpha$ -helical, antiparallel coiled-coil tower domain that is absent in KDM1B (Figure 1c–e). DALI<sup>137</sup> structural similarity analyses indicate that the tower domain fold appears infrequently among known eukaryotic protein structures, with the PI3K $\alpha$ -p85 $\alpha$  subunit complex (PDB 3HHM)<sup>138</sup> and the DNA double-strand break repair ATPase RAD50 (PDB 1L8D)<sup>139</sup> bearing the closest structural similarity. In contrast, the tower fold was heavily represented among a subset of prokaryotic proteins known to utilize such motifs as part of intermolecular protein recruitment, membrane docking, and membrane translocation functions.<sup>140</sup>

Although KDM1B does not contain a tower domain, it does contain two individual zinc fingers and two linker domains that are not reflected in the structure of KDM1A (Figure 1b,e). At the N-terminus of KDM1B, a C4H2C2-type zinc finger is joined to a second CW-type zinc finger (Zf-CW) by a linker formed from two  $\alpha$ -helices (Figure 1b,d). Immediately following the Zf-CW domain, a second linker formed by four  $\alpha$ -helices joined through several large loops bridges these domains to the AOD.<sup>134–136</sup> The surface of the C4H2C2-type zinc finger shows a marked concentration of basic residues, and thus may impact demethylase substrate specificity or positioning within nucleosomal DNA. Additionally, these residues may facilitate interactions with coregulatory molecules or serve to recruit transcriptional machinery, such as phosphorylated RNA polymerase II.<sup>105,134</sup> Interestingly, it appears that the zinc finger domain of KDM1B is required for histone demethylation activity. Wong and coworkers suggest that mutations which disrupt the zinc finger domains or relays of interactions among the zinc finger-SWIRM-AOD likely lead to subtle conformational alterations in the AOD that in turn impair the incorporation of FAD, and consequently its enzymatic activity.<sup>134</sup>

Furthermore, although zinc fingers are common folding motifs, the Cys2<sub>A</sub>-Cys2<sub>B</sub>-His2<sub>A</sub>-Cys2<sub>B</sub> sequence within KDM1B folds into a cross-brace topology that has not been previously observed, raising the possibility that this domain may participate in biomolecular interactions that are exclusive to KDM1B.<sup>134</sup> On the other hand, the Zf-CW of KDM1B bears significant sequence similarity to CW-type zinc finger domains, a class linked to histone H3 binding. Despite this, as



**SCHEME 1** Proposed chemical mechanism of FAD-dependent demethylases KDM1A and KDM1B. Oxidation of the C-N bond of the methylated lysine sidechain to an iminium ion, with concurrent reduction of the flavin enables hydrolysis via bulk water. Collapse of the hemiaminal (not shown) yields formaldehyde and the demethylated amine sidechain. The reduced flavin is reoxidized by molecular oxygen, generating a molar equivalent of hydrogen peroxide.

an isolated recombinant domain, the KDM1B Zf-CW fails to bind histone H3-derived peptides (residues 1–21 containing H3K4me1/2 or unmethylated H3K4), which is atypical to behavior exhibited by other isolated Zf-CW domains.<sup>134,136</sup> However, since ligand binding within Zf-CW domains is mediated by interactions within a well-conserved hydrophobic cleft, which happens to be absent in the KDM1B Zf-CW domain structure, this may partially explain its inability to bind histone H3 peptides.

Taken together, the exclusive presence of the tower domain in KDM1A and the zinc finger motifs in KDM1B strongly suggest that these two demethylases share a related chemical mechanism, but likely participate in associations with non-identical sets of interacting partner biomolecules. These partners may influence individual catalytic activity, substrate specificity, or localization of these enzymes within genetic loci.

## CHEMICAL MECHANISM OF KDM1-FAMILY FLAVIN-DEPENDENT DEMETHYLASES

### KDM1A and KDM1B are Mechanistically Distinct from Iron(II)-Dependent Lysine-Demethylases

KDM1 family human demethylases utilize a FAD cofactor to oxidize C-N bonds with subsequent production of a demethylated lysine residue and formaldehyde byproduct.<sup>141</sup> By contrast, KDM subfamilies 2–6 (Jumonji-C domain-containing demethylases) are mechanistically distinct from the KDM1s since they utilize non-heme iron(II) and  $\alpha$ -ketoglutarate ( $\alpha$ -KG) cofactors to demethylate lysine residues with the concomitant production of succinate and formaldehyde.<sup>4</sup> KDM families 2–6 are also distinguished from KDM1A and KDM1B by their

unique ability to demethylate trimethylated lysine residues.<sup>142</sup> However, KDM1 flavoenzymes have a mechanistic requirement of a protonated iminium intermediate, achievable only with mono- and dimethylated lysines.

### Involvement of Flavin Adenine Dinucleotide as a Cofactor

Experimental and theoretical mechanistic studies have been conducted on flavin-utilizing KDMs, focusing almost exclusively on KDM1A. Mattevi and coworkers first confirmed the participation of the non-covalent FAD in the demethylation reaction using two truncated forms of KDM1A lacking the first N-terminal 157 or 184 aa.<sup>143</sup> They visualized production of the two-electron fully reduced flavin, noting the absence of intermediate one-electron reduced forms of the cofactor. This suggested that KDM1A was likely related by mechanism to the broader family of flavoenzyme oxidases that catalyze two-electron oxidation of substrates with concomitant cofactor reduction.<sup>143</sup> Once the substrate is oxidized, hydrolysis by bulk solvent of the iminium intermediate produces an unstable hemiaminal that spontaneously decomposes into formaldehyde and the mono-demethylated product. Additionally, reoxidation of the FAD cofactor by molecular oxygen produces a molar equivalent of H<sub>2</sub>O<sub>2</sub> and the fully oxidized quinone (Scheme 1).<sup>13,143</sup>

### Evidence for a Direct Hydride Transfer Mechanism

McCafferty, Fitzpatrick, and coworkers conducted a detailed investigation of the chemical mechanism of KDM1A.<sup>144,145</sup> The mechanism was examined using the effects of pH and isotopic substitution on steady-state and pre-equilibrium kinetic parameters. Using a 21-mer derived from histone H3

(H3K4me2, residues 1–21) at pH 7.5, the rate constant for flavin reduction in the transient phase,  $k_{\text{red}}$ , was shown to equal  $k_{\text{cat}}$ , establishing the reductive half-reaction as rate-limiting at physiological pH. Deuteration of the lysyl  $N^\epsilon$ -methyl groups (H3K4me2- $d_6$ ) produced identical kinetic isotope effects of  $3.2 \pm 0.1$  on the  $k_{\text{red}}$ ,  $k_{\text{cat}}$ , and  $k_{\text{cat}}/K_m$  values for the peptide, thus establishing C–H bond cleavage as rate-limiting with this substrate. The  $^D(k_{\text{cat}}/K_m)$  value for the peptide was pH-independent, suggesting that the observed value is the intrinsic deuterium kinetic isotope effect for oxidation of this substrate.<sup>146</sup> No intermediates between oxidized and reduced flavin forms were detected by stopped-flow spectroscopy, consistent with the expectation for a direct hydride transfer catalytic mechanism for amine oxidation. Additionally, the  $k_{\text{cat}}/K_m$  value for the peptide was bell-shaped, consistent with a requirement that the nitrogen at the site of oxidation be uncharged and that at least one of the other lysyl residues be charged for catalysis.<sup>144,145,147</sup>

A subsequent theoretical investigation by Karasulu and coworkers has confirmed that the H3K4me2 residue of the substrate has to be deprotonated in order for catalysis to occur, with K661 of KDM1A acting as the proton acceptor in the active site.<sup>148</sup> Additional support for a direct hydride transfer mechanism was obtained through inhibition studies with tranlycypromine (2-PCPA, Parnate, 1).<sup>118,127</sup> Parnate, which covalently inactivates KDM1A and KDM1B, is known to inactivate FAD-dependent enzymes that function through either the SET<sup>149</sup> or direct hydride transfer mechanisms.<sup>150,151</sup>

As a further point of clarification, in KDM1A, reoxidation of the FAD cofactor by  $O_2$  is a relatively fast process compared to the turnover number measured under steady-state conditions.<sup>152</sup> This entails that reoxidation is not the rate-limiting step of the chemical mechanism. Additionally, the FAD reoxidation rate is not perturbed by the presence of the product peptide<sup>152</sup> and suggests that KDM1A can remain bound to the demethylated product and possibly functions through a ternary complex kinetic mechanism.<sup>153</sup> Using computational approaches, Baron and coworkers suggest that molecular  $O_2$  diffuses through the enzyme for the purpose of reoxidation while the demethylated product remains bound.<sup>123</sup> Despite this prediction, there is no chemical requirement for the demethylated product to remain bound to the enzyme (i.e. the apparent rate of reoxidation is not faster or slower in the presence of the peptide product). Therefore, KDM1A might also function through a ‘ping-pong’ or double displacement kinetic mechanism, in which the release of the demethylated product occurs before reoxidation. Interestingly, in cell culture KDM1A removes a single methyl mark from p53-K370me2 to produce K370me1; however, *in vitro* it completely demethylates this residue.<sup>154,155</sup> Thus, one may argue that the release of the demethylated product may be influenced by coregulatory molecules or other contributing factors capable of tuning its catalytic proficiency or substrate specificity.

Using classical molecular dynamics (MD) and quantum mechanics/molecular mechanics (QM/MM) approaches, Karasulu and coworkers provided theoretical support for a hydride transfer mechanistic pathway for methyl lysine oxidation over SET, carbanion, or polar-nucleophilic mechanisms.<sup>148</sup> Proper alignment of the substrate, transition-state stabilization (due to the protein environment and favorable orbital interactions), and product stabilization via adduct formation were found to be crucial for facilitating the oxidative C–H bond cleavage.<sup>148</sup> Similarly, Truhlar and coworkers provided theoretical support for a hydride transfer mechanism, but also noted that because of the magnitude of the calculated free energy, a mechanism involving concerted transfer of a hydrogen atom and an electron could not be ruled out.<sup>156</sup> Lastly, Kong and coworkers used theoretical calculations to provide support for a hydride transfer mechanism, but also used MD to implicate a conserved Y761 and K661-water-flavin motif in orienting FAD with respect to the substrate.<sup>157</sup> Collectively, these theoretical analyses are in good agreement with the experimentally determined hydride transfer mechanism for KDM1A.<sup>148,156,157</sup>

**KDM1B Chemical Mechanism**

Tentatively, we suspect that KDM1B also adopts a similar hydride transfer chemical mechanism given the overall structural homology it maintains with the AOD of KDM1A, the conservation of active site residues, and subsequent, nearly identical, substrate specificity towards peptide substrates *in vitro*.<sup>14</sup> Additional support for this hypothesis is reflected by the similar pH-rate profile behavior of the kinetic parameters as compared to KDM1A, non-covalent nature of the FAD cofactor, and highly similar catalytic efficiency parameters, with KDM1B being slightly less efficient *in vitro*.<sup>14,134–136</sup>

### Chemical Mechanism Implications

When comparing KDM1A and KDM1B to other amine oxidases, it is important to note that the rate constant of substrate amine oxidation is 2–5 orders of magnitude slower than that of the MAOs and PAOs.<sup>158–164</sup> This suggests that KDM1s likely evolved for substrate specificity rather than catalytic proficiency. Given the physiological role of KDM1 demethylases in the regulation of gene expression, high catalytic efficiency, which is necessary for metabolic enzymes to maintain balance among metabolic pathways, would be much less critical than very high specificity.

## SUBSTRATE SPECIFICITY

### Specificity for Histone Substrates

Shi and coworkers first reported that KDM1A was capable of demethylating methyllysine peptides derived from the highly conserved N-terminus of histone H3, as well as full-length H3 *in vitro*.<sup>13</sup> No cross-reactivity for polyamine substrates was observed, despite the similarity of KDM1A to the PAO superfamily.<sup>13</sup> They also reported that KDM1A is specific for histone H3K4me1/2, as no other methyllysine sites were processed.<sup>13</sup> Forneris and coworkers demonstrated that histone H3 tail peptides greater than 16 aa in length are necessary to achieve demethylase efficiency *in vitro*. Additionally, they revealed that KDM1A demethylated H3K4me1 and H3K4me2 with similar kinetic parameters *in vitro*, illustrating a lack of a strong kinetic preference for either substrate.<sup>147</sup>

Mattevi and coworkers have also examined the contribution of residues within the H3 N-terminal tail to the efficiency of KDM1A demethylase activity, as well as the effects of epigenetic PTMs within this sequence.<sup>144,147,152</sup> For example, Mattevi showed that methylation of H3K9 does not affect enzyme catalysis, yet acetylation at H3K9 increases the  $K_m$  6-fold for H3 peptide substrates methylated on K4. Similarly, phosphorylation of H3S9 abolishes demethylase activity, suggesting that KDM1A 'reads' PTMs along the histone tail.<sup>147,152</sup> It was also proposed that electrostatic interactions likely contribute significantly to substrate binding, since demethylation activity was shown to be sensitive to ionic strength as well as hyperacetylation *in vitro*.<sup>147,152</sup> Additionally, Mattevi showed that unmethylated H3-derived product peptides exhibit inhibition, which may serve to regulate KDM1A activity or localization.<sup>147</sup> Parallel experiments conducted with KDM1B revealed a similar substrate specificity profile,<sup>14</sup> which was anticipated given the significant active site structural similarity shared between the two enzymes in the AOD.<sup>112,134,136</sup>

While the ability of both KDM1A and KDM1B to demethylate H3K4me1/2 is quite striking, both enzymes do not demethylate H3K9me1/2 peptides *in vitro*.<sup>13,14,147</sup> Despite lacking this activity towards peptide substrates, it has been suggested that KDM1A association with AR shifts its substrate specificity to H3K9me1/2 demethylation.<sup>84</sup> However, the mechanisms behind these observations are not yet clear. A simple explanation is that AR association with KDM1A physically occludes its access to H3K4 or triggers recruitment of another demethylase, such as the H3K9me2/3-specific KDM4C (JMJD2C) demethylase.<sup>165</sup> Alternatively, modifications on surrounding histone residues,<sup>166</sup> a conformational change induced by a protein-protein interaction, or a PTM to KDM1A could potentiate this switch in specificity.<sup>167</sup>

As a member of the flavin-dependent oxidases, the KDM1 demethylases exhibit a strict requirement for proper substrate positioning in relation to the FAD cofactor to promote catalysis.<sup>129</sup> However, KDM1s differ from other amine oxidases because their active sites are significantly expanded in order to accommodate the N-terminal residues of the histone H3 peptide (i.e. 1,245 Å<sup>3</sup> in KDM1A).<sup>112</sup> Within KDM1A, for example, there are four major invaginations lined with distinct groupings of residues to form complimentary interactions with H3 substrate side chains as well as for recognition of PTMs.<sup>111</sup> No structural features within the active site of either enzyme have been found that might suggest that the methylation state of H3K4 can be distinguished sterically or electronically, and discrimination against H3K4me3 substrates is due to the inherent chemical mechanism of the enzymes.<sup>111,134</sup> Although more than 16 N-terminal residues of H3 are required for efficient catalysis, a significant portion of the C-terminus of substrates likely extends from the active site and potentially interact along a cleft formed at the interface of the AOD and SWIRM domain.<sup>111,112,115,141</sup> Mutations of residues in this cleft in KDM1A abolish or abrogate demethylation activity, suggesting that interactions with substrates within this region may provide an additional specificity determinant.<sup>111</sup> Additionally, surface plasmon resonance interaction studies have demonstrated that the SWIRM domain of KDM1A interacts with H3-derived peptides.<sup>132</sup> In KDM1B, the surface landscape of this region is quite different and binds the coregulatory protein Nuclear Protein 60kDa/Glyoxylate Reductase 1 Homolog (NPAC/GLYR1).<sup>135,136</sup>

In order to dissect the molecular basis of KDM1A and KDM1B substrate specificity, several three-dimensional structures have been determined of enzyme-substrate like complexes where short peptides occupy the active site in two general conformations (Figure 2).<sup>116,117,123,134–136</sup> The structure of KDM1A bound to a substrate-like peptide inhibitor containing a *N*-methylpropargyl derivatized lysine residue at position four revealed density for residues 1–7 of the peptide and adopted an unusually compacted backbone with three consecutive  $\gamma$ -turns (Figure 2a).<sup>116</sup> Subsequently, a H3 peptide inhibitor containing a K4M mutation (H3K4M, pK4M) was co-crystallized with KDM1A and CoREST,<sup>117</sup> which revealed density for the first 16 residues of the peptide with the first five adopting an  $\alpha$ -helical conformation (Figure 2b). It is important to note that the C-termini of each of these peptides points in opposing directions upon exiting the active site. Additionally, the N-terminal region of SNAI1 and related peptide derivatives have been co-crystallized with KDM1A and display a nearly identical conformation to that of the H3K4M peptide (Figure 2c), thus suggesting some form of molecular mimicry

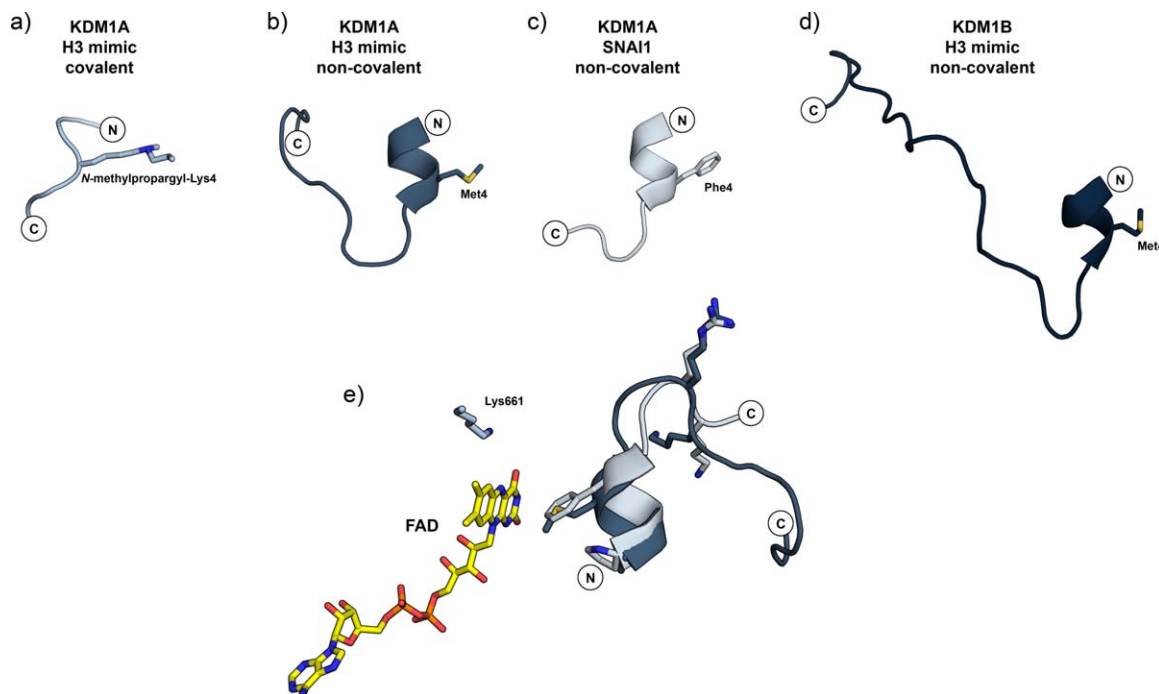


**FIGURE 2** Overview of structural conformations of bound peptide ligands. (a) Conformation of covalently bound N-methylpropargyl-Lys4 H3 peptide in KDM1A (PDB 2UXN). (b) Conformation of non-covalently bound H3K4M (pK4M) in KDM1A (PDB 2V1D). (c) Conformation of non-covalently bound SNAI1 in KDM1A (PDB 2Y48). (d) Conformation of non-covalently bound pK4M in KDM1B (PDB 4HSU). (e) Structural alignment of pK4M and SNAI1 (b and c, respectively) bound to KDM1A, illustrating the overall fold conservation of the peptides and relative position of the non-covalent FAD and active-site Lys661.

in KDM1A inhibition (Figure 2e).<sup>123,124</sup> Finally, when KDM1B was co-crystallized in the presence of the same H3K4M peptide, it exhibited a similar binding conformation to that found in KDM1A (Figure 2d).<sup>134–136</sup> Interestingly, elucidation of the structure of KDM1B bound to the cofactor NPAC/GLYR1 revealed a secondary binding site occupied by the C-terminal region of the H3 peptide tail.<sup>135</sup>

Due to the above conformational differences and identification of the folate binding site within the KDM1A active site, there is some controversy as to which binding mode positions

the K4 residue in the proper geometry that allows catalysis to proceed.<sup>4,117,126,167</sup> Despite this discrepancy, both conformations reveal that the N-terminus of the peptides bind in an anionic pocket with a maximum of three residues N-terminal to the methyllysine residue.<sup>4,141</sup> Additionally, both conformations make extensive contacts with a large set of conserved, negatively charged residues in the active site cavity.<sup>116,117</sup> Overall, these structures exemplify the apparent plasticity of the active sites of KDM1A and KDM1B and only hint at the richness of substrate specificity mechanisms available to this enzyme class.

**Table I** KDM1 Demethylase Family

Name	Synonyms	Histone Substrates	Non-Histone Substrates
KDM1A	LSD1, AOF2, BHC110, KIAA0601	H3K4me1/2, H3K9me1/2	p53 (K370), DNMT1 (K1096), <sup>a</sup> E2F1 (K185), ER $\alpha$ (K266), <sup>b</sup> HIV Tat (K51), HSP90 (K615h/K614m), <sup>c,d</sup> MTA1 (K532), MYPT1 (K442), STAT3 (K140)
KDM1B	LSD2, AOF1, C6orf193	H3K4me1/2	

<sup>a</sup> Not verified to be major site of demethylation.

<sup>b</sup> Inferred site of demethylation, not confirmed.

<sup>c</sup> Confirmed *in vitro*.

<sup>d</sup> Numbering system conventions between *H. sapiens* (K615h) and *M. musculus* (K614m).

Based on these data, it is speculated that KDM1A and KDM1B can recognize and demethylate different substrates in vastly different binding modes.<sup>4</sup>

### Specificity for Non-Histone Substrates

In addition to histone H3, non-histone proteins have been shown to be substrates for KDM1 family enzymes. KDM1A has been shown to demethylate p53, DNMT1, E2F1, MYPT1, STAT3, HIV Tat, HSP90, MTA1, and potentially ER $\alpha$  (Table I).<sup>103,154,155,168–174</sup> To our knowledge, no non-histone substrates have yet been identified for KDM1B; however, we suspect that future work will also define multiple, albeit different substrates and roles for this enzyme. The existence of multiple non-histone substrates for KDM1A has strong implications in apoptosis, cell cycle progression, and the transcriptional activation or repression of associated genes.

The first non-histone substrate of KDM1A identified was the tumor-suppressor p53.<sup>154,155</sup> Like histone proteins, p53 is subject to regulation by various PTMs. In particular, dimethylation of p53 at K370 (K370me<sub>2</sub>) promotes its association with 53BP1 (p53-binding protein 1), a protein that coactivates p53 transcriptional programs.<sup>175–177</sup> Although *in vitro* KDM1A completely removes dimethylation at K370, in cell culture it preferentially removes a single methylation mark, generating the monomethylated species. This mark abrogates transcription through modulating p53-DNA interactions that subsequently repress the pro-apoptotic functions of p53. Further complicating this interaction, Barton and coworkers observed that KDM1A localizes only to genes where p53 represses transcription.<sup>154</sup> This suggests some type of inherent regulation of the KDM1A-p53 interaction and may ensure repression of desired target genes.<sup>178</sup>

In contrast, in p53-deficient tumors, Set7/9 and KDM1A regulate DNA damage-induced cell death in a manner opposite to that observed in p53<sup>+/+</sup> cells, via modulation of the stability of the transcription factor E2F1.<sup>169</sup> Kontaki and Talianidis illustrated that Set7/9 methylates E2F1 at K185 and prevents E2F1 accumulation during DNA damage and subsequent activation of its pro-apoptotic target gene, p73. This PTM is removed by KDM1A, and is required for E2F1 stabilization and downstream pro-apoptotic function. Interestingly, the molecular mechanism of these events involves crosstalk between lysine methylation and other PTMs that affect E2F1 stability and turnover.

Recently, Sakane and coworkers have identified KDM1A as a HIV Tat K51me<sub>1</sub>-specific demethylase that is required for the activation of HIV transcription in latently infected T cells.<sup>103</sup> The RNA-binding domain of Tat is a known region containing PTMs<sup>179</sup> in which K51 is methylated by Set7/9.<sup>180</sup> This PTM

corresponds to an early event in the Tat transactivation cycle and strengthens the interaction of Tat with TAR RNA.<sup>180</sup> On the other hand, acetylation of K50 is mediated by p300/KAT3B, which dissociates the complex formed by Tat, TAR RNA, and the cyclin T1 subunit of the positive transcription elongation factor b (P-TEFb).<sup>181,182</sup> Subsequent to K50 acetylation, the histone acetyltransferase, PCAF/KAT2B, is recruited to the elongating RNA polymerase II complex.<sup>183–185</sup> Interestingly, the association of the KDM1A/CoREST complex with the HIV promoter subsequently activated Tat transcriptional activity in a K51-dependent manner. In accordance with Tat transcriptional activity, shRNAs directed at KDM1A or its inhibition by phenelzine suppressed the activation of HIV transcription in latently infected cells. The study again illustrates the dual nature of KDM1A and its ability to function as both a transcriptional suppressor and activator depending on the context of the substrate and interacting partners.

In addition to p53 and E2F1, Chen and coworkers have identified DNA methyltransferase 1 (DNMT1) as a novel substrate of KDM1A.<sup>168</sup> Targeted deletion of the gene encoding KDM1A (*aof2*) in mouse embryonic stem cells induces the progressive loss of DNA methylation in addition to an increase in the methylation of DNMT1 and a decrease in the DNMT1 protein level. Chen and coworkers illustrated that Set7/9 methylation of K1096 of DNMT1 can be reversed by KDM1A *in vitro*. Despite this evidence, it remains to be determined if K1096 is the major targeted site of KDM1A, since DNMT1 is methylated on multiple sites *in vivo*. By acting on and demethylating DNMT1, KDM1A may play a role in the coordination of DNA and histone methylation.

In another example, like E2F1, the transcription factor STAT3 is subject to PTMs that modulate downstream events in response to different cytokines and growth factors.<sup>186</sup> Following phosphorylation, STAT3 is methylated on K140 by SET7/9 and subsequently demethylated by KDM1A when it is bound to a subset of promoters that it activates.<sup>171</sup> Timing for this process occurs in an ordered sequence on the *SOC3* promoter, illustrating the underlying temporal and spatial control of the methylation and demethylation events. The authors conclude that lysine methylation of promoter-bound STAT3 leads to biologically important downregulation of the dependent responses. This work illustrates the ability of methyltransferases and demethylases to control the methylation status of a transcription factor in a promoter-specific manner and provide a way to modulate the time of residence and promoter occupancy of the protein. Additionally, the transcription factors or the proteins recruited during these events may also provide a docking site for other proteins to carry out important functions, a role suggested for KDM1A by Mattevi and coworkers.<sup>152</sup>

Myosin phosphatase target subunit 1 (MYPT1) is an example of a KDM1A non-histone substrate that has a downstream effect on cell cycle progression.<sup>170</sup> MYPT1, a known regulator of phosphorylation of the transcription factor retinoblastoma protein 1 (RB1), is methylated *in vitro* and in cell culture by SET7/9 and subsequently demethylated by KDM1A, in which K442 is the target residue. The methylation status of MYPT1 influences the affinity the protein maintains for the ubiquitin-proteasome pathway and subsequent protein turnover. Interestingly, overexpression of KDM1A, which is prevalent in many cancer subtypes (see above), could activate RB1 phosphorylation by inducing a destabilization of the MYPT1 protein. Subsequently, the release of E2F could activate transcription of genes required for S phase to enhance cell cycle progression.

An extremely unique target of KDM1A is metastatic tumor antigen 1 (MTA1), a core subunit of the NURD complex (discussed in detail later). Interestingly, it is the only known dual function coregulator with an expected corepressor activity, but unusual ability to also stimulate transcription.<sup>187,188</sup> MTA1 is mono-methylated at residue K532 by G9a (EHMT2) and demethylated by KDM1A.<sup>173</sup> This demethylation event is required for the stable interaction of the two proteins (i.e. KDM1A and MTA1), but also represents a molecular switch, as the methylation state of MTA1 potentiates the nucleation of either the NuRD or NURF complexes. Reconstitution of either complex occurs in a cyclical manner that alternates between opposing biological functions. This activity further compounds the role of KDM1A as both a transcriptional activator and repressor via the demethylation of a non-histone substrates and modulation of subsequent downstream targets.

The least well characterized KDM1A non-histone substrates are HSP90 and ER $\alpha$ .<sup>172,174</sup> Using proteomics and biochemical approaches, Abu-Farha and colleagues determined that HSP90 is methylated at K209 and K615 by SMYD2,<sup>172</sup> the latter of which is present in the dimerization domain (DD) of HSP90. Coincidentally HOP, a co-chaperone known to interact with the DD,<sup>189</sup> blocks methylation at K615 *in vitro*. Although demethylation at this residue was performed *in vitro* by KDM1A, it has not yet been demonstrated *in vivo*. Furthermore, the methylation status of K615 has been implicated in the ability of HSP90 to associate with the sarcomeric protein titin, thereby affecting the maintenance and function of skeletal muscle.<sup>190,191</sup> The role of HSP90 methylation status may also have potential, yet undiscovered, significance in carcinoma maintenance.<sup>192,193</sup> On the other hand, the direct demethylation of ER $\alpha$  at K266 by KDM1A has not been explicitly demonstrated. However, KDM1A seems to negatively regulate the methylation status at this residue.<sup>174</sup> It is interesting to suspect that the presence of KDM1A on estrogen responsive elements (EREs) has a dual role in the demethylation of H3K9me2 and

ER $\alpha$ ,<sup>194</sup> or possibly uses this interaction to recruit an H3K9-selective demethylase enzyme to perform this function.

Interestingly, either SMYD2 (KMT3C) or SET7/9 (KMT7) methylates all but one of the current non-histone substrates that have been identified for KDM1A. In the future it will be informative to investigate more non-histone substrates of KDM1A and KDM1B to determine if they too maintain this same relationship with specific MTases. Such analyses may provide insight into the interplay between ‘writers’ and ‘erasers’ of PTMs *in vivo*.

## INHIBITION OF FLAVIN-DEPENDENT KDM1 DEMETHYLASES

### Discovery and Optimization of Mechanism-Based Inhibitors

The discovery and development of KDM1 family inhibitors has been the subject of several recent comprehensive reviews; therefore, an abbreviated overview of KDM1 inhibitors is presented, which includes many recent developments.<sup>15,21,69,142,195–199</sup> Motivated by the relationship between the AOD of KDM1A to that of MAO-A/B and PAO, the first KDM1A inhibitors were discovered by McCafferty and coworkers.<sup>200</sup> Through screening a focused group of irreversible and reversible amine oxidase inhibitors, tranlycypromine (*trans*-2-phenylcyclopropylamine, 2-PCPA, Parnate<sup>TM</sup>, **1**) was found to exhibit the highest KDM1A inhibitory activity towards methylated bulk histones as well as methylated nucleosomal substrates *in vitro*. Treatment of P19 embryonal carcinoma cells with **1** resulted in the global increase of H3K4 methylation as well as transcriptional derepression of two KDM1A target genes, *Egr1* and the pluripotent stem cell marker *Oct4*. This was the first example of small molecule inhibition of histone demethylation and interruption of transcriptional programs regulated by KDM1A.<sup>200</sup>

In a subsequent study, our group determined that tranlycypromine was a mechanism-based inactivator of KDM1A, forming a covalent adduct with the FAD cofactor and demonstrating inactivation kinetic parameters of  $K_i = 242 \mu\text{M}$  and a  $k_{\text{inact}} = 0.0106 \text{ s}^{-1}$ .<sup>127</sup> Soon after, the laboratories of Cole,<sup>118</sup> Yokohama,<sup>119,122</sup> and Mattevi<sup>121</sup> provided additional support for this inhibitory mechanism, including defining the structure of the tranlycypromine-KDM1A adduct using X-ray methods, which revealed the N5 of the FAD isoalloxazine ring as the site of covalent attachment of the inhibitor.

In addition to tranlycypromine (**1**), our study revealed less potent KDM1A inhibition from the hydrazine-containing phenelzine (**2**) and the propargylamines, represented by pargyline

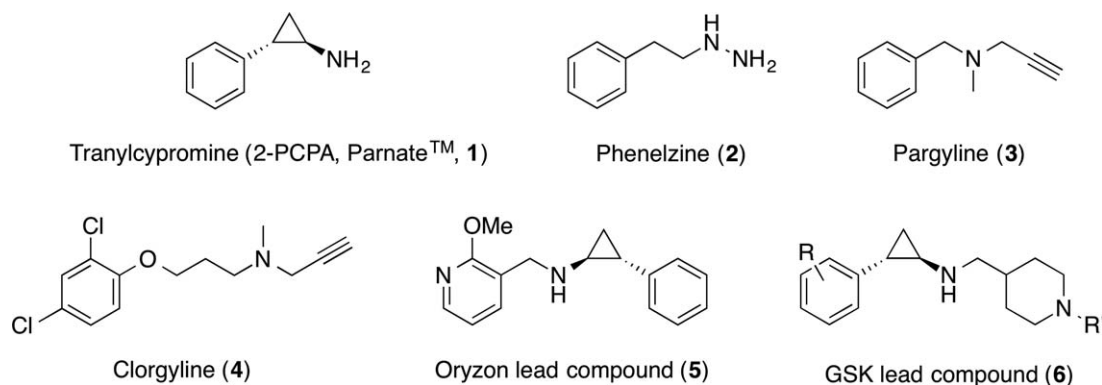


FIGURE 3 Chemical structures of representative mechanism-based, irreversible inhibitors.

(**3**) and clorgyline (**4**) (Figure 3).<sup>200</sup> KDM1A inhibitors **1** and **2** achieved *complete* inhibition *in vitro* at significantly lower concentrations than are physiologically relevant.<sup>127,201</sup> However, propargylamines were not inhibitory at 5 mM, and only *partial* inhibition of KDM1A was observed at 30 mM.<sup>147,200,201</sup> Exposure of cells to such non-physiologically relevant concentrations of **3** causes inhibition of proliferation and alteration of transcriptional programs via mechanisms that do not necessarily involve KDM1A activity.<sup>72</sup> As such, one should approach the use of members of this inhibitor class with caution when attempting to attribute phenotypic effects exclusively to KDM1A inhibition.

Analysis of the crystal structures of KDM1A, MAOs, and PAOs, lead our group to conclude that KDM1A may be distinguished from related amine oxidases since MAO-A/B and PAO have significantly restricted active site volume when compared to KDM1A. As such, we designed, synthesized, and characterized analogues of **1** for the purpose of increasing potency and specificity towards KDM1A through aromatic substitutions and heteroaromatic exchanges.<sup>202</sup> Within this initial group of inhibitors, improved selectivity and potency was observed, and these analogues were subsequently utilized to probe the role of KDM1A activity in estrogen receptor signaling.<sup>72</sup> Since that time, numerous research groups, in addition to our own, have further optimized the potency and selectivity of arylcyclopropylamines for KDM1A inhibition.<sup>121,122,196,203–205</sup>

In fact, several members of the arylcyclopropylamine inhibitor class have achieved pre-clinical and clinical development status industrially. For example, Oryzon researchers reported the discovery of KDM1A inhibitor **5** that exhibited a 100-fold improved potency over the parent inhibitor **1**. In a recent review, it was reported that Oryzon optimized **5** to produce ORY-1001 (structure not yet released), which possesses 1000-fold greater potency than **1** and is highly selective for KDM1A over KDM1B, MAO-A/B, IL4I1, and SMOX (SMO/PAO/

PAO-1/PAOH1).<sup>198</sup> Additionally, GlaxoSmithKline recently reported the discovery, development, and optimization of arylcyclopropylamine-based KDM1A inhibitors (lead compound, **6**) that achieve exclusive selectivity for KDM1A and also exhibit good oral bioavailability.<sup>206</sup>

### Peptide-Based Inhibitors

Protein-protein and protein-ligand interactions provide auspicious starting points for the development of high affinity peptide and peptidomimetic inhibitors. Although this class of molecules has traditionally suffered from poor stability and cell permeability, modifications to the native peptide structure can greatly increase their pharmacokinetic properties and therapeutic value. This inhibition strategy is especially appealing in regard to KDM1A, as it is involved in multiprotein complexes, several of which are beginning to be biophysically characterized in detail (see below). Here we outline the existing peptide-based active site inhibitors of the KDM1 class demethylases with the hope that they will catalyze the development of peptide-based inhibitors that target a wider range of KDM1 interfaces.

In addition to the small molecules discussed above, unmethylated product peptides (**7**) of the KDM1A reaction as well as a related substrate-like inhibitor containing a methionine point mutant (**8**; H3K4M; pK4M) have been shown to be competitive inhibitors of KDM1A with enhanced binding over methylated substrates.<sup>117,147</sup> Recently, Kumarasignhe and Woster have also developed a series of cyclic peptides based on the substrate-like inhibitor pK4M that were more hydrolytically stable than the acyclic analogues. Additionally, moderate anti-tumor effects were observed in MCF7 and Calu-6 cancer cell lines.<sup>207</sup> On the other hand, Mattevi and coworkers have developed a series of short peptide reversible inhibitors based on the N-terminal region of SNAI1, some of which exhibited anti-

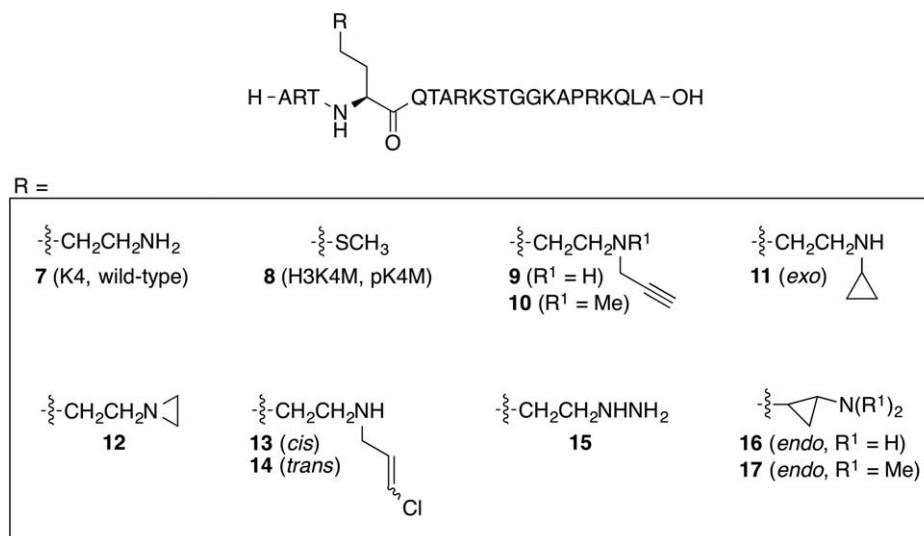


FIGURE 4 Structures of substrate-based peptide inhibitors.

proliferative activity.<sup>123,124</sup> Both classes of peptides show promise and may serve to lay the foundation for the development of peptidomimetic small molecule inhibitors.

In addition to reversible peptide inhibitors, several groups have also adopted an inhibitor design strategy whereby flavin-reactive moieties are grafted as ‘warheads’ onto peptides derived from histone H3, including reactive *N*-propargyl, -cyclopropyl, -aziridine, -phenelzine, -vinylchloride, or -tranylcypromine substituents (compounds **9–17**; Figure 4).<sup>201,208,209</sup> Within this series, phenelzine-containing H3K4-derived peptide (**15**) exhibited the most potent inhibitory activity *in vitro*;<sup>201</sup> however, none of these compounds exhibited significant KDM1A inhibitor activity in cellular models, presumably due to poor cellular uptake or susceptibility to proteolytic degradation.<sup>210</sup> Additionally, although alone propargylamine is a very poor inhibitor of KDM1A,<sup>147,200,201</sup> presentation of the propargylamine group as a pendant substituent within a peptide derived from histone H3 (**9**, **10**) significantly enhanced its activity as a mechanism-based inactivator (Figure 4).<sup>116,201,208</sup>

### Emerging KDM1A Inhibitor Classes

Recently, Jung and coworkers have reported the development of lysine mimetics that possess a propargyl warhead for covalent modification of KDM1A (**18,19**; Figure 5).<sup>211</sup> Although these compounds were inhibitory at low micromolar concentrations, they did not exhibit selectivity over the MAOs and PAO in this first generation series. This class of molecules may likely gain selectivity through future optimization efforts.

Similarly, Suzuki and coworkers have reported a series of KDM1A inactivators in which tranylcypromine (**1**) is coupled

to a lysine carrier moiety at the nitrogen atom (**20**; Figure 5).<sup>212,213</sup> The nonpeptidic small molecules selectively and efficiently delivered **1** to the KDM1A active site creating the inactivated, FAD-adduct in a time-dependent manner. Additionally, the molecules exhibited potent cell growth inhibitory activities against cancer cell lines. Together, the high potency and selectivity towards KDM1A allows this class of molecules to be considered good candidates for further optimization and implementation as chemical biology probes.

The considerable homology KDM1A shares with PAOs, including spermine oxidase (SMOX/SMO/PAO/PAO-1/PAOH1) and others, spurred Woster and Casero to develop a class of reversible KDM1A antagonists capable of derepressing tumor suppressor genes, as well as inducing other beneficial anticancer activities. The first class of polyamine analogues contained bisguanide and bisguanidine functional groups (**21**, **22**) that inhibited KDM1A activity in cell and animal models of cancer.<sup>214–216</sup> Since that time, they have expanded the KDM1A inhibitor repertoire to also include (bis)urea and (bis)thiourea analogues (**23–25**) that have exhibited excellent potency, cell permeability, and selectivity for KDM1A inhibition.<sup>217</sup> In a recent example,<sup>66</sup> the polyamine (1,15-*bis*(*N*<sup>5</sup>-[3,3-(diphenyl)propyl]-*N*<sup>1</sup>-biguanido)-4,12-diazapentadecane) (**22**; Figure 6) induced cytotoxicity and inhibited KDM1A activity in human AML cell lines. Exposure to this agent increased global levels of H3K4me1/2 and exhibited re-expression of the tumor suppressor E-cadherin.

Polyamine analogues have enormous potential as therapeutics for many classes of human cancers, including breast, prostate, and AML. Also, there is potential for these molecules as probes for understanding the contribution of KDM1A to

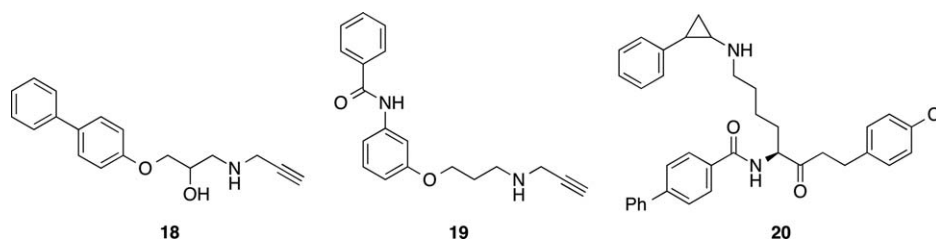


**FIGURE 5** Structures of nonpeptidic, warhead small molecule inhibitors that are substrate derived mimics.

specific epigenetic demethylation events that contribute to cancer pathobiology. As such, the discovery and development of polyamine analogues as reversible KDM1A inhibitors has been the subject of several recent seminal reviews.<sup>19,197,218–222</sup>

Merging key pharmacophoric features of reported KDM1A inhibitors, Dulla and coworkers recently reported the development of 3-amino/guanidine substituted phenyl oxazole-containing inhibitors.<sup>223</sup> Following treatment of cultured cells with nanomolar inhibitor concentrations, viability decreased as compared to the low micromolar range observed for inhibition of KDM1A *in vitro*. Although the basis of the enhanced reactivity in cell culture and the degree of KDM1A selectivity remains to be fully explored, one inhibitor (**26**; Figure 7) avoided zebrafish embryo apoptosis and toxicity and may constitute a lead for further optimization. Additionally, it remains to be determined if this class is selective for KDM1A since these compounds were designed based on existing broad spectrum amine oxidase inhibitors.

Other examples of bifunctional KDM1A inhibitors have also recently been described. First, Zheng and coworkers reported a novel triazole-dithiocarbamate scaffold that inhibits KDM1A more potently than **1**.<sup>54</sup> The 1,2,3-triazole moiety within these inhibitors is readily accessible through the Cu(I)-catalyzed Huisgen 1,3-dipolar cycloaddition of azides with

alkynes (i.e. Sharpless “click” chemistry).<sup>224,225</sup> Additionally, this pharmacophore has been shown to possess numerous biological activities,<sup>226,227</sup> including inhibitory activity towards MAO-A.<sup>228,229</sup> On the other hand, the dithiocarbamate pharmacophore was chosen for its intrinsic inhibitory activity against fungi, bacteria, and malignant cancer.<sup>230–232</sup> One compound synthesized in the series (**27**; Figure 7) effectively reduced tumor growth of human gastric cancer cells *in vivo*.

In another example, Rotili and coworkers synthesized hybrid KDM1A/JmjC bifunctional inhibitors. This was achieved by coupling the skeleton of the KDM1A inhibitor tranlycypromine (**1**), with 4-carboxy-4'-carbomethoxy-2,2'-bipyridine or 5-carboxy-8-hydroxyquinoline chelating groups that were developed as competitive inhibitors for the iron(II)/ $\alpha$ -KG-dependent JmjC demethylases.<sup>86</sup> Two compounds in this series (**28,29**; Figure 7) increase H3K4 and H3K9 methylation levels in cells and cause growth arrest and substantial apoptosis in LNCaP prostate and HCT116 colon cancer cells.<sup>86</sup>

Fortuitously, Yang and coworkers decided to test natural polyphenols as potential inhibitors of KDM1A.<sup>233</sup> Dietary polyphenols are known to have beneficial effects against diabetes, cancer, and cardiovascular disease, and exposure has been linked to both antioxidant activity and modulation of signaling pathways.<sup>234–236</sup> Yang and coworkers demonstrated that resveratrol (**30**), curcumin (**31**), and quercetin (**32**) displayed inhibitory activity against KDM1A *in vitro*, which was independent of their antioxidant properties (Figure 8). However, since quercetin forms colloid-like aggregates in aqueous solution it may inhibit KDM1A *in vitro* non-specifically due to aggregate formation.<sup>237</sup> Based on this precedence, further insight into its mode of action as well as structurally-related compounds is needed.

Screening has also been a means for identifying novel scaffolds against KDM1A and KDM1B and has yielded several anti-KDM1A inhibitor candidates. By combining protein structure similarity clustering and *in vitro* compound screening, Beuttner and coworkers discovered the KDM1A inhibitory activity of the  $\gamma$ -pyrone, Namoline, *in vivo* and *in vitro* (**33**, Figure 9).<sup>85</sup> The IC<sub>50</sub> of this compound was reported to be 51  $\mu$ M against KDM1A and was fully reversible. Namoline

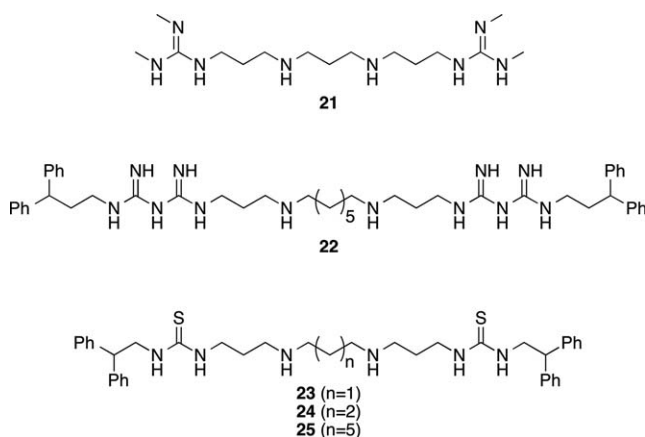


**FIGURE 6** Structures of bisguanide and bisguanidine polyamine inhibitors.

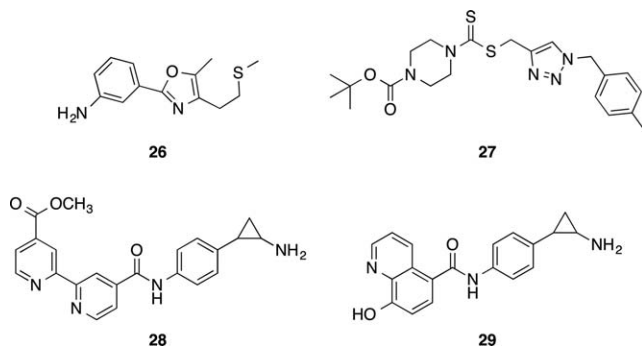


**FIGURE 7** Structures of bifunctional small molecule inhibitors that incorporate multiple pharmacophores.

administration to prostate cancer cells led to silencing of AR-regulated gene expression and impairment of androgen-dependent proliferation *in vitro* and *in vivo*. Namoline may be a promising starting point (i.e. core structure) for the development of therapeutics to treat androgen-dependent prostate cancer.

On the other hand, Sharma and coworkers recently reported a structure-based virtual screen of a compound library containing ~2 million small molecules against KDM1A.<sup>238</sup> Computational docking and scoring followed by biochemical screening led to the identification of a novel *N*'-(1-phenylethylidene)-benzohydrazide series of inhibitors. Hit-to-lead optimization and structure-activity relationship studies aided the discovery of a specific, reversible inhibitor (**34**) of KDM1A with a reported  $K_i$  of 31 nM. Compound **34** inhibits proliferation and survival in breast and colorectal cancer cell lines.

Zha and coworkers have also garnered recent success with a pharmacophore-based virtual screening approach to identify novel inhibitors of KDM1A.<sup>239</sup> Using a moderate database of a commercial compound library and molecular docking tools, the group was able to identify nine candidate KDM1A inhibitors that lacked structural similarity to previously identified inhibitor classes. These compounds were subsequently tested *in vitro* against KDM1A and showed  $IC_{50}$  values in the low micromolar range. One compound, XZ09 (**35**), which showed the highest potency against KDM1A, was also tested versus MAO-A/B and showed moderate selectivity. The XZ09 core structure represents a lead compound that, with further modification, could serve as another tool in probing KDM1A function.

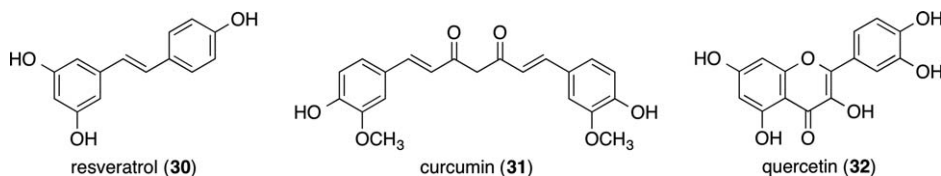


**FIGURE 8** Natural polyphenol inhibitors.

Finally, Cole and coworkers recently reported the design, synthesis, and characterization of the KDM1A inhibitory properties of phenelzine analogues.<sup>240</sup> Bizine (**36**; Figure 10), a novel phenylzine analogue containing a phenyl-butryrylamide appendage, exhibited good *in vitro* activity against KDM1A ( $K_i = 0.06 \mu\text{M}$ ;  $k_{\text{inact}} = 0.15 \text{ min}^{-1}$ ;  $k_{\text{inact}}/K_i = 2.5 \mu\text{M}^{-1} \text{ min}^{-1}$ ) and was selective versus MAO-A/B (26- and 60-fold, respectively) and KDM1B (>100-fold). Bizine exhibited anti-proliferative effects in some cancer cells and was found to be effective at modulating bulk histone methylation. Additionally, these compounds synergistically inhibited cellular proliferation in combination with several histone deacetylase inhibitors. Interestingly, neurons exposed to oxidative stress were protected by the presence of bizine.

## FUNCTIONALLY IMPORTANT INTERACTIONS OF KDM1A AND KDM1B DEMETHYLASES WITH BIOMOLECULES

KDM1 family demethylases typically operate as catalytic subunits within specific stable complexes formed with additional biomolecules and enzymes that perform coregulatory or scaffolding functions. Such interactions link the catalytic activity of KDM1s to distinctive biological occupations, and have been shown to influence the degree of catalytic activity, substrate specificity, and/or localization of these enzymes within chromatin.

### Interaction of KDM1A with CoREST and CoREST-like Proteins in Heteromeric Complexes

CoREST is one of the earliest identified interaction partners of KDM1A and this protein complex assembly (i.e. KDM1A/CoREST complex) is frequently found within several distinct, larger multi-protein complexes.<sup>8,9,34,241–243</sup> Most likely due to this early association, the structural and functional characterization of this particular interaction far outstrips that available for any other KDM1A interaction. CoREST consists of an N-terminal ELM2 domain followed by dual SANT domains (SANT1 and SANT2) with an intervening region colloquially known as the linker domain (Figure 11f). The N-terminal region spanning the ELM2 domain and first SANT domain have been mapped as a binding region for HDAC1,<sup>8</sup> and a

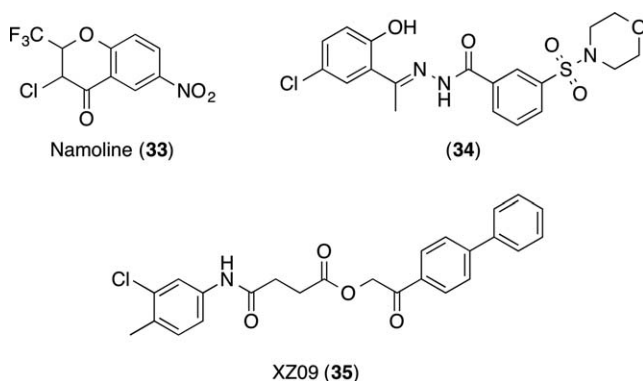


**FIGURE 9** Structures of screen identified and validated inhibitors.

crystal structure of HDAC1 bound to a similar ELM2/SANT region in the CoREST-related protein, MTA1, has recently been reported.<sup>244</sup> Furthermore, Shi and colleagues first mapped the interaction of KDM1A to the CoREST linker domain,<sup>34</sup> indicating that CoREST likely acts as a scaffolding protein that joins deacetylase and demethylase activity into a single catalytic sub-complex. The CoREST SANT2 domain, and possibly the SANT1 domain, has been shown to facilitate demethylation of nucleosomes, presumably by acting as a bridge between KDM1A and its substrate.<sup>34,115,242</sup> A similar mechanism is observed in the SMRT protein, where the C-terminal SANT2 domain stabilizes the protein complex on chromatin by interacting with histone tails.<sup>245</sup> As a point of further clarification, Yang and coworkers highlighted the similarity between the SANT2 domains of CoREST and the viral DNA-binding protein v-Myb, and demonstrated that an isolated CoREST SANT2 domain binds directly to DNA with modest affinity ( $K_d = 84 \mu\text{M}$ ).<sup>115</sup>

Seeking more detailed molecular characterization, Yang and colleagues reported the first crystal structure of KDM1A in complex with the linker and SANT2 domains of CoREST in 2006 (Figure 11a).<sup>115</sup> In this model, the CoREST linker domain forms an L-shaped helical conformation, with the short helix contacting the base of the KDM1A tower domain, the longer helix extending up the T $\alpha$ B helix, and the SANT2 domain contacting the top turn of the tower (Figure 11a, insert). These interactions are mainly hydrophobic in nature, although a few electrostatic interactions may facilitate proper alignment of the CoREST linker with the KDM1A tower domain.<sup>115,130</sup> A second crystal structure of KDM1A and CoREST with a histone substrate-like peptide bound (pK4M) showed little overall conformational change as compared to the non-peptide-bound structure.<sup>117</sup> However, the model does illustrate that the L-shaped short arm formed by the CoREST linker may have an indirect effect on substrate binding by stabilizing the helix formed from KDM1A residues 372–395.

As noted above, although the CoREST SANT2 domain contacts the KDM1A tower in reported crystal structures,<sup>115,117</sup> McCafferty and coworkers have demonstrated that the CoREST linker domain is chiefly responsible for high affinity binding with KDM1A.<sup>130</sup> Specifically, a CoREST fragment consisting of the linker domain (residues 293–380) exhibits low nanomolar binding affinity towards KDM1A ( $K_d = 7.78 \text{ nM}$ ), while inclusion of the SANT2 domain does not substantially alter binding affinity and in isolation lacks significant affinity towards KDM1A.<sup>130</sup> Our group also used mutagenesis and isothermal titration calorimetry to reveal that the energy of binding along the CoREST/KDM1A helix-helix interface is not concentrated into “hotspots,” but is instead distributed almost uniformly along the interaction interface.<sup>246</sup> As CoREST is required for nucleosomal demethylation,<sup>34,242</sup> this argues that inhibitors of the CoREST linker/KDM1A tower interaction may inhibit KDM1A functionality in the cell.

In addition, MD studies by Baron and colleagues have suggested that the KDM1A/CoREST interaction may be dynamic. Specifically, their simulations indicate that the KDM1A SWIRM and CoREST SANT2 domains oscillate in distance and rotational angle in relation to each other, and that substrate binding allosterically rigidifies this fluctuation, favoring an “open” state.<sup>247–249</sup> They further suggest that blocking these ‘hinge sites’ may prevent KDM1A/CoREST association with chromatin or other protein partners and therefore provide another potential strategy for modulating KDM1A function.<sup>250</sup>

In addition to the regulatory mechanisms enforced on KDM1A by CoREST, two CoREST paralogs, CoREST2 (RCOR2, 523 aa) and CoREST3 (RCOR3, four isoforms of 436, 449, 495, and 553 aa), have recently been revealed as further governors of KDM1A activity.<sup>251,252</sup> These paralogs share a similar domain organization, including conserved ELM2 and dual SANT domains. Not surprisingly, CoREST2 and CoREST3 both interact with KDM1A and are capable of incorporation into larger protein complexes.<sup>251,252</sup> Similarly, the crystal structure of KDM1A bound to the linker-SANT2 domain of CoREST3 (residues 273–405; PDB 4CZZ) exhibited a nearly identical conformation as the KDM1A/CoREST (residues 308–440) complex (PDB 2V1D).<sup>251</sup> However, CoREST2 displays a reduced ability to facilitate KDM1A nucleosomal demethylation<sup>252</sup> and transcriptional repression as compared to CoREST.<sup>251</sup> This weakening of repressive activity is attributed to residue L165 in the CoREST2 SANT1 domain, which

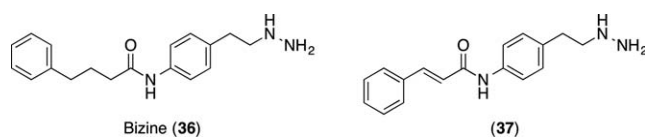


**FIGURE 10** Structures of mechanism-based phenelzine analogs.

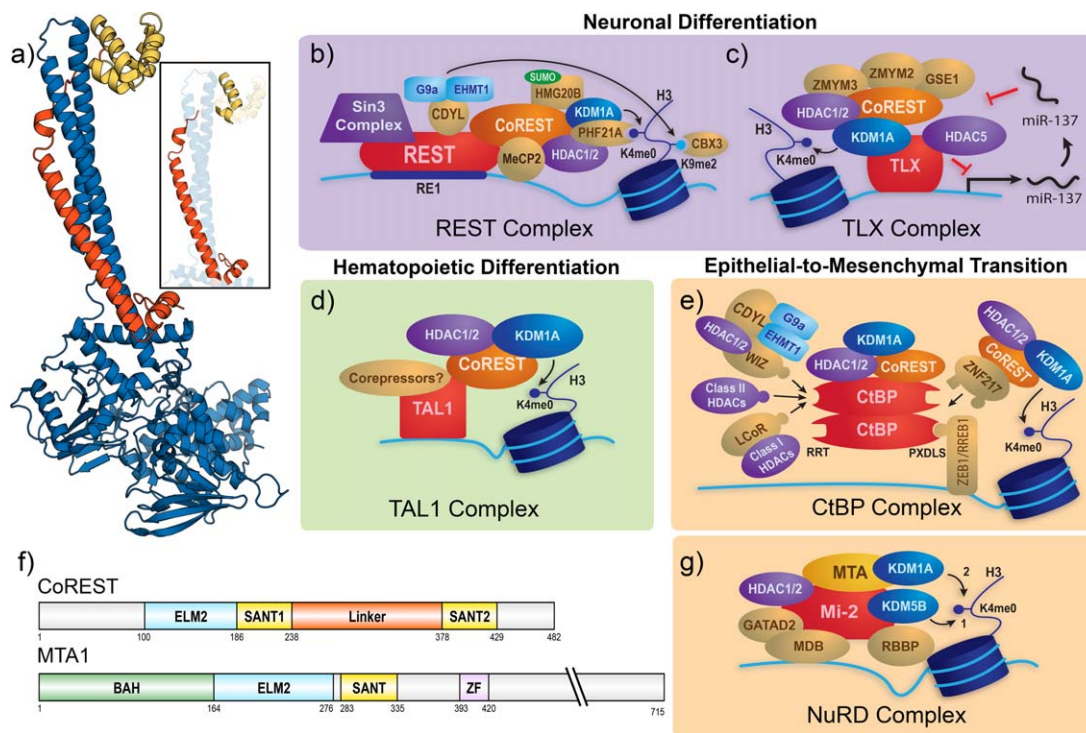


**FIGURE 11** KDM1A complexes that utilize CoREST and CoREST-like interactions. (a) Ribbon representation of KDM1A (blue) in complex with the linker (orange) and SANT2 (yellow) domains of CoREST (PDB 2IW5). Insert highlights the regions of contact between CoREST and the KDM1A tower domain. (b) CoREST recruits a KDM1A complex to suppress neuronal genes through its interaction with REST, which also recruits the Sin3 complex. (c) The CoREST core complex is recruited by a direct interaction between TLX and KDM1A. This complex forms a negative feedback loop with the microRNA miR-137. (d) The transcription factor TAL1 recruits the CoREST complex, and potentially other coregulators, to repress gene transcription as an effector of hematopoietic differentiation. (e) The CtBP proteins associate with DNA-binding proteins for genomic localization and recruit chromatin remodelers, including KDM1A, to regulate the EMT. (f) Domain maps of CoREST and MTA1 are representative of their respective isoforms and show a similar ELM2/SANT domain organization. (g) KDM1A is recruited by its tower domain to the MTA subunit of the NuRD complex, and in this context suppresses the EMT in breast cancer.

diminishes its affinity for HDACs 1 and 2.<sup>251</sup> However, CoREST3 plays an even more antagonistic role, as it competitively inhibits KDM1A nucleosomal demethylation. A CoREST3 chimera with the SANT2 domain replaced by the corresponding domain in CoREST reverses this phenotype and reinstates KDM1A nucleosomal demethylation.<sup>252</sup> Collectively, these studies clearly indicate that CoREST and its paralogs play important roles in a subset of KDM1A-dependent transcriptional regulatory events by acting as a scaffold for the assembly and recruitment of deacetylase/demethylase-containing complexes, and by serving as a bridge to link epigenetic enzymes to nucleosomal substrates.

**REST Complex.** RE1-silencing transcription factor (REST) is a supervisor of cell fate decisions during neuronal differentiation, and functions as a transcription repressor that localizes to

RE1 motifs in the promoters of neuron-specific genes (Figure 11b).<sup>253</sup> In multipotent progenitor cells, these genes are held in a ‘primed-repressed’ state, in which REST recruits corepressor complexes mSin3<sup>254</sup> and CoREST<sup>255–257</sup> to its N- and C-terminal repressor domains, respectively, while simultaneously maintaining an activating chromatin environment and basal-level gene transcription.<sup>258</sup> Upon differentiation into a neuron cell, REST is largely degraded to activate a neuronal expression program, although the CoREST complex sustains a role in tempering the expression of certain genes.<sup>258</sup> Alternately, upon differentiation into a non-neuronal cell type, the REST/mSin3/CoREST repressor machinery persists on RE1-containing promoters and adjusts chromatin in the vicinity of neuron-specific genes to a repressive state.<sup>258</sup> Specifically, H3K4 demethylation is executed by KDM1A,<sup>13</sup> and H3K9 methylation is likely mediated by the histone methyltransferases (HMTs) G9a

and EHMT1, which are bridged to REST by the corepressor protein CDYL.<sup>259</sup> The HMTs SUV39H1 and SETDB1 have also been linked to the CoREST complex and may play a role in H3K9 methylation.<sup>257,260</sup> Increased CpG methylation (mCpG) in RE1 motifs has also been observed in differentiated cells compared to embryonic stem cells,<sup>258</sup> although the DNA methyltransferase responsible has not yet been identified.

The H3K4 and H3K9 methylation status within chromatin encompassing repressed neuron-specific genes further recruits additional corepressors. For example, demethylated H3K4 is bound by PHF21A (BHC80), which stabilizes KDM1A on chromatin and enhances repression.<sup>261,262</sup> However, PHF21A exists as multiple isoforms,<sup>263</sup> is expressed tissue-specifically,<sup>241</sup> and has been reported to paradoxically inhibit KDM1A activity<sup>34</sup> and REST-mediated repression,<sup>264</sup> indicating that its activity may be context-specific. Similarly, REST-associated G9a recruits CBX3 (HP1) to methylated H3K9me2 residues,<sup>265</sup> where it is known to bind through its chromodomain and maintain a heterochromatic state.<sup>266</sup> In another example, the mCpG-binding protein MeCP2 is also recruited to the larger corepressor complex for stable gene silencing,<sup>257</sup> although it also appears to play a role in transient gene repression between neuron depolarization events.<sup>258</sup>

Other accessory proteins that may not directly interact with chromatin are also recruited to regulate gene repression.<sup>34,241</sup> For example, REST repression is reportedly dependent upon sumoylation of HMG20B (BRAAF35)<sup>267</sup> and its recruitment to the CoREST complex.<sup>34,241</sup> Previous studies have suggested that sumoylated regulators may bind the CoREST/KDM1A interaction surface,<sup>268</sup> although it is unclear if this is the case for HMG20B. In contrast, the repressive activity of the REST complex is antagonized by HMG20A (iBRAAF), which forms a heterodimer with HMG20B to prevent its sumoylation and incorporation into the CoREST complex.<sup>267</sup> In fact, HMG20A is a critical regulator of neuronal differentiation that promotes neuron-specific gene expression by recruitment of the H3K4 HMT, MLL.<sup>269</sup>

**TLX Orphan Nuclear Receptor Complex.** KDM1A also regulates neuronal processes through its interaction with the orphan nuclear hormone receptor TLX (NR2E1). In line with KDM1A's role in neuronal differentiation, TLX maintains the proliferative and self-renewal properties of adult neural stem cells and regulates neurogenesis.<sup>270</sup> Yokoyama and coworkers first reported that TLX interacts directly with the AOD and SWIRM domains of KDM1A and further demonstrated that TLX recruits the core CoREST/KDM1A/HDAC1 complex (Figure 11c).<sup>271</sup> Additionally, recruitment of the complex occurs in a KDM1A-dependent manner for H3K4 demethylation, H3 deacetylation, and downstream target gene repression. A subse-

quent report revealed that HDAC5 also associates with this complex.<sup>41</sup> Interestingly, immunoprecipitation of TLX also coprecipitates several other proteins, including ZMYM3 and two that are also found in the SNAI1 complex (see below),<sup>93</sup> namely GSE1 and ZMYM2.<sup>271</sup> Despite these results, it is currently unclear whether any crosstalk exists between these complexes.

Within these complexes, Sun and coworkers also reported that the TLX/KDM1A ensemble regulates neural stem cell proliferation.<sup>41</sup> Specifically, the microRNA, miR-137, antagonizes this proliferative activity and encourages differentiation by downregulating KDM1A. On the other hand, while in complex with KDM1A, TLX represses miR-137 expression. This feedback regulation likely contributes to timely neuronal differentiation events in which KDM1A is intimately involved.<sup>272</sup>

**TAL1 Complex.** TAL1 is a transcription factor that is involved in normal hematopoiesis and leukemogenesis and can act as both a transcriptional activator and repressor, depending upon the genomic context and stage of cellular differentiation.<sup>273</sup> Specifically, TAL1 promotes transcription of erythroid-specific genes through association with p300 and PCAF,<sup>274,275</sup> but can also associate with the mSin3A and ETO2 complexes to induce gene repression.<sup>276–280</sup> KDM1A is recruited by TAL1 along with the core CoREST/HDAC complex to repress erythroid-specific genes in progenitor cells prior to differentiation (Figure 11d), but is dismissed from TAL1 promoters during the early stages of differentiation.<sup>281</sup> The PTM of TAL1 may regulate this gene activation, as phosphorylation of S172 by protein kinase A (PKA) abolishes TAL1 interaction with KDM1A and results in recruitment of the H3K4 HMT, hSET1, activation of target genes, and initiation of erythroid differentiation.<sup>282</sup> It is currently unclear if the KDM1A/CoREST core complex cooperates with any of the other known TAL1-interacting corepressor complexes to stimulate gene repression.

**CtBP Complex.** C-terminal binding proteins (CtBPs) are implicated widely as repressors of mammalian gene expression, and likely function in these varied contexts by recruiting different subsets of corepressors.<sup>283,284</sup> KDM1A was first coprecipitated with the CtBP complex prior to discovery of its demethylase activity<sup>243</sup> and has since been associated with several CtBP functions, including pituitary gland development,<sup>285</sup> suppression of the tumor suppressor BRCA1,<sup>286</sup> and activation of tissue-specific genes in gastrointestinal endocrine cells.<sup>287</sup> However, the best-established role of KDM1A in the CtBP complex is its control of the EMT through suppression of the epithelial gene E-cadherin.<sup>243,288,289</sup>

On the molecular level, CtBPs interact with coregulators (Figure 11e) mainly through two interaction domains: a

hydrophobic pocket that canonically binds proteins containing a Pro-X-Asp-Leu-Ser (PXDLS) sequence motif and a structurally distinct surface crevice that binds an Arg-Arg-Thr (RRT) motif.<sup>290</sup> Additionally, CtBP proteins form extensive scaffolds by dimerization in a manner that positions the PXDLS binding pockets at opposite ends of the dimer, and in such a manner that the PXDLS pocket of one CtBP protein is in relatively close proximity to the RRT binding crevice of the second CtBP molecule.<sup>290</sup> Initial studies indicated that the PXDLS-binding region mediates CtBP genomic localization by associating with DNA-binding transcription factors containing PXDLS motifs.<sup>291</sup> However, later studies revealed that this site also recruits accessory proteins with histone-modification activity.<sup>292</sup> For example, deacetylase activity is recruited by PXDLS motifs in class II HDACs<sup>293</sup> and possibly by class I HDACs bridged through other PXDLS-containing corepressor proteins, such as NRIP140 and LCoR.<sup>294,295</sup> Similarly, PXDLS-like motifs in Wiz recruit the HMTs G9a and EHMT1,<sup>296</sup> and possibly CDYL and HDAC1/2 to the CtBP complex.<sup>292,297</sup> Several other proteins co-precipitate with CtBP, although not all have well-defined functions.<sup>243</sup>

Interestingly, direct binding of CtBP1 to CoREST and HDAC2, respectively, has been reported despite the lack of PXDLS motifs in these proteins, and seem to bridge KDM1A to the complex.<sup>292</sup> However, KDM1A recruitment to the CtBP complex also appears to be mediated by ZNF217,<sup>288,292</sup> a large DNA-binding zinc finger protein that spans the CtBP dimer interface to interact with both PXDLS and RRT domains simultaneously.<sup>290</sup> ZNF217 localizes the CtBP complex for transcriptional repression of several disease-related genes, such as E-cadherin and BRCA1.<sup>286,288</sup> Other DNA-binding proteins have also been reported to bridge KDM1A to the PXDLS-binding pocket and appear to dramatically alter the demethylase's biological function. For example, recruitment by ZEB1 can extend gene repression programs associated with pituitary differentiation,<sup>285</sup> while recruitment by RREB1 can actually promote CtBP/KDM1A-mediate gene activation.<sup>287</sup> Clearly, KDM1A activity within the CtBP complex may have far-reaching biological implications that are most likely determined by the presence of specific coregulatory subunits.

**NuRD Complex.** The nucleosome remodeling and histone deacetylase (NuRD) complex is a large, multi-protein complex that has been implicated as a regulator of a wide variety of cellular processes, from human development to the progression of several cancer types.<sup>298</sup> Since its discovery, the majority of its core protein constituents have been well defined: the ATP-dependent chromatin remodelers Mi-2  $\alpha/\beta$  (CHD3/4), histone deacetylases HDAC1/2, methyl-CpG-binding proteins MDB2/3, retinoblastoma-binding proteins RBBP4/7, corepressors

GATAD2A/B (p66 $\alpha/\beta$ ), and metastasis-associated proteins MTA1/2/3 (Figure 11g).<sup>299</sup>

Interestingly, the MTA proteins share striking similarities with the CoREST proteins. Specifically, the MTA isoforms possess, from N- to C-termini, BAH, ELM2, SANT and GATA-like zinc finger domains (Figure 11f).<sup>299</sup> As previously mentioned, the ELM2 and SANT domains serve to recruit HDACs 1 and 2,<sup>8,244</sup> presumably in similar fashion to CoREST. Wang and coworkers first established that the MTA2 protein, like CoREST, is sufficient to stimulate KDM1A demethylation of nucleosome substrates and mapped an interaction interface involving the KDM1A tower domain and MTA1/2/3 SANT domains.<sup>76</sup> The authors further demonstrated that this interaction recruits H3K4 demethylase activity to the NuRD complex for enhanced gene repression, and that KDM1A association with each MTA isoform corresponds to a unique transcriptional outcome. Functionally, the authors linked KDM1A in the NuRD complex to silencing of the TGF $\beta$  signaling pathway and repression of the EMT and metastatic potential in a breast cancer cell line. Since this initial study, KDM1A has been associated as a corepressor of the NuRD complex in a subset of its biological functions, such as lipid homeostasis,<sup>300</sup> aberrant gene repression in Ewing sarcoma,<sup>301</sup> and enhancer decommissioning during embryonic stem cell differentiation.<sup>27</sup> It is, however, noteworthy that a recent mass spectrometry-proteomics coupled study did not identify KDM1A as a stable component of the NuRD complex in HeLa cell extracts, indicating that it likely interacts in a context-specific manner.<sup>302</sup>

While the MTA proteins resemble CoREST in their ability to recruit HDAC/KDM1A, several domains unique to MTA suggest a unique functionality, possibly through altered interactions with chromatin or coregulatory proteins. In fact, the KDM1A/NuRD complex has been shown to also associate with the  $\alpha$ -KG dependent histone demethylase KDM5B.<sup>303</sup> In this context, KDM5B and KDM1A cooperate to sequentially demethylate H3K4 and repress the metastasis and angiogenesis-associated CCL14 chemokine pathway. However, it remains unclear if KDM5B recruitment is dependent upon a specific MTA isoform. A recent report from Nair and colleagues suggests a regulatory role of KDM1A in NuRD activity.<sup>173</sup> The authors show that G9a methylation of MTA K532 is required for its incorporation into the repressive NuRD complex, while KDM1A-mediated demethylation of the same residue triggers its dissociation from the NuRD complex and recruitment to the coactivator complex, NURE. Although these studies provide much needed insight into the function of KDM1A within the NuRD complex, further investigation into the demethylase activity of KDM1A within the heteromeric complex is needed.

### KDM1A Cooption During Herpes Simplex Virus Infection

Coooption of host KDM1A activity plays a role in infection and latency of herpes simplex virus (HSV) and has recently been reviewed.<sup>18,99</sup> Briefly, HSV establishes an active infection at the portal of entry (typically a mucosal membrane), where the host cell initially silences the inserted viral genome. Through a series of coordinated derepression events, viral immediate-early (IE) stage ( $\alpha$ ) genes are first transcribed and eventually give rise to transcription of late-stage ( $\beta$  and  $\gamma$ ) genes. Although the primary infection produces massive viral titers that are destructive toward the host tissue, the virus also establishes a latent infection in neuronal cells, in which viral genes are present but silenced. This state is non-destructive to the host cell and allows for periodic reemergence of the virus through poorly understood mechanisms.

The HSV genome is parsimonious, lacking much of the cellular machinery required for transcription and regulation of viral genes. The virus instead appropriates host cell transcriptional regulators, including KDM1A, to establish active and latent infections. Gu and coworkers first associated the REST/CoREST/HDAC repressor complex,<sup>304</sup> and later KDM1A, with HSV infection (Figure 12).<sup>305</sup> Consistently, Pinnoji and colleagues identified REST-binding RE1 motifs in the viral genome, suggesting a potential mechanism for cooption of the complex.<sup>306</sup> Indeed, REST appears to aid in repression of viral genes during latent infection, as genomic insertion of a REST mutant incapable of binding corepressor proteins produces a more virulent strain compared to wild-type REST.<sup>307</sup> Similarly, HDAC inhibitors reactivate silenced viral gene expression, while REST antagonizes reactivation.<sup>308</sup>

KDM1A also plays a role in viral gene activation. In order to induce transcription, the viral protein VP16 recruits host proteins HCF1 and OCT1 to target gene promoters.<sup>309</sup> Liang and coworkers report that HCF1 recruits KDM1A and HMTs, SET1 and MLL1, for H3K9 demethylation and H3K4 methylation, respectively (Figure 12).<sup>100</sup> Accordingly, the authors also report that inhibition of KDM1A prevents activation of viral genes and viral reemergence from latency.<sup>100–102</sup> Interestingly, the JMJD2 family H3K9 HDMs work synergistically with KDM1A to activate  $\alpha$  viral genes and inhibition similarly prevents viral activation and emergence from latency.<sup>310,311</sup> Additionally, the histone acetyl transferase, CLOCK, also appears to promote viral gene expression and may interact with HCF1 through the transcription factor BMAL1.<sup>312</sup> The dihydro-tryptido-indole natural product Harmaline reportedly represses  $\alpha$  gene activation, possibly by disrupting this viral-host hybrid protein complex.<sup>313</sup> Gu and coworkers have also suggested that the viral  $\alpha$  protein ICP0 interacts with CoREST and may com-

pete HDAC1 away from the REST/CoREST complex to initiate the switch to  $\beta/\gamma$  genes.<sup>304,314</sup> However, the idea that CoREST plays a role in viral gene repression has been thrown into question by a study that showed no change in virulence when CoREST is knocked-down in an ICP0-deficient HSV strain.<sup>315</sup> Given that KDM1A is a promising target for preventing primary HSV infections and suppressing emergence from latency, it is likely that future work will shed light on such discrepancies and further detail KDM1A's mechanistic role.

### KDM1A Involvement in Nuclear Hormone Signaling AR Complexes.

The AR is a nuclear hormone receptor that is intimately linked to prostate function, regulating processes ranging from normal tissue development to the genesis and progression of prostate cancers, including castration-resistant tumors.<sup>316</sup> Metzger and colleagues first reported KDM1A association with AR, suggesting that a large portion of the two proteins are involved in their mutual interaction and that the demethylase facilitates hormone-dependent AR-mediated transcription by demethylating H3K9 residues.<sup>84</sup> Subsequent studies demonstrated that the Jumonji-domain demethylase, KDM4C, also interacts with KDM1A/AR and works in concert with KDM1A to demethylate H3K9me3 residues.<sup>165</sup> Concurrently, hybrid inhibitors that simultaneously target both KDM1A and KDM4C exhibit anti-proliferative effects in prostate cancer cells.<sup>86</sup> Although KDM1A canonically demethylates H3K4 residues, Metzger and colleagues proposed a mechanism for the observed switch in substrate specificity by which protein kinase C $\beta$ 1 (PKC $\beta$ 1) associates with AR/KDM1A at target genes following hormone treatment and phosphorylates H3T6, a modification that prevents KDM1A demethylation of H3K4 on peptide substrates (Figure 13a).<sup>166</sup>

KDM1A may also play a role in repression of AR target genes. Unlike AR, KDM1A resides on AR target gene promoters even in the absence of androgen treatment, when these gene are presumably repressed.<sup>84,165</sup> Furthermore, the KDM1A/AR complex forms a negative feedback loop at high androgen levels, in which AR recruits KDM1A to an enhancer of the AR gene and mediates gene repression by demethylation of H3K4 (Figure 13a).<sup>317</sup> Although the role of KDM1A as a coregulator of AR signaling is fairly well established, further work will hopefully better delineate its opposing roles as both an activator and repressor.

**ER $\alpha$  Complexes.** Paralleling the function of the AR, the ER $\alpha$  is the main modulator of estrogen (E2) signaling in estrogen-responsive tissues. As such, its dysregulation results in the development and progression of several cancer types.<sup>318</sup> Recently, much attention has focused on the epigenetic

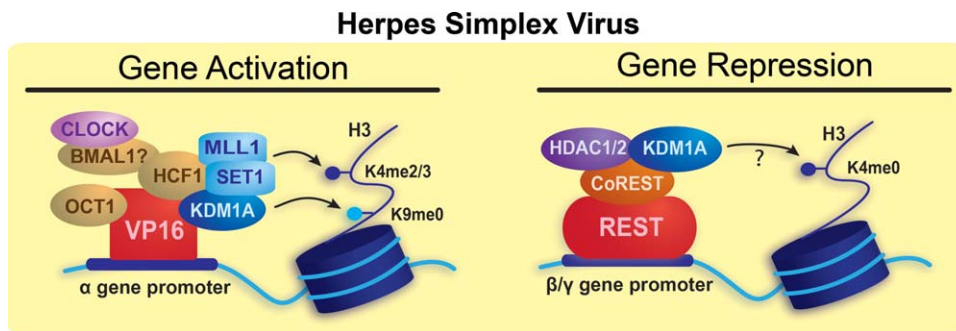


**FIGURE 12** KDM1A involvement in HSV infection and latency. KDM1A, along with other host cell epigenetic machinery, is coopted by HSV for viral gene activation. KDM1A and the CoREST/REST/HDAC complex may also participate in viral gene repression, where KDM1A may demethylate H3K4 residues.

mechanisms that accompany ER $\alpha$  signaling.<sup>319</sup> As observed for KDM1A participation in AR signaling, the demethylase seems to function as both an activator and repressor of ER $\alpha$  signaling. Perillo and coworkers reported that in a ‘resting state’ with no hormone stimulation, KDM1A is constitutively bound to ER $\alpha$  target gene promoters and demethylates H3K4.<sup>194</sup> However, E2 addition causes the recruitment of ER $\alpha$  to these promoters and KDM1A-dependent gene activation, most likely by catalyzing

the demethylation of inhibitory H3K9 methyl marks.<sup>194,320</sup> HMTs such as SET9 and SUV39H1 may also participate in E2-stimulated gene activation by methylating H3K4 (Figure 13b).<sup>194</sup>

The molecular mechanisms governing the activating and repressive roles of KDM1A are beginning to be described. For example, PELP1, an ER $\alpha$  coregulator with no known enzymatic activity, can interact directly with KDM1A, localizes on

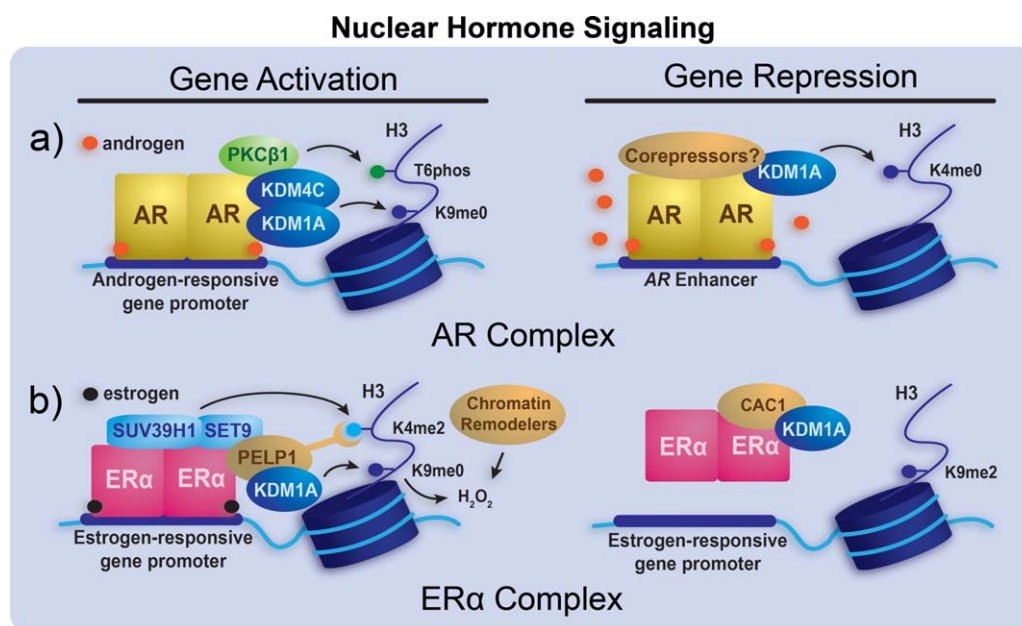


**FIGURE 13** KDM1A as an effector of gene activation and repression with nuclear hormone receptors. (a) KDM1A promotes AR gene activation following hormone stimulation at androgen-responsive gene promoters. At high hormone levels, KDM1A, and potentially other corepressors, repress AR transcription by demethylating H3K4 residues in the corresponding enhancer region. (b) KDM1A and PELP1 are recruited to ER $\alpha$ -occupied promoters. PELP1 reads H3K4me2 marks, and may position KDM1A for H3K9 demethylation. Association of CAC1 with this ER $\alpha$ /KDM1A complex causes dissociation from the promoter, accumulation of H3K9me2 marks, and gene repression.

known KDM1A/ER $\alpha$ -bound genes, and aids in gene activation.<sup>321</sup> When associated with KDM1A/ER $\alpha$ , the histone binding preference of PELP1 switches from H3K9me2 to H3K4me2, presumably to allow the subsequent demethylation of H3K9me2 by KDM1A (Figure 13b).<sup>321</sup> Interestingly, a recent report suggests that targeting this KDM1A/PELP1 activity may be of therapeutic benefit in breast cancer.<sup>78</sup> KDM1A may also demethylate ER $\alpha$  to promote transcriptional activation, although further validation of this activity is required.<sup>174</sup> More indirectly, KDM1A demethylation events and the accompanying production hydrogen peroxide byproducts also reportedly induces controlled DNA damage that attracts chromatin remodelers to enhance chromatin plasticity and promote target gene transcription.<sup>194</sup> In opposition to PELP1-mediated activation, KDM1A also interacts with the ER $\alpha$  corepressor CAC1, which binds KDM1A/ER $\alpha$ , reduces occupancy of the complex on target genes, allows H3K9me2 accumulation, and represses gene transcription (Figure 13b).<sup>322</sup> Additionally, retinoic acid may interfere with the KDM1A-mediated E2 response, as it appears to prevent activation of protein kinase A (PKA) and prohibits H3K9 demethylation, although the mechanism is not yet clear.<sup>323</sup>

In addition to these roles in ER $\alpha$  signaling, KDM1A may also perform ER $\alpha$ -independent functions in breast cancer. For example, inhibition of the demethylase resensitizes hormone-refractory breast cancer cells to anti-estrogen treatment.<sup>78</sup> In ER $\alpha$ -negative breast cancer, an interplay between KDM1A and HDACs is apparently necessary for tumor progression, as both affect the activity of the other towards histone substrates and simultaneous administration of KDM1A and HDAC inhibitors synergistically inhibits proliferation.<sup>79,80</sup> Also, overexpression of the ER $\alpha$  corepressor, CAC1, induces sensitivity to paclitaxel in ER $\alpha$ -positive, paclitaxel-resistant breast cancer cells.<sup>322</sup> These studies collectively imply that KDM1A functions in a wide range of ER $\alpha$  activities, and is additionally involved in various resistance mechanisms.

### SNAG Family Proteins Interact with KDM1A Using Product Mimicry

The Snail/Gfi1 (SNAG) family of proteins encompasses over 70 different members characterized by a conserved SNAG domain and between four to six C<sub>2</sub>H<sub>2</sub> zinc finger domains.<sup>324</sup> Zinc finger domains are generally located near the C-terminal regions of SNAG proteins and function as DNA-recognition domains that frequently localize to E-box sequences (CANNTG), although recruitment of individual proteins is likely tailored by minor variations in zinc fingers domains and DNA sequences.<sup>324</sup> In all but one known example, SNAG domains begin at the most N-terminal residue and are composed of a conserved

“PRSFVLV” sequence, where only the fourth residue is variable (Figure 14a).<sup>324</sup> Proteins in the SNAG family of transcription factors have been reported to regulate KDM1A activity through product-like interactions, in which the SNAG domain mimics the histone H3 N-terminal tail sequence and binds competitively to the KDM1A active site.

Lin and colleagues first identified an interaction between the SNAG domain of SNAI1 and the AOD of KDM1A and demonstrated that it could be disrupted with small molecule inhibitors.<sup>97</sup> Soon after, they showed that SNAI1 recruits KDM1A to target promoters where demethylation of H3K4 is required for gene repression.<sup>90</sup> Following this discovery, Baron and colleagues determined the crystal structure of KDM1A and CoREST in complex with the 20 N-terminal residues of SNAI1 encompassing the SNAG domain, revealing density for the first nine residues (Figure 14b).<sup>123</sup> In this report, the authors indicate that the SNAG domain mimics histone H3 through several conserved, positively charged residues and binds in the active site of KDM1A, resulting in competitive inhibition. Similar to the H3 tail, the first three SNAI1 residues form hydrogen-bonds deep in the active site, while Phe4 (F4), corresponding to Lys4 on H3 (H3K4), forms edge-to-face interactions with the flavin cofactor and KDM1A residue Y761. On the outer rim of the active site, Arg7 and Lys8 (R7 and K8) of SNAI1 seem to occupy the same positions as Arg8 and Lys9 of H3 (H3R8 and H3K9), respectively. Although direct evidence has not yet been provided, KDM1A presumably interacts with other SNAG proteins, including SNAI2, Gfi1, and Gfi1b, in a similar manner. In fact, treatment with either the KDM1A inhibitor tranlylcypromine (**1**) or a cell-permeable SNAG peptide phenocopies down-regulation of either KDM1A or SNAI2 in decreasing the EMT.<sup>325</sup>

However, these studies raise an interesting question: if the SNAG domain is inhibitory toward KDM1A, how does it recruit the enzyme for demethylation of its target genes? One possible scenario is that the SNAG domain recruits KDM1A, but then relinquishes its hold in order to transfer binding to the H3 tail. In a recent study by Tortorici and colleagues, the first six residues of the SNAI1 SNAG domain were found to be sufficient for KDM1A binding, while residues 10–20 increased affinity only marginally and decreased ligand efficiency.<sup>124</sup> On the other hand, the corresponding residues of H3 form multiple interactions with KDM1A,<sup>117</sup> and hence may allow H3 to displace the SNAG domain.

**SNAI1/2 Complexes.** SNAI1 (Snail, Snail1) and SNAI2 (Slug) are master regulators of the EMT and bind to E-box motifs in the promoters of epithelial genes, such as E-cadherin, to repress transcription and provoke an invasive, mesenchymal phenotype.<sup>91,326</sup> KDM1A recruitment to target genes and

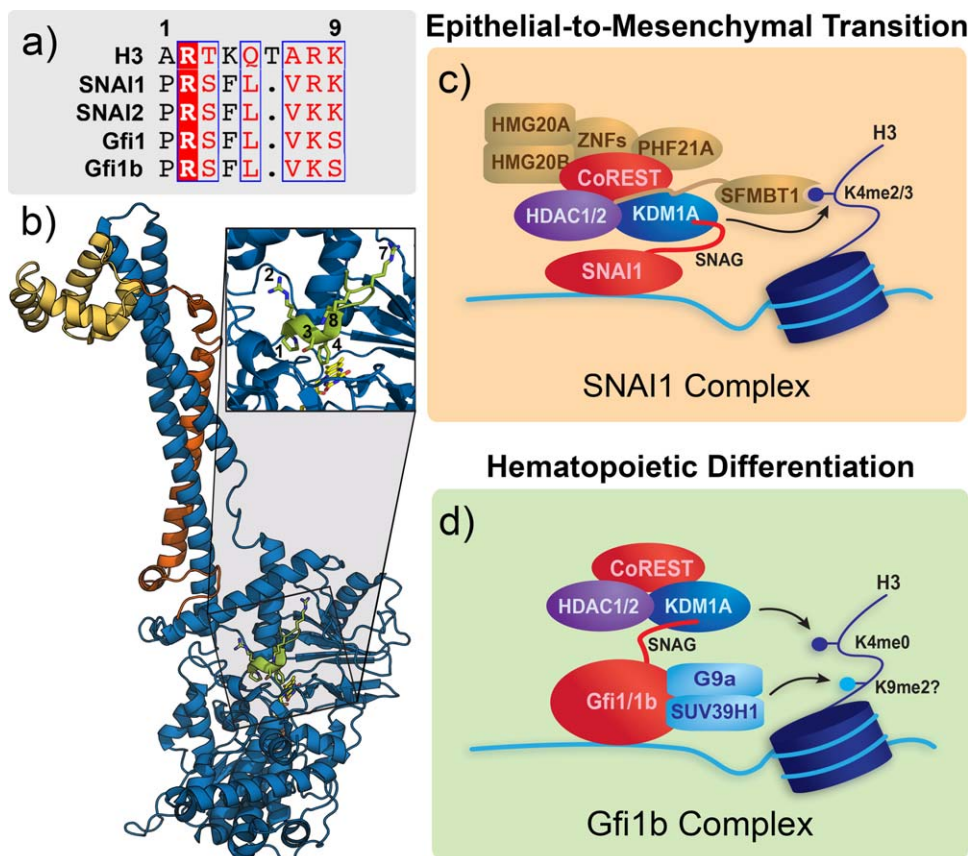


**FIGURE 14** SNAG family proteins recruit KDM1A using product mimicry. (a) Alignment of the H3 tail with the first 8 residues of the SNAI1/2 and Gfi1/1b SNAG domains shows striking similarity, with conserved residues highlighted in red and chemically similar residues boxed in blue. (b) Ribbon representation of the ternary complex formed by KDM1A (blue), CoREST (orange/yellow), and SNAG (green; PDB 2Y48). The insert shows an enlarged view of the SNAG peptide in the KDM1A active site with numbered residues starting with the N-terminal proline. (c) SNAI1 recruits the CoREST core complex and other proteins through its SNAG domain to regulate the EMT. SFMBT1 may also help localize the complex by binding H3K4me2/3. (d) Gfi1 and Gfi1b also recruits the CoREST core complex and cooperates with HMTs to regulate hematopoietic processes.

demethylation of H3K4me2 is required for SNAI1-mediated gene repression.<sup>90</sup> As discussed above, the SNAI1/2 SNAG domains recruit KDM1A via its active site.<sup>97,123</sup> As such, small molecule inhibitors or isolated SNAG domain peptides can displace SNAI1, derepress target genes, and decrease invasiveness and motility in colon and neuroblastoma cancer cell lines without affecting proliferation.<sup>97,325</sup> Interestingly, the chemotherapeutic drug doxorubicin has the opposite effect, enhancing the interaction between SNAI1 and KDM1A by inducing poly(ADP-ribosyl)ation of SNAI1.<sup>327</sup> The authors further suggest that this increased interaction causes repression of the tumor-suppressor gene, PTEN, and may facilitate drug-resistance in cancer.

SNAI1 also coprecipitates the core KDM1A/CoREST/HDAC complex, as well as several auxiliary proteins such as HMG20A/B and PHF21A, which are associated with the REST

complex, and CtBP, GSE1, and several zinc finger proteins, which are associated with the CtBP complex.<sup>93,97</sup> It is currently unclear if SNAI1 recruits these larger KDM1A-containing complexes to further regulate gene expression. Recent studies have also identified the chromatin 'reader' SFMBT1, previously identified with the CoREST complex and other repressive complexes,<sup>328,329</sup> as a member of the SNAI1/KDM1A complex. SFMBT1 binds directly to the CoREST linker region and mediates recruitment of KDM1A to SNAI1, gene repression, and induction of the EMT.<sup>93</sup> Additionally, it recognizes H3K4me2/3 marks,<sup>93</sup> and therefore may help to target the complex to active genes for subsequent repression (Figure 14c).

**Gfi1/1b Complexes.** Gfi1 and Gfi1b are SNAG-containing transcription factors that are critical for hematopoiesis. While

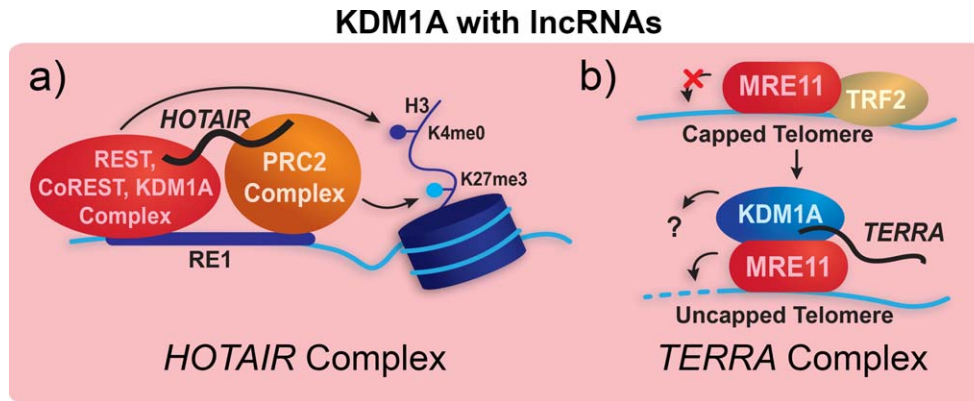


**FIGURE 15** KDM1A forms multi-component complexes with lncRNAs. (a) The lncRNA HOTAIR colocalizes the RE1-silencing transcription factor (REST)/CoREST/KDM1A and PRC2 complexes within the genome for subsequent gene repression. (b) While TRF2 protects telomere ends from degradation, loss of TRF2 allows recruitment of KDM1A and the telomeric repeat-containing lncRNA TERRA to the nuclease MRE11 and promotes telomere end processing.

Gfi1 regulates the differentiation programs of hematopoietic stem cells, small lymphocytes (B and T cells), dendritic cells, granulocytes and macrophages, Gfi1b is involved in the development of megakaryocytes and erythrocytes.<sup>330</sup> As might be expected, both proteins are also involved in hematopoietic-derived cancers, although their roles as promoters or repressors of cancer progression seem to vary significantly depending upon tissue origin.<sup>331–336</sup>

As with the SNAI1 and 2 proteins, Gfi1 and Gfi1b recruit the core KDM1A/CoREST/HDAC complex via their SNAG domains,<sup>29</sup> presumably by binding the KDM1A active site. Furthermore, Gfi1b recruits KDM1A in this manner to the majority of its target genes for demethylation of H3K4me2 residues and transcriptional repression.<sup>29</sup> However, paralleling the tissue-dependent roles of Gfi1/1b, KDM1A differentially affects proliferation depending on the hematopoietic cell type and differentiation status.<sup>29</sup> For example, splice variant Gfi1b p32, is required for erythroid differentiation and recruits the CoREST/KDM1A complex more efficiently than the major Gfi1b isoform when dimethylated on Lys8 (K8) in its SNAG domain.<sup>337</sup> Similarly, the three CoREST isoforms all interact with Gfi1b but have varying effects on its activity (see above).<sup>252</sup> Gfi1b has also been associated with the H3K9 HMTs SUV29H1 and G9a,<sup>338</sup> although these proteins have not been explicitly shown to co-localize with Gfi1b/CoREST (Figure 14d).

### KDM1A Association with Long Non-Coding RNAs

A new class of interactions has recently been identified between KDM1A and long noncoding RNAs (lncRNAs).<sup>339–341</sup> lncRNAs, broadly defined as non-protein coding RNA tran-

scripts greater than 200 nucleotides, are differentially expressed in a number of human cancers and can regulate transcription by acting as scaffolds for chromatin modifying complexes.<sup>342–346</sup> The HOTAIR transcript, which is dramatically overexpressed in several cancers<sup>347–350</sup> and can be induced by estradiol,<sup>351</sup> recruits the PRC2 and KDM1A/CoREST/REST complexes for downregulation of tumor suppressor genes at the HOXD locus.<sup>352,353</sup> Binding interactions for EZH2 and KDM1A were observed at the 5'- and 3'-terminal domains of HOTAIR, respectively, and HOTAIR expression was required for co-immunoprecipitation and genomic co-localization of PRC2 protein complex and KDM1A (Figure 15a).<sup>339</sup> These interactions and the corresponding changes in histone methylation states were also observed *in vivo*.<sup>353</sup> The HOTAIR/PRC2/KDM1A complex has also been implicated as a positive regulator of NFAT5, a transcription factor associated with enhanced metastasis and angiogenesis in breast cancer.<sup>354</sup> In contrast, glioblastoma cell cycle progression appears to be dependent upon HOTAIR and PRC2 but not KDM1A, implying these corepressors may play specific, non-interdependent roles in conjunction with HOTAIR.<sup>355</sup> More extensive reviews of HOTAIR and its role in cancer have recently been published.<sup>356,357</sup>

In 2013, a second breast cancer-associated lncRNA, SRA (steroid receptor RNA activator), was reported to associate with KDM1A-containing repressive complexes, though in this case the interaction was mediated by progesterone receptor (PR).<sup>340,358</sup> Most recently, Porro and colleagues have demonstrated an interaction between KDM1A and the telomeric lncRNA TERRA.<sup>341</sup> The authors report that TERRA, which consists of UUAGGG repeats and has been

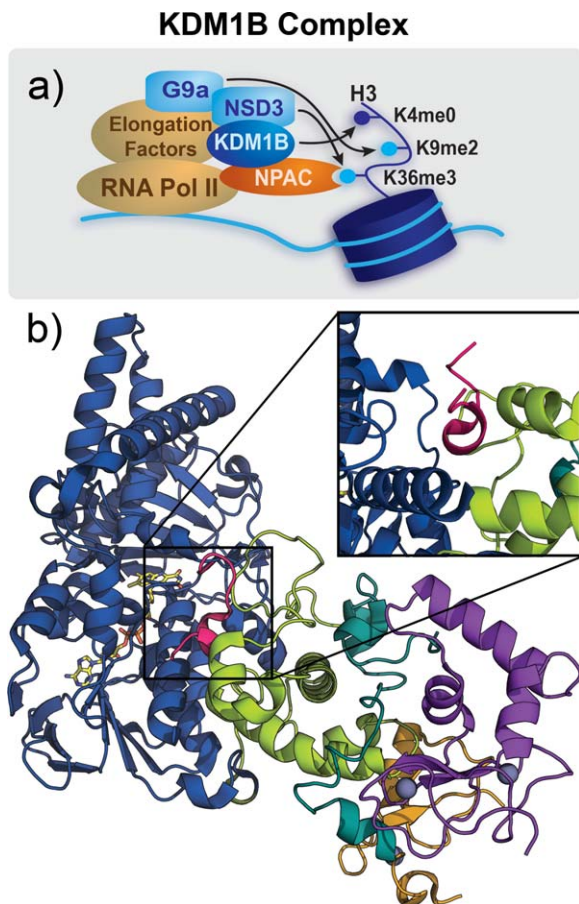


**FIGURE 16** KDM1B forms a multiprotein complex that epigenetically regulates gene expression by altering histone modifications in the coding regions of genes. (a) KDM1B associates with the chromatin reader Nuclear Protein 60kDa/Glyoxylate Reductase 1 Homolog (NPAC/GLYR1), RNA polymerase II, and other elongation factors within active genes. (b) A ribbon representation of KDM1B (colored as described in Figure 1) in complex with a NPAC/GLYR1 fragment peptide (pink). The insert shows an enlarge view of NPAC binding in the cleft between the amine oxidase catalytic domain and SWIRM domains of KDM1B.

implicated in the progressive shortening of telomeres, recruits KDM1A to telomeric DNA in the absence of the protective telomere repeat-binding factor 2 (TRF2). KDM1A does not seem to affect histone methylation levels in this context but instead promotes the removal of telomere 3' guanine overhangs by enhancing the nuclease activity of MRE11, an enzyme involved in telomere 3' end processing. Both TERRA and MRE11 interact with the SWIRM and N-terminal AOD region of KDM1A, but do not interact directly themselves. The authors therefore speculate that TERRA enhances the affinity of KDM1A for MRE11 and hence promotes telomeric shortening, although a direct substrate of KDM1A was not identified (Figure 15b). Given that the biological significance of lncRNAs is

just beginning to be appreciated, future reports of KDM1A interactions with lncRNAs are anticipated.

### Interaction of KDM1B with Proteins and Multi-Protein Complexes

Compared to the identified roles of KDM1A described above, much less is known about the interactions and biological significance of KDM1B. In contrast to KDM1A, KDM1B does not possess a coiled-coil tower domain, and hence does not interact with CoREST<sup>14</sup> nor cooperate with HDACs in breast cancer.<sup>79</sup> However, it has been reported as an effector of genomic imprinting,<sup>106</sup> and its activity is required for somatic cell reprogramming<sup>108,109</sup> and liver development.<sup>107</sup> KDM1B has more recently been implicated as a regulator of breast cancer proliferation, where inhibition works synergistically with DNMT and KDM1B inhibitors to derepress aberrantly silenced genes and decrease cell growth.<sup>359</sup>

KDM1B has been reported to function as a positive regulator of gene transcription by binding to chromatin in the highly transcribed, H3K36me3-enriched coding regions down-stream of gene promoters.<sup>105</sup> Here it helps to maintain H3K4 and H3K9 methylation by associating with a larger complex that includes Pol II and other elongation factors, as well as the SET-family HMTs NSD3 and G9a, which methylate histone H3K36 and H3K9 sites, respectively (Figure 16a).<sup>105</sup> Later studies indicated that the H3K36me3 reader NPAC/GLYR1 is likely part of this complex as well, and enhances KDM1B demethylation of H3K4me1/2 by binding at its AOD/SWIRM interface (Figure 16b).<sup>136</sup> Finally, KDM1B is recruited to the promoters of inflammatory genes by the NF- $\kappa$ B subunit c-Rel and is required for subsequent H3K9 demethylation, recruitment of NF- $\kappa$ B, and gene expression.<sup>110</sup> Given the intricate mechanisms involved in regulating and modulating KDM1A activity, it is likely that future work will uncover an analogous but unique set of protein partners that govern KDM1B activity.

### CONCLUSIONS

KDM1s function as oxidative demethylases, removing methyl marks on protein substrates that provide chemical cues for the regulation of transcription. As such, KDM1A and KDM1B are central to numerous transcriptional programs in normal and disease-associated biology. These include regulating differentiation processes of both hematopoietic and neuronal tissues, cancer proliferation and metastasis, and viral replication and emergence from latency. Within these enzymes exist interaction motifs unique to each KDM1 isoform that facilitate interactions with biomolecules that regulate catalysis, promote KDM1 enzyme recruitment, and direct access to specific

substrates at explicit sites within the cell. These coregulatory molecules include proteins, product-like inhibitors, and lncRNAs. Recently, transcriptional outcomes have been correlated to specific interactions of KDM1A or KDM1B with coregulatory biomolecules. In fact, interactions with differing subsets of coregulators can lead to KDM1 involvement in opposing transcriptional programs. Although several classes of KDM1-selective small molecule inhibitors have been recently developed, pan-inhibition strategies lack the selectivity capable of discriminating between KDM1 activities in these specific functional contexts. The development of next-generation chemical biology probes and therapeutics that modulate these interactions may further deconvolute the complex biology of epigenetic regulation. We suspect that due to the sheer size of these multiprotein complexes that these probes will either be peptides, peptoids, or peptide-like in nature.

We wish to thank the members of the McCafferty and Hargrove laboratories for their thoughtful insights during the preparation of this manuscript.

## REFERENCES

- Allfrey, V. G.; Mirsky, A. E. *Science* 1964, 144, 559.
- Allfrey, V. G.; Faulkner, R.; Mirsky, A. E. *Proc Natl Acad Sci USA* 1964, 51, 786–794.
- Kooistra, S. M.; Helin, K. *Nat Rev Mol Cell Biol* 2012, 13, 297–311.
- Hou, H.; Yu, H. *Curr Opin Struct Biol* 2010, 20, 739–748.
- Qian, C.; Zhou, M. M. *Cell Mol Life Sci* 2006, 63, 2755–2763.
- Tong, J. K.; Hassig, C. A.; Schnitzler, G. R.; Kingston, R. E.; Schreiber, S. L. *Nature* 1998, 395, 917–921.
- Humphrey, G. W.; Wang, Y.; Russanova, V. R.; Hirai, T.; Qin, J.; Nakatani, Y.; Howard, B. H. *J Biol Chem* 2001, 276, 6817–6824.
- You, A.; Tong, J. K.; Grozinger, C. M.; Schreiber, S. L. *Proc Natl Acad Sci USA* 2001, 98, 1454–1458.
- Hakimi, M. A.; Dong, Y.; Lane, W. S.; Speicher, D. W.; Shiekhattar, R. *J Biol Chem* 2003, 278, 7234–7239.
- He, Y.; Michaels, S. D.; Amasino, R. M. *Science* 2003, 302, 1751–1754.
- Aravind, L.; Iyer, L. M. *Genome Biol* 2002, 3, RESEARCH0039.
- Da, G.; Lenkart, J.; Zhao, K.; Shiekhattar, R.; Cairns, B. R.; Marmorstein, R. *Proc Natl Acad Sci USA* 2006, 103, 2057–2062.
- Shi, Y.; Lan, F.; Matson, C.; Mulligan, P.; Whetstone, J. R.; Cole, P. A.; Casero, R. A.; Shi, Y. *Cell* 2004, 119, 941–953.
- Karytinis, A.; Forneris, F.; Profumo, A.; Ciozzani, G.; Battaglioli, E.; Binda, C.; Mattevi, A. *J Biol Chem* 2009, 284, 17775–17782.
- Spannhoff, A.; Hauser, A. T.; Heinke, R.; Sippl, W.; Jung, M. *ChemMedChem* 2009, 4, 1568–1582.
- Tian, X.; Fang, J. *Acta Biochim Biophys Sin (Shanghai)* 2007, 39, 81–88.
- Nottke, A.; Colaiacovo, M. P.; Shi, Y. *Development* 2009, 136, 879–889.
- Roizman, B.; Zhou, G.; Du, T. *J Neurovirol* 2011, 17, 512–517.
- Rotili, D.; Mai, A. *Genes Cancer* 2011, 2, 663–679.
- Chen, Y.; Jie, W.; Yan, W.; Zhou, K.; Xiao, Y. *Crit Rev Eukaryot Gene Expr* 2012, 22, 53–59.
- Lynch, J. T.; Harris, W. J.; Somerville, T. C. *Expert Opin Ther Targets* 2012, 16, 1239–1249.
- Amente, S.; Lania, L.; Majello, B. *Biochim Biophys Acta* 2013, 1829, 981–986.
- Dent, S. Y.; Chandra, J. *Elife* 2013, 2, e00963.
- Meissner, A. *Nat Biotechnol* 2010, 28, 1079–1088.
- Voigt, P.; Tee, W. W.; Reinberg, D. *Genes Dev* 2013, 27, 1318–1338.
- Puri, D.; Gala, H.; Mishra, R.; Dhawan, J. *FEBS J* 2014. [Epub ahead of print].
- Whyte, W. A.; Bilodeau, S.; Orlando, D. A.; Hoke, H. A.; Frampton, G. M.; Foster, C. T.; Cowley, S. M.; Young, R. A. *Nature* 2012, 482, 221–225.
- Adamo, A.; Sese, B.; Boue, S.; Castano, J.; Paramonov, I.; Barrero, M. J.; Izpisua Belmonte, J. C. *Nat Cell Biol* 2011, 13, 652–659.
- Saleque, S.; Kim, J.; Rooke, H. M.; Orkin, S. H. *Mol Cell* 2007, 27, 562–572.
- Kerenyi, M. A.; Shao, Z.; Hsu, Y. J.; Guo, G.; Luc, S.; O'Brien, K.; Fujiwara, Y.; Peng, C.; Nguyen, M.; Orkin, S. H. *Elife* 2013, 2, e00633.
- Sprussel, A.; Schulte, J. H.; Weber, S.; Necke, M.; Handschke, K.; Thor, T.; Pajtlar, K. W.; Schramm, A.; Konig, K.; Diehl, L.; Mestdagh, P.; Vandesompele, J.; Speleman, F.; Jastrow, H.; Heukamp, L. C.; Schule, R.; Duhrsen, U.; Buettner, R.; Eggert, A.; Gothert, J. R. *Leukemia* 2012, 26, 2039–2051.
- Butler, J. S.; Dent, S. Y. *Blood* 2013, 121, 3076–3084.
- Yang, R. F.; Zhao, G. W.; Liang, S. T.; Chen, H. Z.; Liu, D. P. *Chin Med Sci J* 2013, 28, 82–87.
- Shi, Y. J.; Matson, C.; Lan, F.; Iwase, S.; Baba, T.; Shi, Y. *Mol Cell* 2005, 19, 857–864.
- Kim, H. J.; Rosenfeld, M. G. *Arch Pharm Res* 2010, 33, 1467–1473.
- Fuentes, P.; Canovas, J.; Berndt, F. A.; Noctor, S. C.; Kukuljan, M. *Cereb Cortex* 2012, 22, 1431–1441.
- He, Y.; Yu, H.; Sun, S.; Wang, Y.; Liu, I.; Chen, Z.; Li, H. *Int J Dev Biol* 2013, 57, 365–373.
- Lyons, D. B.; Allen, W. E.; Goh, T.; Tsai, L.; Barnea, G.; Lomvardas, S. *Cell* 2013, 154, 325–336.
- Zhu, X.; Wang, J.; Ju, B. G.; Rosenfeld, M. G. *Curr Opin Cell Biol* 2007, 19, 605–611.
- Ge, W.; Liu, Y.; Chen, T.; Zhang, X.; Lv, L.; Jin, C.; Jiang, Y.; Shi, L.; Zhou, Y. *Biomaterials* 2014, 35, 6015–6025.
- Sun, G.; Alzayady, K.; Stewart, R.; Ye, P.; Yang, S.; Li, W.; Shi, Y. *Mol Cell Biol* 2010, 30, 1997–2005.
- Jie, Z.; Li, T.; Jia-Yun, H.; Qiu, J.; Ping-Yao, Z.; Houyan, S. *Brain Res Bull* 2009, 80, 79–84.
- Neelamegam, R.; Ricq, E. L.; Malvaez, M.; Patnaik, D.; Norton, S.; Carlin, S. M.; Hill, I. T.; Wood, M. A.; Haggarty, S. J.; Hooker, J. M. *ACS Chem Neurosci* 2012, 3, 120–128.
- Harris, W. J.; Huang, X.; Lynch, J. T.; Spencer, G. J.; Hitchin, J. R.; Li, Y.; Ciceri, F.; Blaser, J. G.; Greystoke, B. F.; Jordan, A. M.; Miller, C. J.; Ogilvie, D. J.; Somerville, T. C. *Cancer Cell* 2012, 21, 473–487.

45. Niebel, D.; Kirfel, J.; Janzen, V.; Holler, T.; Majores, M.; Gutgemann, I. *Blood* 2014, 124, 151–152.
46. Hayami, S.; Kelly, J. D.; Cho, H. S.; Yoshimatsu, M.; Unoki, M.; Tsunoda, T.; Field, H. I.; Neal, D. E.; Yamaue, H.; Ponder, B. A.; Nakamura, Y.; Hamamoto, R. *Int J Cancer* 2011, 128, 574–586.
47. Schildhaus, H. U.; Riegel, R.; Hartmann, W.; Steiner, S.; Wardelmann, E.; Merkelbach-Bruse, S.; Tanaka, S.; Sonobe, H.; Schule, R.; Buettner, R.; Kirfel, J. *Hum Pathol* 2011, 42, 1667–1675.
48. Lv, T.; Yuan, D.; Miao, X.; Lv, Y.; Zhan, P.; Shen, X.; Song, Y. *PLoS One* 2012, 7, e35065.
49. Yu, Y.; Wang, B.; Zhang, K.; Lei, Z.; Guo, Y.; Xiao, H.; Wang, J.; Fan, L.; Lan, C.; Wei, Y.; Ma, Q.; Lin, L.; Mao, C.; Yang, X.; Chen, X.; Li, Y.; Bai, Y.; Chen, D. *Biochem Biophys Res Commun* 2013, 437, 192–198.
50. Kononov, S.; Garcia-Bassets, I. *J Ovarian Res* 2013, 6, 75.
51. Ding, D.; Liu, X.; Guo, S. W. *Fertil Steril* 2014, 101, 740–749.
52. Singh, M. M.; Manton, C. A.; Bhat, K. P.; Tsai, W. W.; Aldape, K.; Barton, M. C.; Chandra, J. *Neuro Oncol* 2011, 13, 894–903.
53. Sareddy, G. R.; Nair, B. C.; Krishnan, S. K.; Gonugunta, V. K.; Zhang, Q. G.; Suzuki, T.; Miyata, N.; Brenner, A. J.; Brann, D. W.; Vadlamudi, R. K. *Oncotarget* 2013, 4, 18–28.
54. Zheng, Y. C.; Duan, Y. C.; Ma, J. L.; Xu, R. M.; Zi, X.; Lv, W. L.; Wang, M. M.; Ye, X. W.; Zhu, S.; Mobley, D.; Zhu, Y. Y.; Wang, J. W.; Li, J. F.; Wang, Z. R.; Zhao, W.; Liu, H. M. *J Med Chem* 2013, 56, 8543–8560.
55. Sankar, S.; Theisen, E. R.; Bearss, J.; Mulvihill, T.; Hoffman, L. M.; Sorna, V.; Beckerle, M. C.; Sharma, S.; Lessnick, S. L. *Clin Cancer Res* 2014, 20, 4584–4597.
56. Theisen, E. R.; Gajiwala, S.; Bearss, J.; Sorna, V.; Sharma, S.; Janat-Amsbury, M. *BMC Cancer* 2014, 14, 752.
57. Schulte, J. H.; Lim, S.; Schramm, A.; Friedrichs, N.; Koster, J.; Versteeg, R.; Ora, I.; Pajtlar, K.; Klein-Hitpass, L.; Kuhfittig-Kulle, S.; Metzger, E.; Schule, R.; Eggert, A.; Buettner, R.; Kirfel, J. *Cancer Res* 2009, 69, 2065–2071.
58. Althoff, K.; Beckers, A.; Odersky, A.; Mestdagh, P.; Koster, J.; Bray, I. M.; Bryan, K.; Vandosomespele, J.; Speleman, F.; Stallings, R. L.; Schramm, A.; Eggert, A.; Sprussel, A.; Schulte, J. H. *Int J Cancer* 2013, 133, 1064–1073.
59. Yang, H.; Li, Q.; Zhao, W.; Yuan, D.; Zhao, H.; Zhou, Y. *FEBS Lett* 2014, 588, 192–197.
60. Xu, G.; Xiao, Y.; Hu, J.; Xing, L.; Zhao, O.; Wu, Y. *Cell Physiol Biochem* 2013, 31, 854–862.
61. Pajtlar, K. W.; Weingarten, C.; Thor, T.; Kunkele, A.; Heukamp, L. C.; Buttner, R.; Suzuki, T.; Miyata, N.; Grotzer, M.; Rieb, A.; Sprussel, A.; Eggert, A.; Schramm, A.; Schulte, J. H. *Acta Neuropathol Commun* 2013, 1, 19.
62. Huang, Z.; Li, S.; Song, W.; Li, X.; Li, Q.; Zhang, Z.; Han, Y.; Zhang, X.; Miao, S.; Du, R.; Wang, L. *PLoS One* 2013, 8, e70077.
63. Jie, D.; Zhongmin, Z.; Guoqing, L.; Sheng, L.; Yi, Z.; Jing, W.; Liang, Z. *Dig Dis Sci* 2013, 58, 1581–1589.
64. Ding, J.; Zhang, Z. M.; Xia, Y.; Liao, G. Q.; Pan, Y.; Liu, S.; Zhang, Y.; Yan, Z. *Br J Cancer* 2013, 109, 994–1003.
65. Jin, L.; Hanigan, C. L.; Wu, Y.; Wang, W.; Park, B. H.; Woster, P. M.; Casero, R. A. *Biochem J* 2013, 449, 459–468.
66. Murray-Stewart, T.; Woster, P. M.; Casero, R. A., Jr. *Amino Acids* 2014, 46, 585–594.
67. Fiskus, W.; Sharma, S.; Shah, B.; Portier, B. P.; Devaraj, S. G.; Liu, K.; Iyer, S. P.; Bearss, D.; Bhalla, K. N. *Leukemia* 2014, 28, 2155–2164.
68. Schenk, T.; Chen, W. C.; Gollner, S.; Howell, L.; Jin, L.; Hebestreit, K.; Klein, H. U.; Popescu, A. C.; Burnett, A.; Mills, K.; Casero, R. A., Jr.; Marton, L.; Woster, P.; Minden, M. D.; Dugas, M.; Wang, J. C.; Dick, J. E.; Muller-Tidow, C.; Petrie, K.; Zelent, A. *Nat Med* 2012, 18, 605–611.
69. Mould, D. P.; McGonagle, A. E.; Wiseman, D. H.; Williams, E. L.; Jordan, A. M. *Med Res Rev* 2014. [Epub ahead of print].
70. Lim, S.; Janzer, A.; Becker, A.; Zimmer, A.; Schule, R.; Buettner, R.; Kirfel, J. *Carcinogenesis* 2010, 31, 512–520.
71. Serce, N.; Gnatzy, A.; Steiner, S.; Lorenzen, H.; Kirfel, J.; Buettner, R. *BMC Clin Pathol* 2012, 12, 13.
72. Pollock, J. A.; Larrea, M. D.; Jasper, J. S.; McDonnell, D. P.; McCafferty, D. G. *ACS Chem Biol* 2012, 7, 1221–1231.
73. Derr, R. S.; van Hoesel, A. Q.; Benard, A.; Goossens-Beumer, I. J.; Sajet, A.; Dekker-Ensink, N. G.; de Kruijf, E. M.; Bastiaannet, E.; Smit, V. T.; van de Velde, C. J.; Kuppen, P. J. *BMC Cancer* 2014, 14, 604.
74. Wu, Y.; Wang, Y.; Yang, X. H.; Kang, T.; Zhao, Y.; Wang, C.; Evers, B. M.; Zhou, B. P. *Cell Rep* 2013, 5, 224–236.
75. Zhu, Q.; Huang, Y.; Marton, L. J.; Woster, P. M.; Davidson, N. E.; Casero, R. A., Jr. *Amino Acids* 2012, 42, 887–898.
76. Wang, Y.; Zhang, H.; Chen, Y.; Sun, Y.; Yang, F.; Yu, W.; Liang, J.; Sun, L.; Yang, X.; Shi, L.; Li, R.; Li, Y.; Zhang, Y.; Li, Q.; Yi, X.; Shang, Y. *Cell* 2009, 138, 660–672.
77. Patani, N.; Jiang, W. G.; Newbold, R. F.; Mokbel, K. *Anticancer Res* 2011, 31, 4115–4125.
78. Cortez, V.; Mann, M.; Tekmal, S.; Suzuki, T.; Miyata, N.; Rodriguez-Aguayo, C.; Lopez-Berestein, G.; Sood, A. K.; Vadlamudi, R. K. *Breast Cancer Res* 2012, 14, 404.
79. Huang, Y.; Vasilatos, S. N.; Boric, L.; Shaw, P. G.; Davidson, N. E. *Breast Cancer Res Treat* 2012, 131, 777–789.
80. Vasilatos, S. N.; Katz, T. A.; Oesterreich, S.; Wan, Y.; Davidson, N. E.; Huang, Y. *Carcinogenesis* 2013, 34, 1196–1207.
81. Kahl, P.; Gullotti, L.; Heukamp, L. C.; Wolf, S.; Friedrichs, N.; Vorreuther, R.; Solleder, G.; Bastian, P. J.; Ellinger, J.; Metzger, E.; Schule, R.; Buettner, R. *Cancer Res* 2006, 66, 11341–11347.
82. Urbanucci, A.; Waltering, K. K.; Suikki, H. E.; Helenius, M. A.; Visakorpi, T. *BMC Cancer* 2008, 8, 219.
83. Suikki, H. E.; Kujala, P. M.; Tammela, T. L.; van Weerden, W. M.; Vessella, R. L.; Visakorpi, T. *Prostate* 2010, 70, 889–898.
84. Metzger, E.; Wissmann, M.; Yin, N.; Muller, J. M.; Schneider, R.; Peters, A. H.; Gunther, T.; Buettner, R.; Schule, R. *Nature* 2005, 437, 436–439.
85. Willmann, D.; Lim, S.; Wetzler, S.; Metzger, E.; Jandausch, A.; Wilk, W.; Jung, M.; Forne, I.; Imhof, A.; Janzer, A.; Kirfel, J.; Waldmann, H.; Schule, R.; Buettner, R. *Int J Cancer* 2012, 131, 2704–2709.
86. Rotili, D.; Tomassi, S.; Conte, M.; Benedetti, R.; Tortorici, M.; Ciossani, G.; Valente, S.; Marrocco, B.; Labella, D.; Novellino, E.; Mattevi, A.; Altucci, L.; Tumber, A.; Yapp, C.; King, O. N.; Hopkinson, R. J.; Kawamura, A.; Schofield, C. J.; Mai, A. *J Med Chem* 2014, 57, 42–55.
87. Kashyap, V.; Ahmad, S.; Nilsson, E. M.; Helczynski, L.; Kenna, S.; Persson, J. L.; Gudas, L. J.; Mongan, N. P. *Mol Oncol* 2013, 7, 555–566.

88. Crea, F.; Sun, L.; Mai, A.; Chiang, Y. T.; Farrar, W. L.; Danesi, R.; Helgason, C. D. *Mol Cancer* 2012, 11, 52.
89. De Craene, B.; Berx, G. *Nat Rev Cancer* 2013, 13, 97–110.
90. Lin, T.; Ponn, A.; Hu, X.; Law, B. K.; Lu, J. *Oncogene* 2010, 29, 4896–4904.
91. Peinado, H.; Olmeda, D.; Cano, A. *Nat Rev Cancer* 2007, 7, 415–428.
92. McDonald, O. G.; Wu, H.; Timp, W.; Doi, A.; Feinberg, A. P. *Nat Struct Mol Biol* 2011, 18, 867–874.
93. Tang, M.; Shen, H.; Jin, Y.; Lin, T.; Cai, Q.; Pinard, M. A.; Biswas, S.; Tran, Q.; Li, G.; Shenoy, A. K.; Tongdee, E.; Lin, S.; Gu, Y.; Law, B. K.; Zhou, L.; McKenna, R.; Wu, L.; Lu, J. *J Biol Chem* 2013, 288, 27680–27691.
94. Wu, Z. Q.; Li, X. Y.; Hu, C. Y.; Ford, M.; Kleer, C. G.; Weiss, S. J. *Proc Natl Acad Sci USA* 2012, 109, 16654–16659.
95. Mulligan, P.; Yang, F.; Di Stefano, L.; Ji, J. Y.; Ouyang, J.; Nishikawa, J. L.; Toiber, D.; Kulkarni, M.; Wang, Q.; Najafi-Shoushtari, S. H.; Mostoslavsky, R.; Gygi, S. P.; Gill, G.; Dyson, N. J.; Naar, A. M. *Mol Cell* 2011, 42, 689–699.
96. Yatim, A.; Benne, C.; Sobhian, B.; Laurent-Chabalier, S.; Deas, O.; Judde, J. G.; Lelievre, J. D.; Levy, Y.; Benkirane, M. *Mol Cell* 2012, 48, 445–458.
97. Lin, Y.; Wu, Y.; Li, J.; Dong, C.; Ye, X.; Chi, Y. I.; Evers, B. M.; Zhou, B. P. *EMBO J* 2010, 29, 1803–1816.
98. Phillips, S.; Prat, A.; Sedic, M.; Proia, T.; Wronski, A.; Mazumdar, S.; Skibinski, A.; Shirley, S. H.; Perou, C. M.; Gill, G.; Gupta, P. B.; Kuperwasser, C. *Stem Cell Reports* 2014, 2, 633–647.
99. Zhou, G.; Du, T.; Roizman, B. *Viruses* 2013, 5, 1208–1218.
100. Liang, Y.; Vogel, J. L.; Narayanan, A.; Peng, H.; Kristie, T. M. *Nat Med* 2009, 15, 1312–1317.
101. Liang, Y.; Quenelle, D.; Vogel, J. L.; Mascaro, C.; Ortega, A.; Kristie, T. M. *MBio* 2013, 4, e00558–00512.
102. Hill, J. M.; Quenelle, D. C.; Cardin, R. D.; Vogel, J. L.; Clement, C.; Bravo, F. J.; Foster, T. P.; Bosch-Marce, M.; Raja, P.; Lee, J. S.; Bernstein, D. I.; Krause, P. R.; Knipe, D. M.; Kristie, T. M. *Sci Transl Med* 2014, 6, 265ra169.
103. Sakane, N.; Kwon, H. S.; Pagans, S.; Kaehlcke, K.; Mizusawa, Y.; Kamada, M.; Lassen, K. G.; Chan, J.; Greene, W. C.; Schnoelzer, M.; Ott, M. *PLoS Pathog* 2011, 7, e1002184.
104. Le Douce, V.; Colin, L.; Redel, L.; Cherrier, T.; Herbein, G.; Aunis, D.; Rohr, O.; Van Lint, C.; Schwartz, C. *Nucleic Acids Res* 2012, 40, 1904–1915.
105. Fang, R.; Barbera, A. J.; Xu, Y.; Rutenberg, M.; Leonor, T.; Bi, Q.; Lan, F.; Mei, P.; Yuan, G. C.; Lian, C.; Peng, J.; Cheng, D.; Sui, G.; Kaiser, U. B.; Shi, Y.; Shi, Y. G. *Mol Cell* 2010, 39, 222–233.
106. Ciccone, D. N.; Su, H.; Hevi, S.; Gay, F.; Lei, H.; Bajko, J.; Xu, G.; Li, E.; Chen, T. *Nature* 2009, 461, 415–418.
107. Lu, H.; Cui, J. Y.; Gunewardena, S.; Yoo, B.; Zhong, X. B.; Klaassen, C. D. *Epigenetics* 2012, 7, 914–929.
108. Lin, S. L.; Chang, D. C.; Lin, C. H.; Ying, S. Y.; Leu, D.; Wu, D. T. *Nucleic Acids Res* 2011, 39, 1054–1065.
109. Bourguignon, L. Y.; Wong, G.; Earle, C.; Chen, L. *J Biol Chem* 2012, 287, 32800–32824.
110. van Essen, D.; Zhu, Y.; Saccani, S. *Mol Cell* 2010, 39, 750–760.
111. Stavropoulos, P.; Blobel, G.; Hoelz, A. *Nat Struct Mol Biol* 2006, 13, 626–632.
112. Chen, Y.; Yang, Y.; Wang, F.; Wan, K.; Yamane, K.; Zhang, Y.; Lei, M. *Proc Natl Acad Sci USA* 2006, 103, 13956–13961.
113. Kubicek, S.; Jenuwein, T. *Cell* 2004, 119, 903–906.
114. Jin, Y.; Kim, T. Y.; Kim, M. S.; Kim, M. A.; Park, S. H.; Jang, Y. K. *J Biochem* 2014, 156, 305–313.
115. Yang, M.; Gocke, C. B.; Luo, X.; Borek, D.; Tomchick, D. R.; Machius, M.; Otwinowski, Z.; Yu, H. *Mol Cell* 2006, 23, 377–387.
116. Yang, M.; Culhane, J. C.; Szewczuk, L. M.; Gocke, C. B.; Brautigam, C. A.; Tomchick, D. R.; Machius, M.; Cole, P. A.; Yu, H. *Nat Struct Mol Biol* 2007, 14, 535–539.
117. Forneris, F.; Binda, C.; Adamo, A.; Battaglioli, E.; Mattevi, A. *J Biol Chem* 2007, 282, 20070–20074.
118. Yang, M.; Culhane, J. C.; Szewczuk, L. M.; Jalili, P.; Ball, H. L.; Machius, M.; Cole, P. A.; Yu, H. *Biochemistry* 2007, 46, 8058–8065.
119. Mimasu, S.; Sengoku, T.; Fukuzawa, S.; Umehara, T.; Yokoyama, S. *Biochem Biophys Res Commun* 2008, 366, 15–22.
120. Zibetti, C.; Adamo, A.; Binda, C.; Forneris, F.; Toffolo, E.; Verpelli, C.; Ginelli, E.; Mattevi, A.; Sala, C.; Battaglioli, E. *J Neurosci* 2010, 30, 2521–2532.
121. Binda, C.; Valente, S.; Romanenghi, M.; Pilotto, S.; Cirilli, R.; Karytinos, A.; Ciossani, G.; Botrugno, O. A.; Forneris, F.; Tardugno, M.; Edmondson, D. E.; Minucci, S.; Mattevi, A.; Mai, A. *J Am Chem Soc* 2010, 132, 6827–6833.
122. Mimasu, S.; Umezawa, N.; Sato, S.; Higuchi, T.; Umehara, T.; Yokoyama, S. *Biochemistry* 2010, 49, 6494–6503.
123. Baron, R.; Binda, C.; Tortorici, M.; McCammon, J. A.; Mattevi, A. *Structure* 2011, 19, 212–220.
124. Tortorici, M.; Borrello, M. T.; Tardugno, M.; Chiarelli, L. R.; Pilotto, S.; Ciossani, G.; Vellore, N. A.; Bailey, S. G.; Cowan, J.; O’Connell, M.; Crabb, S. J.; Packham, G.; Mai, A.; Baron, R.; Ganesan, A.; Mattevi, A. *ACS Chem Biol* 2013, 8, 1677–1682.
125. Toffolo, E.; Rusconi, F.; Paganini, L.; Tortorici, M.; Pilotto, S.; Heise, C.; Verpelli, C.; Tedeschi, G.; Maffioli, E.; Sala, C.; Mattevi, A.; Battaglioli, E. *J Neurochem* 2014, 128, 603–616.
126. Luka, Z.; Pakhomova, S.; Loukachevitch, L. V.; Calcutt, M. W.; Newcomer, M. E.; Wagner, C. *Protein Sci* 2014, 23, 993–998.
127. Schmidt, D. M.; McCafferty, D. G. *Biochemistry* 2007, 46, 4408–4416.
128. De Colibus, L.; Mattevi, A. *Curr Opin Struct Biol* 2006, 16, 722–728.
129. Fraaije, M. W.; Mattevi, A. *Trends Biochem Sci* 2000, 25, 126–132.
130. Hwang, S.; Schmitt, A. A.; Luteran, A. E.; Toone, E. J.; McCafferty, D. G. *Biochemistry* 2011, 50, 546–557.
131. Qian, C.; Zhang, Q.; Li, S.; Zeng, L.; Walsh, M. J.; Zhou, M. M. *Nat Struct Mol Biol* 2005, 12, 1078–1085.
132. Tochio, N.; Umehara, T.; Koshihara, S.; Inoue, M.; Yabuki, T.; Aoki, M.; Seki, E.; Watanabe, S.; Tomo, Y.; Hanada, M.; Ikari, M.; Sato, M.; Terada, T.; Nagase, T.; Ohara, O.; Shirouzu, M.; Tanaka, A.; Kigawa, T.; Yokoyama, S. *Structure* 2006, 14, 457–468.
133. Luka, Z.; Moss, F.; Loukachevitch, L. V.; Bornhop, D. J.; Wagner, C. *Biochemistry* 2011, 50, 4750–4756.
134. Zhang, Q.; Qi, S.; Xu, M.; Yu, L.; Tao, Y.; Deng, Z.; Wu, W.; Li, J.; Chen, Z.; Wong, J. *Cell Res* 2013, 23, 225–241.

135. Chen, F.; Yang, H.; Dong, Z.; Fang, J.; Wang, P.; Zhu, T.; Gong, W.; Fang, R.; Shi, Y. G.; Li, Z.; Xu, Y. *Cell Res* 2013, 23, 306–309.
136. Fang, R.; Chen, F.; Dong, Z.; Hu, D.; Barbera, A. J.; Clark, E. A.; Fang, J.; Yang, Y.; Mei, P.; Rutenberg, M.; Li, Z.; Zhang, Y.; Xu, Y.; Yang, H.; Wang, P.; Simon, M. D.; Zhou, Q.; Li, J.; Marynick, M. P.; Li, X.; Lu, H.; Kaiser, U. B.; Kingston, R. E.; Xu, Y.; Shi, Y. G. *Mol Cell* 2013, 49, 558–570.
137. Holm, L.; Rosenstrom, P. *Nucleic Acids Res* 2010, 38, W545–W549.
138. Mandelker, D.; Gabelli, S. B.; Schmidt-Kittler, O.; Zhu, J.; Cheong, I.; Huang, C. H.; Kinzler, K. W.; Vogelstein, B.; Amzel, L. M. *Proc Natl Acad Sci USA* 2009, 106, 16996–17001.
139. Hopfner, K. P.; Craig, L.; Moncalian, G.; Zinkel, R. A.; Usui, T.; Owen, B. A.; Karcher, A.; Henderson, B.; Bodmer, J. L.; McMurray, C. T.; Carney, J. P.; Petrini, J. H.; Tainer, J. A. *Nature* 2002, 418, 562–566.
140. Barta, M. L.; Dickenson, N. E.; Patil, M.; Keightley, A.; Wyckoff, G. J.; Picking, W. D.; Picking, W. L.; Geisbrecht, B. V. *J Mol Biol* 2012, 417, 395–405.
141. Culhane, J. C.; Cole, P. A. *Curr Opin Chem Biol* 2007, 11, 561–568.
142. Højfeldt, J. W.; Agger, K.; Helin, K. *Nat Rev Drug Discov* 2013, 12, 917–930.
143. Forneris, F.; Binda, C.; Vanoni, M. A.; Mattevi, A.; Battaglioli, E. *FEBS Lett* 2005, 579, 2203–2207.
144. Gaweska, H. M.; University of Pennsylvania, 2009.
145. Gaweska, H.; Henderson Pozzi, M.; Schmidt, D. M.; McCafferty, D. G.; Fitzpatrick, P. F. *Biochemistry* 2009, 48, 5440–5445.
146. Cook, P. F.; Cleland, W. W. *Biochemistry* 1981, 20, 1797–1805.
147. Forneris, F.; Binda, C.; Vanoni, M. A.; Battaglioli, E.; Mattevi, A. *J Biol Chem* 2005, 280, 41360–41365.
148. Karasulu, B.; Patil, M.; Thiel, W. *J Am Chem Soc* 2013, 135, 13400–13413.
149. Silverman, R. B. *Accounts of Chemical Research* 1995, 28, 335–342.
150. McCann, A. E.; Sampson, N. S. *Journal of the American Chemical Society* 2000, 122, 35–39.
151. Chen, Z. W.; Zhao, G.; Martinovic, S.; Jorns, M. S.; Mathews, F. S. *Biochemistry* 2005, 44, 15444–15450.
152. Forneris, F.; Binda, C.; Dall'Aglio, A.; Fraaije, M. W.; Battaglioli, E.; Mattevi, A. *J Biol Chem* 2006, 281, 35289–35295.
153. Mattevi, A. *Trends Biochem Sci* 2006, 31, 276–283.
154. Tsai, W. W.; Nguyen, T. T.; Shi, Y.; Barton, M. C. *Mol Cell Biol* 2008, 28, 5139–5146.
155. Huang, J.; Sengupta, R.; Espejo, A. B.; Lee, M. G.; Dorsey, J. A.; Richter, M.; Opravil, S.; Shiekhattar, R.; Bedford, M. T.; Jenuwein, T.; Berger, S. L. *Nature* 2007, 449, 105–108.
156. Yu, T.; Higashi, M.; Cembran, A.; Gao, J.; Truhlar, D. G. *J Phys Chem B* 2013, 117, 8422–8429.
157. Kong, X.; Ouyang, S.; Liang, Z.; Lu, J.; Chen, L.; Shen, B.; Li, D.; Zheng, M.; Li, K. K.; Luo, C.; Jiang, H. *PLoS One* 2011, 6, e25444.
158. Henderson Pozzi, M.; Gawandi, V.; Fitzpatrick, P. F. *Biochemistry* 2009, 48, 1508–1516.
159. Polticelli, F.; Basran, J.; Faso, C.; Cona, A.; Minervini, G.; Angelini, R.; Federico, R.; Scrutton, N. S.; Tavladoraki, P. *Biochemistry* 2005, 44, 16108–16120.
160. Massey, V.; Curti, B. *J Biol Chem* 1967, 242, 1259–1264.
161. Massey, V.; Gibson, Q. H. *Fed Proc* 1964, 23, 18–29.
162. Walker, M. C.; Edmondson, D. E. *Biochemistry* 1994, 33, 7088–7098.
163. Emanuele, J. J.; Fitzpatrick, P. F. *Biochemistry* 1995, 34, 3710–3715.
164. Basran, J.; Bhanji, N.; Basran, A.; Nietlispach, D.; Mistry, S.; Meskys, R.; Scrutton, N. S. *Biochemistry* 2002, 41, 4733–4743.
165. Wissmann, M.; Yin, N.; Muller, J. M.; Greschik, H.; Fodor, B. D.; Jenuwein, T.; Vogler, C.; Schneider, R.; Gunther, T.; Buettner, R.; Metzger, E.; Schule, R. *Nat Cell Biol* 2007, 9, 347–353.
166. Metzger, E.; Imhof, A.; Patel, D.; Kahl, P.; Hoffmeyer, K.; Friedrichs, N.; Muller, J. M.; Greschik, H.; Kirfel, J.; Ji, S.; Kunowska, N.; Beisenherz-Huss, C.; Gunther, T.; Buettner, R.; Schule, R. *Nature* 2010, 464, 792–796.
167. Forneris, F.; Binda, C.; Battaglioli, E.; Mattevi, A. *Trends Biochem Sci* 2008, 33, 181–189.
168. Wang, J.; Hevi, S.; Kurash, J. K.; Lei, H.; Gay, F.; Bajko, J.; Su, H.; Sun, W.; Chang, H.; Xu, G.; Gaudet, F.; Li, E.; Chen, T. *Nat Genet* 2009, 41, 125–129.
169. Kontaki, H.; Talianidis, I. *Mol Cell* 2010, 39, 152–160.
170. Cho, H. S.; Suzuki, T.; Dohmae, N.; Hayami, S.; Unoki, M.; Yoshimatsu, M.; Toyokawa, G.; Takawa, M.; Chen, T.; Kurash, J. K.; Field, H. I.; Ponder, B. A.; Nakamura, Y.; Hamamoto, R. *Cancer Res* 2011, 71, 655–660.
171. Yang, J.; Huang, J.; Dasgupta, M.; Sears, N.; Miyagi, M.; Wang, B.; Chance, M. R.; Chen, X.; Du, Y.; Wang, Y.; An, L.; Wang, Q.; Lu, T.; Zhang, X.; Wang, Z.; Stark, G. R. *Proc Natl Acad Sci USA* 2010, 107, 21499–21504.
172. Abu-Farha, M.; Lanouette, S.; Elisma, F.; Tremblay, V.; Butson, J.; Figeys, D.; Couture, J. F. *J Mol Cell Biol* 2011, 3, 301–308.
173. Nair, S. S.; Li, D. Q.; Kumar, R. *Mol Cell* 2013, 49, 704–718.
174. Zhang, X.; Tanaka, K.; Yan, J.; Li, J.; Peng, D.; Jiang, Y.; Yang, Z.; Barton, M. C.; Wen, H.; Shi, X. *Proc Natl Acad Sci USA* 2013, 110, 17284–17289.
175. Iwabuchi, K.; Li, B.; Massa, H. F.; Trask, B. J.; Date, T.; Fields, S. *J Biol Chem* 1998, 273, 26061–26068.
176. Iwabuchi, K.; Bartel, P. L.; Li, B.; Marraccino, R.; Fields, S. *Proc Natl Acad Sci USA* 1994, 91, 6098–6102.
177. Brummelkamp, T. R.; Fabius, A. W.; Mullenders, J.; Madiredjo, M.; Velds, A.; Kerkhoven, R. M.; Bernards, R.; Beijersbergen, R. L. *Nat Chem Biol* 2006, 2, 202–206.
178. Nicholson, T. B.; Chen, T. *Epigenetics* 2009, 4, 129–132.
179. Hauber, J.; Malim, M. H.; Cullen, B. R. *J Virol* 1989, 63, 1181–1187.
180. Pagans, S.; Kauder, S. E.; Kaehlcke, K.; Sakane, N.; Schroeder, S.; Dormeyer, W.; Trievel, R. C.; Verdin, E.; Schnolzer, M.; Ott, M. *Cell Host Microbe* 2010, 7, 234–244.
181. Ott, M.; Schnolzer, M.; Garnica, J.; Fischle, W.; Emiliani, S.; Rackwitz, H. R.; Verdin, E. *Curr Biol* 1999, 9, 1489–1492.
182. Kiernan, R. E.; Vanhulle, C.; Schiltz, L.; Adam, E.; Xiao, H.; Maudoux, F.; Calomme, C.; Burny, A.; Nakatani, Y.; Jeang, K. T.; Benkirane, M.; Van Lint, C. *EMBO J* 1999, 18, 6106–6118.

183. Dorr, A.; Kiermer, V.; Pedal, A.; Rackwitz, H. R.; Henklein, P.; Schubert, U.; Zhou, M. M.; Verdin, E.; Ott, M. *EMBO J* 2002, 21, 2715–2723.
184. Mujtaba, S.; He, Y.; Zeng, L.; Farooq, A.; Carlson, J. E.; Ott, M.; Verdin, E.; Zhou, M. M. *Mol Cell* 2002, 9, 575–586.
185. Kaehlcke, K.; Dorr, A.; Hetzer-Egger, C.; Kiermer, V.; Henklein, P.; Schnoelzer, M.; Loret, E.; Cole, P. A.; Verdin, E.; Ott, M. *Mol Cell* 2003, 12, 167–176.
186. Akira, S.; Nishio, Y.; Inoue, M.; Wang, X. J.; Wei, S.; Matsusaka, T.; Yoshida, K.; Sudo, T.; Naruto, M.; Kishimoto, T. *Cell* 1994, 77, 63–71.
187. Manavathi, B.; Kumar, R. *J Biol Chem* 2007, 282, 1529–1533.
188. Li, D. Q.; Pakala, S. B.; Reddy, S. D.; Ohshiro, K.; Peng, S. H.; Lian, Y.; Fu, S. W.; Kumar, R. *J Biol Chem* 2010, 285, 10044–10052.
189. Pratt, W. B.; Toft, D. O. *Exp Biol Med (Maywood)* 2003, 228, 111–133.
190. Donlin, L. T.; Andresen, C.; Just, S.; Rudensky, E.; Pappas, C. T.; Kruger, M.; Jacobs, E. Y.; Unger, A.; Zieseniss, A.; Dobenecker, M. W.; Voelkel, T.; Chait, B. T.; Gregorio, C. C.; Rottbauer, W.; Tarakhovskiy, A.; Linke, W. A. *Genes Dev* 2012, 26, 114–119.
191. Voelkel, T.; Andresen, C.; Unger, A.; Just, S.; Rottbauer, W.; Linke, W. A. *Biochim Biophys Acta* 2013, 1833, 812–822.
192. Greenman, C.; Stephens, P.; Smith, R.; Dalgliesh, G. L.; Hunter, C.; Bignell, G.; Davies, H.; Teague, J.; Butler, A.; Stevens, C.; Edkins, S.; O'Meara, S.; Vastrik, I.; Schmidt, E. E.; Avis, T.; Barthorpe, S.; Bhamra, G.; Buck, G.; Choudhury, B.; Clements, J.; Cole, J.; Dicks, E.; Forbes, S.; Gray, K.; Halliday, K.; Harrison, R.; Hills, K.; Hinton, J.; Jenkinson, A.; Jones, D.; Menzies, A.; Mironenko, T.; Perry, J.; Raine, K.; Richardson, D.; Shepherd, R.; Small, A.; Tofts, C.; Varian, J.; Webb, T.; West, S.; Widaa, S.; Yates, A.; Cahill, D. P.; Louis, D. N.; Goldstraw, P.; Nicholson, A. G.; Brasseur, F.; Looijenga, L.; Weber, B. L.; Chiew, Y. E.; DeFazio, A.; Greaves, M. F.; Green, A. R.; Campbell, P.; Birney, E.; Easton, D. F.; Chenevix-Trench, G.; Tan, M. H.; Khoo, S. K.; Teh, B. T.; Yuen, S. T.; Leung, S. Y.; Wooster, R.; Futreal, P. A.; Stratton, M. R. *Nature* 2007, 446, 153–158.
193. Trepel, J.; Mollapour, M.; Giaccone, G.; Neckers, L. *Nat Rev Cancer* 2010, 10, 537–549.
194. Perillo, B.; Ombra, M. N.; Bertoni, A.; Cuozzo, C.; Sacchetti, S.; Sasso, A.; Chiariotti, L.; Malorni, A.; Abbondanza, C.; Avvedimento, E. V. *Science* 2008, 319, 202–206.
195. Itoh, Y.; Suzuki, T.; Miyata, N. *Mol Biosyst* 2013, 9, 873–896.
196. Khan, M. N.; Suzuki, T.; Miyata, N. *Med Res Rev* 2013, 33, 873–910.
197. Lohse, B.; Kristensen, J. L.; Kristensen, L. H.; Agger, K.; Helin, K.; Gajhede, M.; Clausen, R. P. *Bioorg Med Chem* 2011, 19, 3625–3636.
198. Helin, K.; Dhanak, D. *Nature* 2013, 502, 480–488.
199. Stavropoulos, P.; Hoelz, A. *Expert Opin Ther Targets* 2007, 11, 809–820.
200. Lee, M. G.; Wynder, C.; Schmidt, D. M.; McCafferty, D. G.; Shiekhhattar, R. *Chem Biol* 2006, 13, 563–567.
201. Culhane, J. C.; Wang, D.; Yen, P. M.; Cole, P. A. *J Am Chem Soc* 2010, 132, 3164–3176.
202. Gooden, D. M.; Schmidt, D. M.; Pollock, J. A.; Kabadi, A. M.; McCafferty, D. G. *Bioorg Med Chem Lett* 2008, 18, 3047–3051.
203. Ueda, R.; Suzuki, T.; Mino, K.; Tsumoto, H.; Nakagawa, H.; Hasegawa, M.; Sasaki, R.; Mizukami, T.; Miyata, N. *J Am Chem Soc* 2009, 131, 17536–17537.
204. Vianello, P.; Botrugno, O. A.; Cappa, A.; Ciossani, G.; Dessanti, P.; Mai, A.; Mattevi, A.; Meroni, G.; Minucci, S.; Thaler, F.; Tortorici, M.; Trifiro, P.; Valente, S.; Villa, M.; Varasi, M.; Mercurio, C. *Eur J Med Chem* 2014, 86, 352–363.
205. Benelkebir, H.; Hodgkinson, C.; Duriez, P. J.; Hayden, A. L.; Bulleid, R. A.; Crabb, S. J.; Packham, G.; Ganesan, A. *Bioorg Med Chem* 2011, 19, 3709–3716.
206. Johnson, N. W.; Kaspavec, J.; Rouse, M. B.; Tian, X.; Suarez, D. P.; McNulty, K. C.; Blackledge, C. W.; Van Aller, G. S.; Schneck, J.; Carson, J. D.; Kruger, R. G.; Mohammad, H. P.; Crouthamel, M. H.; Smitheman, K. N.; Liu, Y.; Gorman, S.; McHugh, C. F.; Bonnette, W.; Concha, N. O.; Patel, M.; Tummino, P. J.; Miller, W. H. In 246th ACS National Meeting and Exposition: Indiana Convention Center, 2013.
207. Kumarasinghe, I. R.; Woster, P. M. *ACS Med Chem Lett* 2014, 5, 29–33.
208. Culhane, J. C.; Szewczuk, L. M.; Liu, X.; Da, G.; Marmorstein, R.; Cole, P. A. *J Am Chem Soc* 2006, 128, 4536–4537.
209. Szewczuk, L. M.; Culhane, J. C.; Yang, M.; Majumdar, A.; Yu, H.; Cole, P. A. *Biochemistry* 2007, 46, 6892–6902.
210. Gongora-Benitez, M.; Tulla-Puche, J.; Albericio, F. *Chem Rev* 2014, 114, 901–926.
211. Schmitt, M. L.; Hauser, A. T.; Carlino, L.; Pippel, M.; Schulz-Fincke, J.; Metzger, E.; Willmann, D.; Yiu, T.; Barton, M.; Schule, R.; Sippl, W.; Jung, M. *J Med Chem* 2013, 56, 7334–7342.
212. Ogasawara, D.; Itoh, Y.; Tsumoto, H.; Kakizawa, T.; Mino, K.; Fukuhara, K.; Nakagawa, H.; Hasegawa, M.; Sasaki, R.; Mizukami, T.; Miyata, N.; Suzuki, T. *Angew Chem Int Ed Engl* 2013, 52, 8620–8624.
213. Itoh, Y.; Ogasawara, D.; Ota, Y.; Mizukami, T.; Suzuki, T. *Comput Struct Biotechnol J* 2014, 9, e201402002.
214. Huang, Y.; Stewart, T. M.; Wu, Y.; Baylin, S. B.; Marton, L. J.; Perkins, B.; Jones, R. J.; Woster, P. M.; Casero, R. A., Jr. *Clin Cancer Res* 2009, 15, 7217–7228.
215. Huang, Y.; Greene, E.; Murray Stewart, T.; Goodwin, A. C.; Baylin, S. B.; Woster, P. M.; Casero, R. A., Jr. *Proc Natl Acad Sci USA* 2007, 104, 8023–8028.
216. Bi, X.; Lopez, C.; Bacchi, C. J.; Rattendi, D.; Woster, P. M. *Bioorg Med Chem Lett* 2006, 16, 3229–3232.
217. Sharma, S. K.; Wu, Y.; Steinbergs, N.; Crowley, M. L.; Hanson, A. S.; Casero, R. A.; Woster, P. M. *J Med Chem* 2010, 53, 5197–5212.
218. Sharma, S. K.; Hazeldine, S.; Crowley, M. L.; Hanson, A.; Beattie, R.; Varghese, S.; Senanayake, T. M.; Hirata, A.; Hirata, F.; Huang, Y.; Wu, Y.; Steinbergs, N.; Murray-Stewart, T.; Bytheway, I.; Casero, R. A., Jr.; Woster, P. M. *Medchemcomm* 2012, 3, 14–21.
219. Pachaiyappan, B.; Woster, P. M. *Bioorg Med Chem Lett* 2014, 24, 21–32.
220. Huang, Y.; Marton, L. J.; Woster, P. M.; Casero, R. A. *Essays Biochem* 2009, 46, 95–110.
221. Wang, Z.; Patel, D. J. *Q Rev Biophys* 2013, 46, 349–373.

222. Nowotarski, S. L.; Woster, P. M.; Casero, R. A., Jr. *Expert Rev Mol Med* 2013, 15, e3.
223. Dulla, B.; Kirla, K. T.; Rathore, V.; Deora, G. S.; Kavela, S.; Maddika, S.; Chatti, K.; Reiser, O.; Iqbal, J.; Pal, M. *Org Biomol Chem* 2013, 11, 3103–3107.
224. Kolb, H. C.; Finn, M. G.; Sharpless, K. B. *Angew Chem Int Ed Engl* 2001, 40, 2004–2021.
225. Kolb, H. C.; Sharpless, K. B. *Drug Discov Today* 2003, 8, 1128–1137.
226. Zificsak, C. A.; Hlasta, D. J. *Tetrahedron* 2004, 60, 8991–9016.
227. Davies, J. R.; Kane, P. D.; Moody, C. J. *Tetrahedron* 2004, 60, 3967–3977.
228. Jia, Z.; Zhu, Q. *Bioorg Med Chem Lett* 2010, 20, 6222–6225.
229. Reck, F.; Zhou, F.; Girardot, M.; Kern, G.; Eyermann, C. J.; Hales, N. J.; Ramsay, R. R.; Gravestock, M. B. *J Med Chem* 2005, 48, 499–506.
230. Len, C.; BoulogneMerlot, A. S.; Postel, D.; Ronco, G.; Villa, P.; Goubert, C.; Jeufrault, E.; Mathon, B.; Simon, H. *Journal of Agricultural and Food Chemistry* 1996, 44, 2856–2858.
231. Imamura, H.; Ohtake, N.; Jona, H.; Shimizu, A.; Moriya, M.; Sato, H.; Sugimoto, Y.; Ikeura, C.; Kiyonaga, H.; Nakano, M.; Nagano, R.; Abe, S.; Yamada, K.; Hashizume, T.; Morishima, H. *Bioorg Med Chem* 2001, 9, 1571–1578.
232. Ronconi, L.; Marzano, C.; Zanello, P.; Corsini, M.; Miolo, G.; Macca, C.; Trevisan, A.; Fregona, D. *J Med Chem* 2006, 49, 1648–1657.
233. Abdulla, A.; Zhao, X.; Yang, F. *J Biochem Pharmacol Res* 2013, 1, 56–63.
234. Yu, W.; Fu, Y. C.; Wang, W. *J Cell Biochem* 2012, 113, 752–759.
235. Zhou, H.; Beevers, C. S.; Huang, S. *Curr Drug Targets* 2011, 12, 332–347.
236. Boots, A. W.; Haenen, G. R.; Bast, A. *Eur J Pharmacol* 2008, 585, 325–337.
237. Seidler, J.; McGovern, S. L.; Doman, T. N.; Shoichet, B. K. *J Med Chem* 2003, 46, 4477–4486.
238. Sorna, V.; Theisen, E. R.; Stephens, B.; Warner, S. L.; Bearss, D. J.; Vankayalapati, H.; Sharma, S. *J Med Chem* 2013, 56, 9496–9508.
239. Zhou, C.; Kang, D.; Xu, Y.; Zhang, L.; Zha, X. *Chem Biol Drug Des* 2014.
240. Prusevich, P.; Kalin, J. H.; Ming, S. A.; Basso, M.; Givens, J.; Li, X.; Hu, J.; Taylor, M. S.; Cieniewicz, A. M.; Hsiao, P. Y.; Huang, R.; Roberson, H.; Adejola, N.; Avery, L. B.; Casero, R. A., Jr.; Taverna, S. D.; Qian, J.; Tackett, A. J.; Ratan, R. R.; McDonald, O. G.; Feinberg, A. P.; Cole, P. A. *ACS Chem Biol* 2014, 9, 1284–1293.
241. Hakimi, M. A.; Bochar, D. A.; Chenoweth, J.; Lane, W. S.; Mandel, G.; Shiekhhattar, R. *Proc Natl Acad Sci USA* 2002, 99, 7420–7425.
242. Lee, M. G.; Wynder, C.; Cooch, N.; Shiekhhattar, R. *Nature* 2005, 437, 432–435.
243. Shi, Y.; Sawada, J.; Sui, G.; Affar el, B.; Whetstone, J. R.; Lan, F.; Ogawa, H.; Luke, M. P.; Nakatani, Y.; Shi, Y. *Nature* 2003, 422, 735–738.
244. Millard, C. J.; Watson, P. J.; Celardo, I.; Gordiyenko, Y.; Cowley, S. M.; Robinson, C. V.; Fairall, L.; Schwabe, J. W. *Mol Cell* 2013, 51, 57–67.
245. Yu, J.; Li, Y.; Ishizuka, T.; Guenther, M. G.; Lazar, M. A. *EMBO J* 2003, 22, 3403–3410.
246. Hwang, S.; Duke University, 2012.
247. Baron, R.; Vellore, N. A. *Proc Natl Acad Sci USA* 2012, 109, 12509–12514.
248. Baron, R.; Vellore, N. A. *Biochemistry* 2012, 51, 3151–3153.
249. Vellore, N. A.; Baron, R. *BMC Biophys* 2013, 6, 15.
250. Robertson, J. C.; Hurley, N. C.; Tortorici, M.; Ciossani, G.; Borrello, M. T.; Vellore, N. A.; Ganesan, A.; Mattevi, A.; Baron, R. *PLoS Comput Biol* 2013, 9, e1003158.
251. Barrios, A. P.; Gomez, A. V.; Saez, J. E.; Ciossani, G.; Toffolo, E.; Battaglioli, E.; Mattevi, A.; Andres, M. E. *Mol Cell Biol* 2014, 34, 2760–2770.
252. Upadhyay, G.; Chowdhury, A. H.; Vaidyanathan, B.; Kim, D.; Saleque, S. *Proc Natl Acad Sci USA* 2014, 111, 8071–8076.
253. Ballas, N.; Mandel, G. *Curr Opin Neurobiol* 2005, 15, 500–506.
254. Grimes, J. A.; Nielsen, S. J.; Battaglioli, E.; Miska, E. A.; Speh, J. C.; Berry, D. L.; Atouf, F.; Holdener, B. C.; Mandel, G.; Kouzarides, T. *Journal of Biological Chemistry* 2000, 275, 9461–9467.
255. Andres, M. E.; Burger, C.; Peral-Rubio, M. J.; Battaglioli, E.; Anderson, M. E.; Grimes, J.; Dallman, J.; Ballas, N.; Mandel, G. *Proc Natl Acad Sci USA* 1999, 96, 9873–9878.
256. Ballas, N.; Battaglioli, E.; Atouf, F.; Andres, M. E.; Chenoweth, J.; Anderson, M. E.; Burger, C.; Moniwa, M.; Davie, J. R.; Bowers, W. J.; Federoff, H. J.; Rose, D. W.; Rosenfeld, M. G.; Brehm, P.; Mandel, G. *Neuron* 2001, 31, 353–365.
257. Lunyak, V. V.; Burgess, R.; Prefontaine, G. G.; Nelson, C.; Sze, S. H.; Chenoweth, J.; Schwartz, P.; Pevzner, P. A.; Glass, C.; Mandel, G.; Rosenfeld, M. G. *Science* 2002, 298, 1747–1752.
258. Ballas, N.; Grunseich, C.; Lu, D. D.; Speh, J. C.; Mandel, G. *Cell* 2005, 121, 645–657.
259. Mulligan, P.; Westbrook, T. F.; Ottinger, M.; Pavlova, N.; Chang, B. J.; Macia, E.; Shi, Y. J.; Barretina, J.; Liu, J.; Howley, P. M.; Elledge, S. J.; Shi, Y. *Mol Cell* 2008, 32, 718–726.
260. Kim, B. J.; Kang, K. M.; Jung, S. Y.; Choi, H. K.; Seo, J. H.; Chae, J. H.; Cho, E. J.; Youn, H. D.; Qin, J.; Kim, S. T. *Biochem Biophys Res Commun* 2008, 372, 298–304.
261. Lan, F.; Collins, R. E.; De Cegli, R.; Alpatov, R.; Horton, J. R.; Shi, X.; Gozani, O.; Cheng, X.; Shi, Y. *Nature* 2007, 448, 718–722.
262. Kim, H. G.; Kim, H. T.; Leach, N. T.; Lan, F.; Ullmann, R.; Silahtaroglu, A.; Kurth, I.; Nowka, A.; Seong, I. S.; Shen, Y.; Talkowski, M. E.; Ruderfer, D.; Lee, J. H.; Glotzbach, C.; Ha, K.; Kjaergaard, S.; Levin, A. V.; Romeike, B. F.; Kleefstra, T.; Bartsch, O.; Elsea, S. H.; Jabs, E. W.; MacDonald, M. E.; Harris, D. J.; Quade, B. J.; Ropers, H. H.; Shaffer, L. G.; Kutsche, K.; Layman, L. C.; Tommerup, N.; Kalscheuer, V. M.; Shi, Y.; Morton, C. C.; Kim, C. H.; Gusella, J. F. *Am J Hum Genet* 2012, 91, 56–72.
263. Iwase, S.; Januma, A.; Miyamoto, K.; Shono, N.; Honda, A.; Yanagisawa, J.; Baba, T. *Biochem Biophys Res Commun* 2004, 322, 601–608.
264. Klajn, A.; Ferrai, C.; Stucchi, L.; Prada, I.; Podini, P.; Baba, T.; Rocchi, M.; Meldolesi, J.; D’Alessandro, R. *J Neurosci* 2009, 29, 6296–6307.
265. Roopra, A.; Qazi, R.; Schoenike, B.; Daley, T. J.; Morrison, J. F. *Mol Cell* 2004, 14, 727–738.
266. Lachner, M.; O’Carroll, D.; Rea, S.; Mechtler, K.; Jenuwein, T. *Nature* 2001, 410, 116–120.

267. Ceballos-Chavez, M.; Rivero, S.; Garcia-Gutierrez, P.; Rodriguez-Paredes, M.; Garcia-Dominguez, M.; Bhattacharya, S.; Reyes, J. C. *Proc Natl Acad Sci USA* 2012, 109, 8085–8090.
268. Rosendorff, A.; Sakakibara, S.; Lu, S.; Kieff, E.; Xuan, Y.; DiBacco, A.; Shi, Y.; Shi, Y.; Gill, G. *Proc Natl Acad Sci USA* 2006, 103, 5308–5313.
269. Wynder, C.; Hakimi, M. A.; Epstein, J. A.; Shilatfard, A.; Shiekhatar, R. *Nat Cell Biol* 2005, 7, 1113–1117.
270. Islam, M. M.; Zhang, C. L. *Biochim Biophys Acta* 2015, 1849, 210–216.
271. Yokoyama, A.; Takezawa, S.; Schule, R.; Kitagawa, H.; Kato, S. *Mol Cell Biol* 2008, 28, 3995–4003.
272. Sun, G.; Ye, P.; Murai, K.; Lang, M. F.; Li, S.; Zhang, H.; Li, W.; Fu, C.; Yin, J.; Wang, A.; Ma, X.; Shi, Y. *Nat Commun* 2011, 2, 529.
273. Hu, X.; Ybarra, R.; Qiu, Y.; Bungert, J.; Huang, S. *Epigenetics* 2009, 4, 357–361.
274. Huang, S. M.; Qiu, Y.; Stein, R. W.; Brandt, S. J. *Oncogene* 1999, 18, 4958–4967.
275. Huang, S.; Qiu, Y.; Shi, Y.; Xu, Z.; Brandt, S. J. *EMBO J* 2000, 19, 6792–6803.
276. Huang, S.; Brandt, S. J. *Mol Cell Biol* 2000, 20, 2248–2259.
277. O'Neil, J.; Shank, J.; Cusson, N.; Murre, C.; Kelliher, M. *Cancer Cell* 2004, 5, 587–596.
278. Xu, Z.; Meng, X.; Cai, Y.; Koury, M. J.; Brandt, S. J. *Biochem J* 2006, 399, 297–304.
279. Schuh, A. H.; Tipping, A. J.; Clark, A. J.; Hamlett, I.; Guyot, B.; Iborra, F. J.; Rodriguez, P.; Strouboulis, J.; Enver, T.; Vyas, P.; Porcher, C. *Mol Cell Biol* 2005, 25, 10235–10250.
280. Cai, Y.; Xu, Z.; Xie, J.; Ham, A. J.; Koury, M. J.; Hiebert, S. W.; Brandt, S. J. *Biochem Biophys Res Commun* 2009, 390, 295–301.
281. Hu, X.; Li, X.; Valverde, K.; Fu, X.; Noguchi, C.; Qiu, Y.; Huang, S. *Proc Natl Acad Sci USA* 2009, 106, 10141–10146.
282. Li, Y.; Deng, C.; Hu, X.; Patel, B.; Fu, X.; Qiu, Y.; Brand, M.; Zhao, K.; Huang, S. *Oncogene* 2012, 31, 5007–5018.
283. Chinnadurai, G. *Int J Biochem Cell Biol* 2007, 39, 1593–1607.
284. Chinnadurai, G. *Cancer Res* 2009, 69, 731–734.
285. Wang, J.; Scully, K.; Zhu, X.; Cai, L.; Zhang, J.; Prefontaine, G. G.; Krones, A.; Ohgi, K. A.; Zhu, P.; Garcia-Bassets, I.; Liu, F.; Taylor, H.; Lozach, J.; Jayes, F. L.; Korach, K. S.; Glass, C. K.; Fu, X. D.; Rosenfeld, M. G. *Nature* 2007, 446, 882–887.
286. Banck, M. S.; Li, S.; Nishio, H.; Wang, C.; Beutler, A. S.; Walsh, M. J. *Epigenetics* 2009, 4, 100–106.
287. Ray, S. K.; Li, H. J.; Metzger, E.; Schule, R.; Leiter, A. B. *Mol Cell Biol* 2014, 34, 2308–2317.
288. Cowger, J. J.; Zhao, Q.; Isovich, M.; Torchia, J. *Oncogene* 2007, 26, 3378–3386.
289. Gocke, C. B.; Yu, H. *PLoS One* 2008, 3, e3255.
290. Quinlan, K. G.; Nardini, M.; Verger, A.; Francescato, P.; Yaswen, P.; Corda, D.; Bolognesi, M.; Crossley, M. *Mol Cell Biol* 2006, 26, 8159–8172.
291. Quinlan, K. G.; Verger, A.; Kwok, A.; Lee, S. H.; Perdomo, J.; Nardini, M.; Bolognesi, M.; Crossley, M. *Mol Cell Biol* 2006, 26, 8202–8213.
292. Kuppaswamy, M.; Vijayalingam, S.; Zhao, L. J.; Zhou, Y.; Subramanian, T.; Ryerse, J.; Chinnadurai, G. *Mol Cell Biol* 2008, 28, 269–281.
293. Zhang, C. L.; McKinsey, T. A.; Lu, J. R.; Olson, E. N. *J Biol Chem* 2001, 276, 35–39.
294. Castet, A.; Boulahtouf, A.; Versini, G.; Bonnet, S.; Augereau, P.; Vignon, F.; Khochbin, S.; Jalaguier, S.; Cavailles, V. *Nucleic Acids Res* 2004, 32, 1957–1966.
295. Fernandes, I.; Bastien, Y.; Wai, T.; Nygard, K.; Lin, R.; Cormier, O.; Lee, H. S.; Eng, F.; Bertos, N. R.; Pelletier, N.; Mader, S.; Han, V. K.; Yang, X. J.; White, J. H. *Mol Cell* 2003, 11, 139–150.
296. Ueda, J.; Tachibana, M.; Ikura, T.; Shinkai, Y. *J Biol Chem* 2006, 281, 20120–20128.
297. Caron, C.; Pivot-Pajot, C.; van Grunsven, L. A.; Col, E.; Lestrat, C.; Rousseaux, S.; Khochbin, S. *EMBO Rep* 2003, 4, 877–882.
298. Basta, J.; Rauchman, M. *Transl Res* 2015, 165, 36–47.
299. Allen, H. F.; Wade, P. A.; Kutateladze, T. G. *Cell Mol Life Sci* 2013, 70, 3513–3524.
300. Ouyang, H.; Qin, Y.; Liu, Y.; Xie, Y.; Liu, J. *PLoS One* 2013, 8, e62192.
301. Sankar, S.; Bell, R.; Stephens, B.; Zhuo, R.; Sharma, S.; Bearss, D. J.; Lessnick, S. L. *Oncogene* 2013, 32, 5089–5100.
302. Smits, A. H.; Jansen, P. W.; Poser, I.; Hyman, A. A.; Vermeulen, M. *Nucleic Acids Res* 2013, 41, e28.
303. Li, Q.; Shi, L.; Gui, B.; Yu, W.; Wang, J.; Zhang, D.; Han, X.; Yao, Z.; Shang, Y. *Cancer Res* 2011, 71, 6899–6908.
304. Gu, H.; Liang, Y.; Mandel, G.; Roizman, B. *Proc Natl Acad Sci USA* 2005, 102, 7571–7576.
305. Gu, H.; Roizman, B. *J Virol* 2009, 83, 4376–4385.
306. Pinnoji, R. C.; Bedadala, G. R.; George, B.; Holland, T. C.; Hill, J. M.; Hsia, S. C. V. *Virology Journal* 2007, 4, 56–66.
307. Du, T.; Zhou, G.; Khan, S.; Gu, H.; Roizman, B. *Proc Natl Acad Sci USA* 2010, 107, 15904–15909.
308. Zhou, G.; Du, T.; Roizman, B. *Proc Natl Acad Sci USA* 2013, 110, E498–506.
309. Wysocka, J.; Herr, W. *Trends Biochem Sci* 2003, 28, 294–304.
310. Liang, Y.; Vogel, J. L.; Arbuckle, J. H.; Rai, G.; Jadhav, A.; Simeonov, A.; Maloney, D. J.; Kristie, T. M. *Sci Transl Med* 2013, 5, 167ra165.
311. Rai, G.; Kawamura, A.; Tumber, A.; Liang, Y.; Vogel, J. L.; Arbuckle, J. H.; Rose, N. R.; Dexheimer, T. S.; Foley, T. L.; King, O. N.; Quinn, A.; Mott, B. T.; Schofield, C. J.; Oppermann, U.; Jadhav, A.; Simeonov, A.; Kristie, T. M.; Maloney, D. J. In *Probe Reports from the NIH Molecular Libraries Program*; National Center for Biotechnology Information: Bethesda, MD, 2012.
312. Kalamvoki, M.; Roizman, B. *Proc Natl Acad Sci USA* 2010, 107, 17721–17726.
313. Bag, P.; Ojha, D.; Mukherjee, H.; Halder, U. C.; Mondal, S.; Biswas, A.; Sharon, A.; Van Kaer, L.; Chakrabarty, S.; Das, G.; Mitra, D.; Chattopadhyay, D. *Antiviral Res* 2014, 105, 126–134.
314. Gu, H.; Roizman, B. *Proc Natl Acad Sci USA* 2007, 104, 17134–17139.
315. Everett, R. D. *J Virol* 2010, 84, 3695–3698.
316. Zhou, Y.; Bolton, E. C.; Jones, J. O. *J Mol Endocrinol* 2015, 54, R15–29.
317. Cai, C.; He, H. H.; Chen, S.; Coleman, I.; Wang, H.; Fang, Z.; Chen, S.; Nelson, P. S.; Liu, X. S.; Brown, M.; Balk, S. P. *Cancer Cell* 2011, 20, 457–471.
318. Thomas, C.; Gustafsson, J. A. *Nat Rev Cancer* 2011, 11, 597–608.

319. Hervouet, E.; Cartron, P. F.; Jouvenot, M.; Delage-Mourroux, R. *Epigenetics* 2013, 8, 237–245.
320. Garcia-Bassets, I.; Kwon, Y. S.; Telese, F.; Prefontaine, G. G.; Hutt, K. R.; Cheng, C. S.; Ju, B. G.; Ohgi, K. A.; Wang, J.; Escoubet-Lozach, L.; Rose, D. W.; Glass, C. K.; Fu, X. D.; Rosenfeld, M. G. *Cell* 2007, 128, 505–518.
321. Nair, S. S.; Nair, B. C.; Cortez, V.; Chakravarty, D.; Metzger, E.; Schule, R.; Brann, D. W.; Tekmal, R. R.; Vadlamudi, R. K. *EMBO Rep* 2010, 11, 438–444.
322. Kim, J.; Park, U. H.; Moon, M.; Um, S. J.; Kim, E. J. *FEBS Lett* 2013, 587, 17–22.
323. Ombra, M. N.; Di Santi, A.; Abbondanza, C.; Migliaccio, A.; Avvedimento, E. V.; Perillo, B. *Biochim Biophys Acta* 2013, 1829, 480–486.
324. Chiang, C.; Ayyanathan, K. *Cytokine Growth Factor Rev* 2013, 24, 123–131.
325. Ferrari-Amorotti, G.; Fragliasso, V.; Esteki, R.; Prudente, Z.; Soliera, A. R.; Cattelani, S.; Manzotti, G.; Grisendi, G.; Dominici, M.; Pieraccioli, M.; Raschella, G.; Chiodoni, C.; Colombo, M. P.; Calabretta, B. *Cancer Res* 2013, 73, 235–245.
326. Lin, Y.; Dong, C.; Zhou, B. P. *Curr Pharm Des* 2014, 20, 1698–1705.
327. Lin, Y.; Kang, T.; Zhou, B. P. *Cell Cycle* 2014, 13, 1708–1716.
328. Lin, S.; Shen, H.; Li, J. L.; Tang, S.; Gu, Y.; Chen, Z.; Hu, C.; Rice, J. C.; Lu, J.; Wu, L. *J Biol Chem* 2013, 288, 6238–6247.
329. Zhang, J.; Bonasio, R.; Strino, F.; Kluger, Y.; Holloway, J. K.; Modzelewski, A. J.; Cohen, P. E.; Reinberg, D. *Genes Dev* 2013, 27, 749–766.
330. van der Meer, L. T.; Jansen, J. H.; van der Reijden, B. A. *Leukemia* 2010, 24, 1834–1843.
331. Kazanjian, A.; Gross, E. A.; Grimes, H. L. *Crit Rev Oncol Hematol* 2006, 59, 85–97.
332. Huang, M.; Hu, Z.; Chang, W.; Ou, D.; Zhou, J.; Zhang, Y. *Acta Haematol* 2010, 123, 1–5.
333. Valk, P. J.; Verhaak, R. G.; Beijen, M. A.; Erpelinck, C. A.; Barjesteh van Waalwijk van Doorn-Khosrovani, S.; Boer, J. M.; Beverloo, H. B.; Moorhouse, M. J.; van der Spek, P. J.; Lowenberg, B.; Delwel, R. *N Engl J Med* 2004, 350, 1617–1628.
334. Vassen, L.; Khandanpour, C.; Ebeling, P.; van der Reijden, B. A.; Jansen, J. H.; Mahlmann, S.; Duhren, U.; Moroy, T. *Int J Hematol* 2009, 89, 422–430.
335. Xu, W.; Kee, B. L. *Blood* 2007, 109, 4406–4414.
336. Chowdhury, A. H.; Ramroop, J. R.; Upadhyay, G.; Sengupta, A.; Andrzejczyk, A.; Saleque, S. *PLoS One* 2013, 8, e53666.
337. Laurent, B.; Randrianarison-Huetz, V.; Frisan, E.; Andrieu-Soler, C.; Soler, E.; Fontenay, M.; Dusanter-Fourt, I.; Dumenil, D. *J Cell Sci* 2012, 125, 993–1002.
338. Vassen, L.; Fiolka, K.; Moroy, T. *EMBO J* 2006, 25, 2409–2419.
339. Tsai, M. C.; Manor, O.; Wan, Y.; Mosammaparast, N.; Wang, J. K.; Lan, F.; Shi, Y.; Segal, E.; Chang, H. Y. *Science* 2010, 329, 689–693.
340. Vicent, G. P.; Nacht, A. S.; Zaurin, R.; Font-Mateu, J.; Soronellas, D.; Le Dily, F.; Reyes, D.; Beato, M. *Genes Dev* 2013, 27, 1179–1197.
341. Porro, A.; Feuerhahn, S.; Lingner, J. *Cell Rep* 2014, 6, 765–776.
342. Lee, J. T. *Science* 2012, 338, 1435–1439.
343. Moran, V. A.; Perera, R. J.; Khalil, A. M. *Nucleic Acids Res* 2012, 40, 6391–6400.
344. Prensner, J. R.; Chinnaiyan, A. M. *Cancer Discov* 2011, 1, 391–407.
345. Tsai, M. C.; Spitale, R. C.; Chang, H. Y. *Cancer Res* 2011, 71, 3–7.
346. Spitale, R. C.; Tsai, M. C.; Chang, H. Y. *Epigenetics* 2011, 6, 539–543.
347. Gupta, R. A.; Shah, N.; Wang, K. C.; Kim, J.; Horlings, H. M.; Wong, D. J.; Tsai, M. C.; Hung, T.; Argani, P.; Rinn, J. L.; Wang, Y.; Brzoska, P.; Kong, B.; Li, R.; West, R. B.; van de Vijver, M. J.; Sukumar, S.; Chang, H. Y. *Nature* 2010, 464, 1071–1076.
348. Li, X.; Wu, Z.; Mei, Q.; Li, X.; Guo, M.; Fu, X.; Han, W. *Br J Cancer* 2013, 109, 2266–2278.
349. Kim, K.; Jutooru, I.; Chadalapaka, G.; Johnson, G.; Frank, J.; Burghardt, R.; Kim, S.; Safe, S. *Oncogene* 2013, 32, 1616–1625.
350. Kogo, R.; Shimamura, T.; Mimori, K.; Kawahara, K.; Imoto, S.; Sudo, T.; Tanaka, F.; Shibata, K.; Suzuki, A.; Komune, S.; Miyano, S.; Mori, M. *Cancer Res* 2011, 71, 6320–6326.
351. Bhan, A.; Hussain, I.; Ansari, K. I.; Kasiri, S.; Bashyal, A.; Mandal, S. S. *J Mol Biol* 2013, 425, 3707–3722.
352. Rinn, J. L.; Kertesz, M.; Wang, J. K.; Squazzo, S. L.; Xu, X.; Bruggmann, S. A.; Goodnough, L. H.; Helms, J. A.; Farnham, P. J.; Segal, E.; Chang, H. Y. *Cell* 2007, 129, 1311–1323.
353. Li, L.; Liu, B.; Wapinski, O. L.; Tsai, M. C.; Qu, K.; Zhang, J.; Carlson, J. C.; Lin, M.; Fang, F.; Gupta, R. A.; Helms, J. A.; Chang, H. Y. *Cell Rep* 2013, 5, 3–12.
354. Li, J. T.; Wang, L. F.; Zhao, Y. L.; Yang, T.; Li, W.; Zhao, J.; Yu, F.; Wang, L.; Meng, Y. L.; Liu, N. N.; Zhu, X. S.; Gao, C. F.; Jia, L. T.; Yang, A. G. *Breast Cancer Res* 2014, 16, 454.
355. Zhang, K.; Sun, X.; Zhou, X.; Han, L.; Chen, L.; Shi, Z.; Zhang, A.; Ye, M.; Wang, Q.; Liu, C.; Wei, J.; Ren, Y.; Yang, J.; Zhang, J.; Pu, P.; Li, M.; Kang, C. *Oncotarget* 2015, 6, 537–546.
356. Cai, B.; Song, X. Q.; Cai, J. P.; Zhang, S. *Neoplasma* 2014, 61, 379–391.
357. Wu, Y.; Zhang, L.; Wang, Y.; Li, H.; Ren, X.; Wei, F.; Yu, W.; Wang, X.; Zhang, L.; Yu, J.; Hao, X. *Tumour Biol* 2014, 35, 9531–9538.
358. Beato, M.; Vicent, G. P. *Transcription* 2013, 4, 167–171.
359. Katz, T. A.; Vasilatos, S. N.; Harrington, E.; Oesterreich, S.; Davidson, N. E.; Huang, Y. *Breast Cancer Res Treat* 2014, 146, 99–108.



## A rationally-designed chimeric KDM1A/KDM1B histone demethylase tower domain deletion mutant retaining enzymatic activity



Jonathan M. Burg<sup>a</sup>, Alan T. Makhoul<sup>b</sup>, Charles W. Pemble IV<sup>c,1</sup>, Jennifer E. Link<sup>a</sup>, Frederick J. Heller<sup>b</sup>, Dewey G. McCafferty<sup>a,\*</sup>

<sup>a</sup>Department of Chemistry, Duke University, Durham, NC, USA

<sup>b</sup>Trinity College of Arts & Sciences, Duke University, Durham, NC, USA

<sup>c</sup>Duke University Human Vaccine Institute Macromolecular Crystallography Center, Duke University School of Medicine, Durham, NC, USA

### ARTICLE INFO

#### Article history:

Received 13 May 2015

Revised 19 July 2015

Accepted 20 July 2015

Available online 29 July 2015

Edited by Ned Mantei

#### Keywords:

KDM1A/LSD1

Tower domain

Chimera

Deletion mutant

Enzyme engineering

CoREST

### ABSTRACT

**A target with therapeutic potential, lysine-specific demethylase 1A (KDM1A) is a regulator of gene expression whose tower domain is a protein–protein interaction motif. This domain facilitates the interaction of KDM1A with coregulators and multiprotein complexes that direct its activity to nucleosomes. We describe the design and characterization of a chimeric ‘towerless’ KDM1A, termed nΔ150 KDM1AΔTower KDM1B chimera (chKDM1AΔTower), which incorporates a region from the paralog lysine-specific demethylase 1B (KDM1B). This chimera copurifies with FAD and displays demethylase activity, but fails to bind the partner protein corepressor of the RE1-silencing transcription factor (CoREST). We conclude that KDM1A catalysis can be decoupled from tower-dependent interactions, lending chKDM1AΔTower useful for dissecting molecular contributions to KDM1A function.**

© 2015 Published by Elsevier B.V. on behalf of the Federation of European Biochemical Societies.

### 1. Introduction

In 2004, lysine-specific demethylase 1A (KDM1A also known as LSD1/BHC110/AOF2/KIAA0601/p110b) became the first histone demethylase to be isolated and characterized [1] and has subsequently been identified as a potential therapeutic target [2–4]. KDM1A is a flavin-dependent amine oxidase that demethylates mono- and dimethylated lysine residues at positions 4 and 9 on histone H3 (H3K4me1/2 and H3K9me1/2), leading to gene activation and repression, respectively [1,5,6]. This 852 amino acid (aa)

**Abbreviations:** AOD, amine oxidase domain; chKDM1AΔTower, nΔ150 KDM1AΔTower KDM1B chimera; CoREST, corepressor of the RE1-silencing transcription factor; KDM1A, lysine-specific demethylase 1A; KDM1B, lysine-specific demethylase 1B; SWIRM, SWI3p, Rsc8p, and Moira

**Author Contributions:** J.B. and D.M. conceived this study; J.B., C.P., and D.M. planned experiments; J.B., A.M., C.P., J.L., and F.H. executed experiments and gathered data; J.B. and D.M. analyzed data; J.B., J.L., and D.M. wrote and edited the manuscript; D.M. supervised all aspects of this study.

\* Corresponding author at: Department of Chemistry, Duke University, B120 Levine Science Research Center, Box 90346, 450 Research Drive, Durham, NC 27708-0346, USA.

E-mail address: [dewey.mccafferty@duke.edu](mailto:dewey.mccafferty@duke.edu) (D.G. McCafferty).

<sup>1</sup> Present address: Rigaku Americas Corporation, The Woodlands, TX, USA.

<http://dx.doi.org/10.1016/j.febslet.2015.07.028>

0014-5793/© 2015 Published by Elsevier B.V. on behalf of the Federation of European Biochemical Societies.

polypeptide is composed of three structured domains (Fig. 1A). The catalytic amine oxidase domain (AOD) houses a single, non-covalently bound flavin adenine dinucleotide (FAD) cofactor required for catalysis while the N-terminal SWI3p, Rsc8p, and Moira (SWIRM) domain is commonly found in chromatin-associating proteins (Fig. 1B) [7–10]. The ‘tower’ domain is a nearly 100 aa AOD insert that forms an approximately 90 Å long antiparallel coiled-coil from two α-helices (termed TαA and TαB) linked by a tight turn (Fig. 1B) [7,8]. Unprecedented among related amine oxidases [1], the tower domain serves as a protein interaction motif and facilitates KDM1A incorporation into multiprotein regulatory complexes that dictate its cellular function [11].

One of the best-studied tower domain interaction partners is the corepressor of the RE1-silencing transcription factor (CoREST/RCOR1/KIAA0071), which facilitates demethylation of nucleosomal substrates by bridging KDM1A to chromatin through its DNA-binding SANT domains [8,12–17]. Additionally, CoREST orchestrates the inclusion of enzymes such as KDM1A and histone deacetylases as catalytic subunits within modular multiprotein complexes [18,19]. KDM1A activity is further governed by other homologous proteins that bind the tower domain and perform similar functions in different molecular contexts, such as the

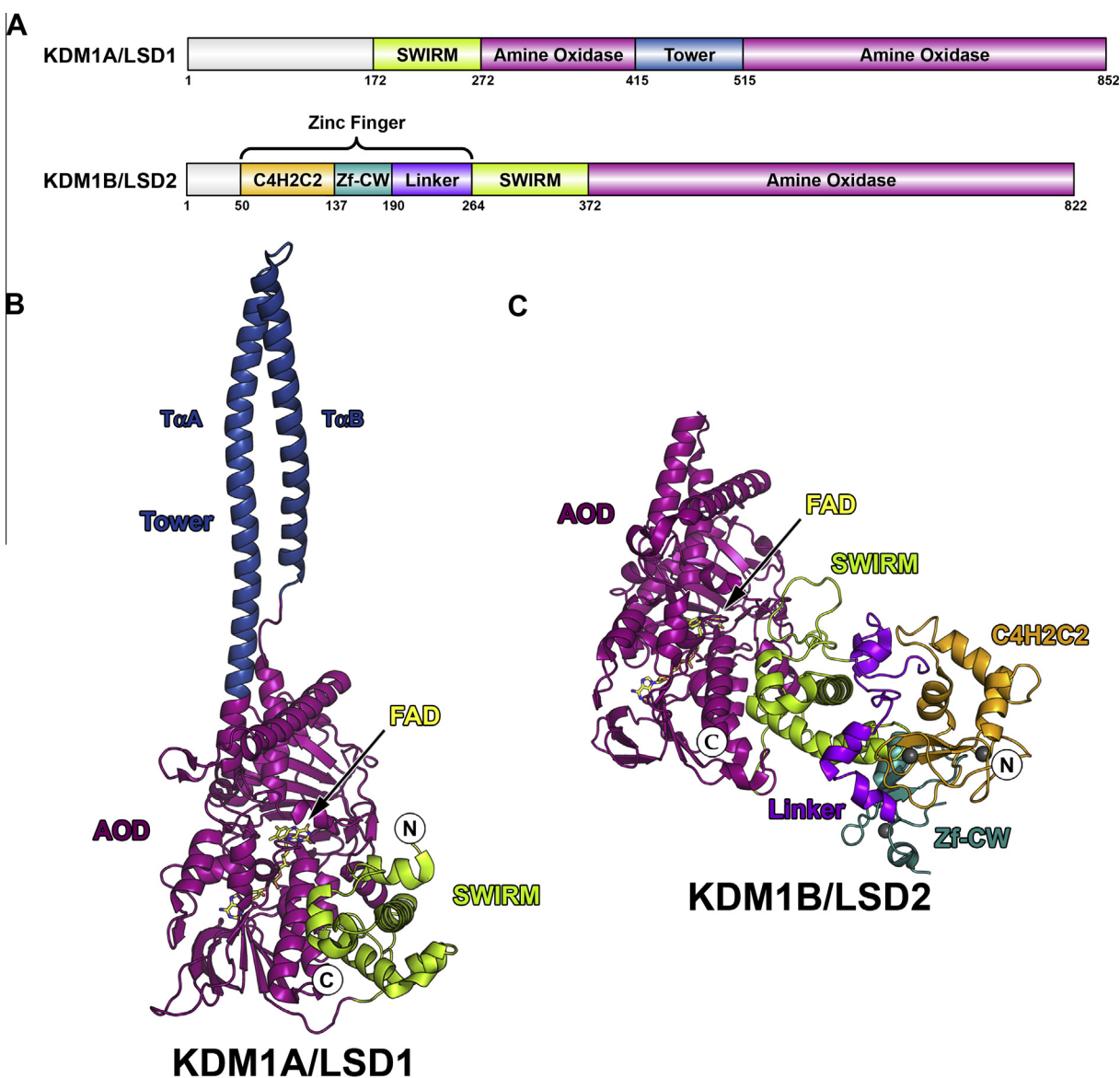


**Fig. 1.** Domain maps and structural overview of KDM1A and KDM1B. (A) Domain maps of KDM1A and KDM1B. SWIRM domains are shown in green, AODs are shown in magenta, tower domain is shown in blue, C4H2C2 domain is shown in orange, Zf-CW domain is shown in cyan, and linker is shown in purple. Structural overview of (B) KDM1A (PDB 2IW5) and (C) KDM1B (PDB 4HSU). Coloring scheme follows that of domain map above, FAD cofactor is shown in yellow, and N and C-termini are labeled. Zinc ions in KDM1B structure are shown as gray spheres.

CoREST paralogs RCOR2 and RCOR3 and the MTA proteins [17,20–22]. Therefore, one of the most significant challenges is understanding the impact of these tower-dependent interactions on KDM1A specificity, catalysis, and positioning within chromatin.

In order to evaluate these tower-dependent interactions independent of demethylase activity, a KDM1A tower domain deletion mutant is highly desired. Indeed, several groups have generated such mutants, but were limited by a lack of enzymatic activity [7,8,21,23]. These studies suggest that either the tower domain is inherently required for KDM1A catalysis or that the methods chosen to bridge the tower region were not conducive to proper active site folding. Interestingly the recent characterization of the KDM1A paralog KDM1B provides a unique opportunity to investigate this dichotomy [24]. KDM1B lacks a tower domain (Fig. 1A) but conserves the AOD architecture, sharing a 2.0 Å RMSD compared to KDM1A, despite a modest sequence similarity (<25%) (Fig. 1B and C). As this paralog overcomes exclusion of the tower

domain in a manner that preserves a KDM1A-like active site conformation, we sought to use it as a template for engineering a chimeric KDM1A enzyme.

Here we report the rational design and characterization of a KDM1A tower domain deletion chimera. KDM1A and KDM1B sequence and structural alignments suggested that KDM1B residues V494–L531 could replace the KDM1A tower domain (residues T389–R524) with minimal active site disturbance. This construct, termed chKDM1A $\Delta$ Tower, copurified from *Escherichia coli* cellular lysates with a stoichiometric equivalent of FAD. As expected, chKDM1A $\Delta$ Tower failed to bind CoREST. However, unlike previous tower deletion mutants, our chimera exhibits kinetic parameters nearly identical to those of unaltered KDM1A and KDM1B, suggesting that the tower domain is not required for catalytic activity. The chKDM1A $\Delta$ Tower chimera therefore decouples tower-dependent protein interactions from catalysis and provides a tool to assess the effects of KDM1A mistargeting and orphanization.

## 2. Materials and methods

### 2.1. Reagents and materials

Clones of genes encoding *Homo sapiens* n $\Delta$ 150 KDM1A (UniProtKB accession No. O60341) and full-length KDM1B (UniProtKB accession No. Q8NB78) were codon optimized for *E. coli* by GenScript (Piscataway, NJ) and subcloned into pET-15b (Novagen) with NdeI and XhoI (New England Biolabs; NEB). The pDB-HisGST vector was obtained from the DNASU Plasmid Repository. Buffer salts were obtained from Sigma, EMD Millipore, and JT Baker. Tween 20 was obtained from AMRESCO. Protein purification was conducted using an ÄKTA FPLC (Amersham Biosciences).

### 2.2. Alignment of KDM1A and KDM1B and generation of a chimera model

Primary amino acid sequences of KDM1A and KDM1B were aligned using Clustal Omega [25]. A sequence alignment figure (Fig. 2A) was generated utilizing ESPript 3.0 [26]. Structural alignment of PDB files 2IW5 and 4HSU (KDM1A [13] and KDM1B [27], respectively) was conducted with PyMOL [28] (Fig. 2B). To generate a composite model of the chimera, the headers of PDB files 2IW5 and 4HSU were deleted and coordinates superimposed using Coot [29]. KDM1A tower domain residues T389–R524 were replaced with KDM1B residues V494–L531. The resultant chain was renumbered and coordinates of the chimera composite model exported into PyMOL (Fig. 2C). All-atom contacts were validated with MolProbity [30].

### 2.3. Cloning of chKDM1A $\Delta$ Tower

Joining KDM1A fragments L151–A388 and D525–M852 to KDM1B residues V494–L531 formed the chimera sequence. A previously described pET-15b vector containing 6 $\times$ His n $\Delta$ 150 KDM1A (residues 151–852) [31] was used as a template for construction of the chimera. This entire vector was amplified with exclusion of the KDM1A tower domain (residues T389–R524) using primers that incorporated Sall and KpnI restriction sites and PFU Turbo DNA polymerase (Agilent) under the following conditions: an initial denaturation step for 2 min at 95 °C, 30 cycles of denaturation for 30 s at 95 °C, annealing for 30 s over a gradient from 54 to 65 °C, elongation for 8 min at 72 °C, and a final elongation step for 10 min at 72 °C. The KDM1B insert (residues V494–L531) was amplified with complementary restriction sites under similar conditions, but with an elongation of 1 min at 72 °C. The resulting insert and vector were digested and ligated utilizing a Quick Ligation Kit (NEB). Restriction sites were removed using a Q5 Site-Directed Mutagenesis Kit (NEB) under the following conditions: an initial denaturation step for 1 min at 98 °C, 30 cycles of denaturation for 30 s at 98 °C, annealing for 30 s over a gradient from 59 to 70 °C, elongation for 4 min at 72 °C, and a final elongation step for 2 min at 72 °C. For primers, see Table S1.

### 2.4. Expression and purification of KDM1A and chKDM1A $\Delta$ Tower

Expression and purification of wild type n $\Delta$ 150 KDM1A was conducted as previously described [15,31]. The 6 $\times$ His-tagged n $\Delta$ 150 KDM1A $\Delta$ Tower KDM1B chimera in pET-15b (i.e. chKDM1A $\Delta$ Tower) was expressed in BL21 Star (DE3) *E. coli* (Invitrogen) at 15 °C. chKDM1A $\Delta$ Tower was purified under similar conditions to wild type n $\Delta$ 150 KDM1A with minor modifications. Approximately 4.5 mg of chKDM1A $\Delta$ Tower per liter of culture were obtained at >95% purity. For more details, please see the Supplementary Material.

### 2.5. Cofactor analysis of chKDM1A $\Delta$ Tower

The method of Aliverti et al. was employed to determine the FAD molar extinction coefficient [32]. chKDM1A $\Delta$ Tower in gel filtration buffer at 1.5–2.0 mg/mL was incubated with SDS to a final concentration of 0.3% (w/v) and monitored until the UV trace stabilized. 15  $\mu$ M FAD disodium salt hydrate (Sigma) in gel filtration buffer was used as a standard. The chimera was calculated to copurify with FAD in 1.1:1 ratio (FAD:protein) and to have a molar extinction coefficient of 10350 M<sup>-1</sup> cm<sup>-1</sup> at 455 nm using  $\epsilon_{450} = 11300$  M<sup>-1</sup> cm<sup>-1</sup> for free FAD (FAD<sub>free</sub>). This value was routinely used to determine protein concentration.

### 2.6. Expression and purification of His-GST-CoREST-C and His-GST

The His-GST-CoREST-C construct was expressed in BL21 (DE3) *E. coli* (Novagen) at 19 °C. Protein was purified by immobilized metal affinity chromatography (IMAC) and ion exchange chromatography (IEC). Approximately 2.0 mg protein per liter of culture were obtained at >75% purity. The His-GST construct was expressed and purified in a similar manner. For more details, see the Supplementary Material.

### 2.7. Steady-state demethylase assay

A peptide corresponding to the N-terminal 21 amino acids of histone H3 with a dimethylated K4 residue (H3K4me<sup>2</sup>-<sup>21</sup>) was prepared as previously described [31,33]. A continuous, fluorescence-based, steady-state kinetic assay was employed as previously described with slight modifications [31,33]. An HRP-coupled (1 U/mL of HRP) assay monitored enzymatic peroxide production in 50 mM Tris-HCl (pH 7.85) with 0.01% (w/v) CHAPS using Amplex Red (50  $\mu$ M) as the fluorogenic electron acceptor. All measurements were performed in a final volume of 60  $\mu$ L at 25 °C in 96-well format (Corning 3693). Reactions were initiated with the addition of enzyme (0.35  $\mu$ M final concentration). The product, resorufin, was monitored with 535 nm excitation and 597 nm emission wavelengths. Data were analyzed using GraphPad Prism 6.0 (GraphPad Software, San Diego, CA). All data sets were corrected for background and zero by subtraction of the no enzyme control and the initial time point, respectively. Initial velocities within the 10% product conversion limit were fit to the Henri-Michaelis-Menten equation with non-linear regression analysis.

### 2.8. His-GST-CoREST-C pull-down interaction assay

A total of 15  $\mu$ g of purified His-GST-CoREST-C (residues 286–482) or 9  $\mu$ g His-GST were incubated with 12  $\mu$ g n $\Delta$ 150 KDM1A or 10  $\mu$ g chKDM1A $\Delta$ Tower at 4 °C for 16 h in 100  $\mu$ L of binding buffer (137 mM NaCl, 2.7 mM KCl, 10 mM Na<sub>2</sub>HPO<sub>4</sub>, 1.8 mM KH<sub>2</sub>PO<sub>4</sub> (pH 7.4), 10 mM DTT, and 0.05% (v/v) Tween 20) containing 20  $\mu$ L of Glutathione Sepharose 4 Fast Flow beads (GE Healthcare). Flow-through (supernatant) was removed and beads were washed 3 times with 400  $\mu$ L of binding buffer, resuspended in 80  $\mu$ L of 2 $\times$  SDS sample buffer, and denatured for 2 min at 100 °C. Input, beads (bound), and flow-through were analyzed by SDS-PAGE (4–20% gradient, Bio-Rad) and visualized with Coomassie Brilliant Blue.

## 3. Results

### 3.1. Design of the chKDM1A $\Delta$ Tower chimera from KDM1A and KDM1B alignments

To rationally design a tower domain deletion mutant of KDM1A, we looked to its 'towerless' paralog KDM1B, which performs



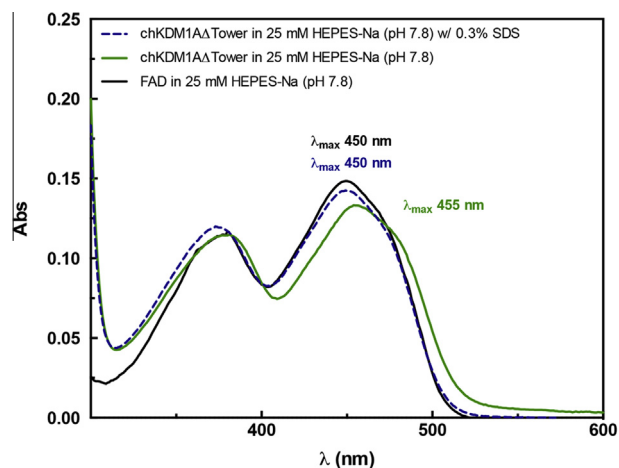


**Fig. 3.** chKDM1AΔTower copurifies with a non-covalently bound FAD cofactor. chKDM1AΔTower was evaluated by UV–Vis and has absorption maxima at 380 and 455 nm (solid green line). The chimera was denatured by treatment with SDS, releasing the cofactor (dashed blue line). The spectrum of the denatured sample directly overlays with a FAD standard (solid black line).

### 3.3. chKDM1AΔTower exhibits similar demethylase activity as KDM1A and KDM1B

As the chKDM1AΔTower-bound flavin chromophore is suggestive of properly assembled catalytic machinery, we next tested for bona fide enzymatic activity. Steady-state kinetic parameters of chKDM1AΔTower were evaluated by monitoring enzymatic production of H<sub>2</sub>O<sub>2</sub> using a peptide substrate. As shown in Fig. 4, chKDM1AΔTower exhibited well-behaved linear velocities and demethylated H3K4me2<sup>1–21</sup> with a  $K_m^{app}$  of  $3.21 \pm 0.16 \mu\text{M}$ , a  $k_{cat}^{app}$  of  $0.57 \pm 0.01 \text{ min}^{-1}$ , and a catalytic efficiency of  $0.18 \pm 0.01 \mu\text{M}^{-1} \text{ min}^{-1}$ . These values compare very favorably to that of wild type KDM1A and KDM1B enzymes (Table 1). In fact, the  $k_{cat}^{app}/K_m^{app}$  of chKDM1AΔTower was identical to that of KDM1B, and only approximately 10-fold lower than that of KDM1A [24,31]. Interestingly, values of both  $K_m^{app}$  and  $k_{cat}^{app}$  of the chimera were situated neatly near those of the two enzymes (Table 1). These data suggest that chKDM1AΔTower preserves elements from both KDM1A and KDM1B as anticipated, and clearly maintains integrity of the amine oxidase active site. Thus, by grafting the KDM1B loop onto KDM1A, we generated a tower domain deletion mutant that retains wild type-like demethylase activity.

### 3.4. chKDM1AΔTower does not interact with KDM1A binding partner CoREST

Having achieved one of our goals in engineering an active KDM1A tower deletion mutant, we next determined if a known tower domain interacting protein was precluded from binding to the chimera. The tower domain of wild type KDM1A is a well-known protein recruitment motif for CoREST [8,12,13]. We therefore hypothesized that this interaction would be abrogated in the chimera. A GST pull-down assay previously used to evaluate CoREST binding to wild type KDM1A was employed to assess if chKDM1AΔTower interacts with the C-terminal region of CoREST (CoREST-C; residues 286–482) [12]. Immobilized His-GST-CoREST-C or His-GST were incubated with either wild type KDM1A or chKDM1AΔTower, extensively washed, and the input, flow-through, and bound proteins visualized by SDS-PAGE. As previously reported, His-GST-CoREST-C significantly bound wild type KDM1A as compared to the GST control. Conversely, immobilized His-GST-CoREST-C showed no enrichment for chKDM1AΔTower

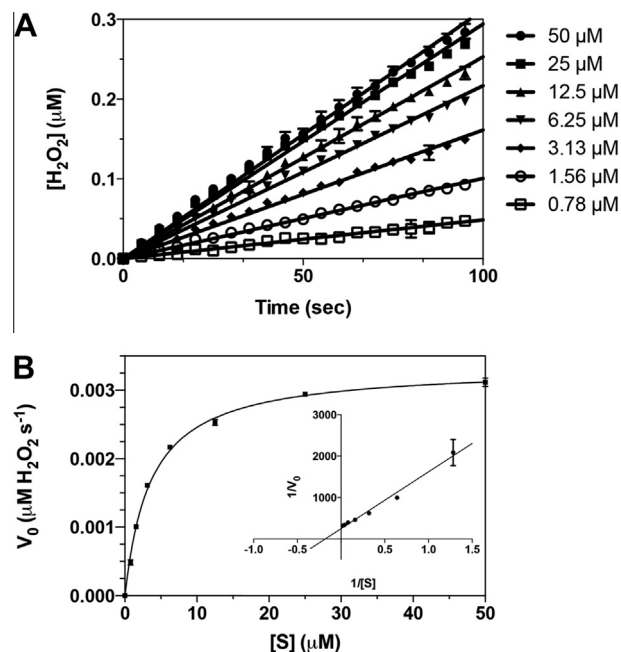


**Fig. 4.** chKDM1AΔTower is an active enzyme. (A) Representative linear fit of initial rates from substrate titration against chKDM1AΔTower. Plots are within 10% product conversion. Concentrations indicated are that of the H3K4me2<sup>1–21</sup> peptide substrate. (B) Representative initial velocity curve of the catalytic activity of chKDM1AΔTower. Data are fit to the Henri–Michaelis–Menten equation. Inset is a reciprocal plot,  $1/V_0$  ( $\text{s } \mu\text{M}^{-1} \text{ H}_2\text{O}_2$ ) vs.  $1/[S]$  ( $\mu\text{M}^{-1}$ ), to illustrate linear nature of data.

**Table 1**  
Kinetic Parameters of the Catalytic Activity of chKDM1AΔTower with the First 21 Amino Acids of H3 Dimethylated at K4 (H3K4me2<sup>1–21</sup>).

Enzyme Name	$K_m^{app}$ ( $\mu\text{M}$ )	$k_{cat}^{app}$ ( $\text{min}^{-1}$ )	$k_{cat}^{app}/K_m^{app}$ ( $\mu\text{M}^{-1} \text{ min}^{-1}$ )
nΔ150 KDM1A wt <sup>a,b</sup>	$2.60 \pm 0.2$	$5.97 \pm 0.78$	$2.28 \pm 0.12$
nΔ25 mKDM1B wt <sup>c</sup>	$11.3 \pm 1.3$	$2.00 \pm 0.60$	$0.18 \pm 0.04$
chKDM1AΔTower <sup>a</sup>	$3.21 \pm 0.16$	$0.57 \pm 0.01$	$0.18 \pm 0.01$

<sup>a</sup> In 50 mM Tris–HCl (pH 7.85), 0.01% CHAPS (w/v), 50  $\mu\text{M}$  Amplex Red & 1 U/mL HRP at 25 °C in air saturated buffer; peptide titrated from 50  $\mu\text{M}$  to 0 in 2-fold dilution series ( $n = 3$ ).

<sup>b</sup> Values reported by Gaweska et al. [31].

<sup>c</sup> Values reported by Karytinis et al. [24].

compared to the control (Fig. 5). These data are in agreement with previous reports that KDM1A interaction with the C-terminal fragment of CoREST in vitro is mediated mainly through the tower domain and does not receive significant contributions from the AOD and SWIRM domains [8,13]. Hence our chimera effectively abrogates association with CoREST, and presumably any other protein that relies predominantly on the tower domain for binding.

## 4. Discussion

There is currently a remarkable lack of tools for studying the influence of tower-dependent interactions on KDM1A recruitment into modular multiprotein complexes, substrate specificity, and chromatin localization. To address this issue, we here report what is, to the best of our knowledge, the first KDM1A tower deletion enzyme that retains catalytic activity comparable to wild type KDM1A and KDM1B. Using sequence and structure-driven design principles, we have rationally selected boundaries for excision of the KDM1A tower domain and replacement with a bridging segment from KDM1B. This chimera, termed chKDM1AΔTower, copurifies with a stoichiometric equivalent of FAD and exhibits catalytic

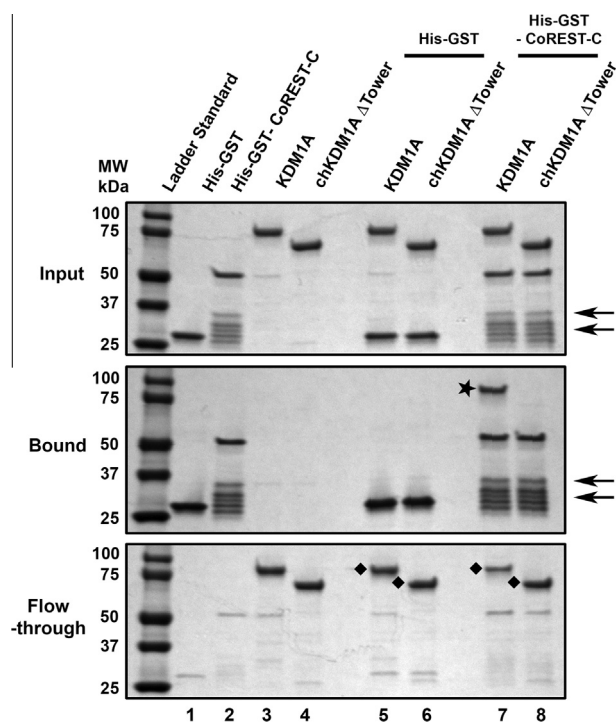


**Fig. 5.** Unlike wild type KDM1A, chKDM1A $\Delta$ Tower is incapable of interacting with CoREST. Comparable wild type and deletion mutant of KDM1A (chKDM1A $\Delta$ Tower) were incubated with glutathione Sepharose beads in the presence or absence of His-GST-CoREST-C or His-GST (negative control). The input (top), bound (middle), and flow-through (bottom) proteins were analyzed by SDS-PAGE. The star (★) in middle indicates bound KDM1A (lane 7) and the diamonds (◆) in bottom indicate the unbound KDM1A (lanes 5 and 7) and chKDM1A $\Delta$ Tower (lanes 6 and 8) after incubation with His-GST-CoREST-C or His-GST. The arrows indicate major truncation products of the His-GST-CoREST-C protein.

demethylase activity commensurate with its parent enzymes. Additionally, our *in vitro* pull-down studies demonstrate that the absence of a tower domain in chKDM1A $\Delta$ Tower precludes the tower-dependent binding interaction observed between CoREST and KDM1A, effectively uncoupling catalysis from tower-dependent interactions.

Our rational design demonstrates that the tower domain is not required for catalytic demethylation, thereby overcoming the catalytic inactivity of previously reported KDM1A tower deletion mutants. We suspect the catalytic deficiencies of these mutants may be attributed to subtle changes in active site geometry that alter substrate positioning [35]. However, it appears that insertion of the bridging KDM1B sequence instead mimics the native span between KDM1A residues A388 and D525 and facilitates folding of the chimera into a catalytically competent conformation. Although the catalytic efficiency of chKDM1A $\Delta$ Tower varies only minimally from that of KDM1A, we cannot rule out the possibility that our design may yet be catalytically suboptimal.

By combining catalytic activity with the lack of a tower domain, our chimera provides a much-needed probe for dissecting the influence of tower-dependent protein interactions on KDM1A function. KDM1A and KDM1B are believed to assemble in a modular fashion into larger, multivalent complexes that dictate their intracellular function [11]. As the tower domain is responsible for a large number of KDM1A interactions, chKDM1A $\Delta$ Tower provides an ideal tool for determining the effects of removing KDM1A from the control of its interaction partners. We predict this will likely result in mistargeting of the enzyme on chromatin and alteration of downstream genetic programming. For example, we suspect that chKDM1A $\Delta$ Tower will no longer localize with CoREST

in their coregulated promoter regions, thereby functionally disrupting the transcriptional programs for this subset of genes. Beyond KDM1A, this strategy of splicing related regions between functionally related proteins may prove to be an invaluable tool for investigating domains for which standard domain deletion proves intractable. This strategy is specifically useful when investigating enzymes that exist as subunits of multimeric complexes.

## Acknowledgements

We thank members of the McCafferty laboratory for their thoughtful insight during the preparation of this manuscript. This work was kindly supported by the U.S. DoD CDMRP Grant W81XWH-13-1-0400 (to D.G.M.) and by NIH Predoctoral Training Grants and T32-GM008487-19 in Structural Biology and Biophysics (to J.M.B.) and T32-GM007105-39 in Pharmacological Sciences (to J.E.L.).

## Appendix A. Supplementary data

Supplementary data associated with this article can be found, in the online version, at <http://dx.doi.org/10.1016/j.febslet.2015.07.028>.

## References

- Shi, Y., Lan, F., Matson, C., Mulligan, P., Whetstone, J.R., Cole, P.A., Casero, R.A. and Shi, Y. (2004) Histone demethylation mediated by the nuclear amine oxidase homolog LSD1. *Cell* 119, 941–953.
- Friso, S., Carvajal, C.A., Fardella, C.E. and Olivieri, O. (2015) Epigenetics and arterial hypertension: the challenge of emerging evidence. *Transl. Res.* 165, 154–165.
- Kristie, T.M. (2015) Dynamic modulation of HSV chromatin drives initiation of infection and provides targets for epigenetic therapies. *Virology* 479–480, 555–561.
- Hojfeldt, J.W., Agger, K. and Helin, K. (2013) Histone lysine demethylases as targets for anticancer therapy. *Nat. Rev. Drug Discovery* 12, 917–930.
- Metzger, E., Wissmann, M., Yin, N., Muller, J.M., Schneider, R., Peters, A.H., Gunther, T., Buettner, R. and Schule, R. (2005) LSD1 demethylates repressive histone marks to promote androgen-receptor-dependent transcription. *Nature* 437, 436–439.
- Laurent, B., Ruitu, L., Murn, J., Hempel, K., Ferrao, R., Xiang, Y., Liu, S., Garcia, B.A., Wu, H., Wu, F., Steen, H. and Shi, Y. (2015) A specific LSD1/KDM1A isoform regulates neuronal differentiation through H3K9 demethylation. *Mol. Cell* 57, 957–970.
- Stavropoulos, P., Blobel, G. and Hoelz, A. (2006) Crystal structure and mechanism of human lysine-specific demethylase-1. *Nat. Struct. Mol. Biol.* 13, 626–632.
- Chen, Y., Yang, Y., Wang, F., Wan, K., Yamane, K., Zhang, Y. and Lei, M. (2006) Crystal structure of human histone lysine-specific demethylase 1 (LSD1). *Proc. Natl. Acad. Sci. U.S.A.* 103, 13956–13961.
- Da, G., Lenkart, J., Zhao, K., Shiekhattar, R., Cairns, B.R. and Marmorstein, R. (2006) Structure and function of the SWIRM domain, a conserved protein module found in chromatin regulatory complexes. *Proc. Natl. Acad. Sci. U.S.A.* 103, 2057–2062.
- Aravind, L. and Iyer, L.M. (2002) The SWIRM domain: a conserved module found in chromosomal proteins points to novel chromatin-modifying activities. *Genome Biol.* 3, Research0039.
- Burg, J.M., Link, J.E., Morgan, B.S., Heller, F.J., Hargrove, A.E. and McCafferty, D.G. (2015) KDM1 class flavin-dependent protein lysine demethylases. *Biopolymers* 104, 213–246.
- Shi, Y.J., Matson, C., Lan, F., Iwase, S., Baba, T. and Shi, Y. (2005) Regulation of LSD1 histone demethylase activity by its associated factors. *Mol. Cell* 19, 857–864.
- Yang, M., Gocke, C.B., Luo, X., Borek, D., Tomchick, D.R., Machius, M., Otwinowski, Z. and Yu, H. (2006) Structural basis for CoREST-dependent demethylation of nucleosomes by the human LSD1 histone demethylase. *Mol. Cell* 23, 377–387.
- Lee, M.G., Wynder, C., Cooch, N. and Shiekhattar, R. (2005) An essential role for CoREST in nucleosomal histone 3 lysine 4 demethylation. *Nature* 437, 432–435.
- Hwang, S., Schmitt, A.A., Luteran, A.E., Toone, E.J. and McCafferty, D.G. (2011) Thermodynamic characterization of the binding interaction between the histone demethylase LSD1/KDM1 and CoREST. *Biochemistry* 50, 546–557.
- Kim, S.A., Chatterjee, N., Jennings, M.J., Bartholomew, B. and Tan, S. (2015) Extracellular DNA enhances the activity of the LSD1/CoREST histone demethylase complex. *Nucleic Acids Res.* 43, 4868–4880.

- [17] Pilotto, S., Speranzini, V., Tortorici, M., Durand, D., Fish, A., Valente, S., Forneris, F., Mai, A., Sixma, T.K., Vachette, P. and Mattevi, A. (2015) Interplay among nucleosomal DNA, histone tails, and corepressor CoREST underlies LSD1-mediated H3 demethylation. *Proc. Natl. Acad. Sci. U.S.A.* 112, 2752–2757.
- [18] You, A., Tong, J.K., Grozinger, C.M. and Schreiber, S.L. (2001) CoREST is an integral component of the CoREST-human histone deacetylase complex. *Proc. Natl. Acad. Sci. U.S.A.* 98, 1454–1458.
- [19] Lee, M.G., Wynder, C., Bochar, D.A., Hakimi, M.A., Cooch, N. and Shiekhhattar, R. (2006) Functional interplay between histone demethylase and deacetylase enzymes. *Mol. Cell. Biol.* 26, 6395–6402.
- [20] Upadhyay, G., Chowdhury, A.H., Vaidyanathan, B., Kim, D. and Saleque, S. (2014) Antagonistic actions of Rcor proteins regulate LSD1 activity and cellular differentiation. *Proc. Natl. Acad. Sci. U.S.A.* 111, 8071–8076.
- [21] Wang, Y., Zhang, H., Chen, Y., Sun, Y., Yang, F., Yu, W., Liang, J., Sun, L., Yang, X., Shi, L., Li, R., Li, Y., Zhang, Y., Li, Q., Yi, X. and Shang, Y. (2009) LSD1 is a subunit of the NuRD complex and targets the metastasis programs in breast cancer. *Cell* 138, 660–672.
- [22] Barrios, A.P., Gomez, A.V., Saez, J.E., Ciossani, G., Toffolo, E., Battaglioli, E., Mattevi, A. and Andres, M.E. (2014) Differential properties of transcriptional complexes formed by the CoREST family. *Mol. Cell. Biol.* 34, 2760–2770.
- [23] Lin, Y., Wu, Y., Li, J., Dong, C., Ye, X., Chi, Y.L., Evers, B.M. and Zhou, B.P. (2010) The SNAG domain of Snail1 functions as a molecular hook for recruiting lysine-specific demethylase 1. *EMBO J.* 29, 1803–1816.
- [24] Karytinis, A., Forneris, F., Profumo, A., Ciossani, G., Battaglioli, E., Binda, C. and Mattevi, A. (2009) A novel mammalian flavin-dependent histone demethylase. *J. Biol. Chem.* 284, 17775–17782.
- [25] Larkin, M.A., Blackshields, G., Brown, N.P., Chenna, R., McGettigan, P.A., McWilliam, H., Valentin, F., Wallace, I.M., Wilm, A., Lopez, R., Thompson, J.D., Gibson, D.G. and Higgins, D.G. (2007) Clustal W and Clustal X version 2.0. *Bioinformatics* 23, 2947–2948.
- [26] Robert, X. and Gouet, P. (2014) Deciphering key features in protein structures with the new ENDscript server. *Nucleic Acids Res.* 42, W320–W324.
- [27] Chen, F., Yang, H., Dong, Z., Fang, J., Wang, P., Zhu, T., Gong, W., Fang, R., Shi, Y.G., Li, Z. and Xu, Y. (2013) Structural insight into substrate recognition by histone demethylase LSD2/KDM1b. *Cell Res.* 23, 306–309.
- [28] The PyMOL Molecular Graphics System, Version 1.5.0.4, Schrödinger, LLC.
- [29] Emsley, P., Lohkamp, B., Scott, W.G. and Cowtan, K. (2010) Features and development of Coot. *Acta Crystallogr. D Biol. Crystallogr.* 66, 486–501.
- [30] Chen, V.B., Arendall 3rd, W.B., Headd, J.J., Keedy, D.A., Immormino, R.M., Kapral, G.J., Murray, L.W., Richardson, J.S. and Richardson, D.C. (2010) MolProbity: all-atom structure validation for macromolecular crystallography. *Acta Crystallogr. D Biol. Crystallogr.* 66, 12–21.
- [31] Gaweska, H., Henderson Pozzi, M., Schmidt, D.M., McCafferty, D.G. and Fitzpatrick, P.F. (2009) Use of pH and kinetic isotope effects to establish chemistry as rate-limiting in oxidation of a peptide substrate by LSD1. *Biochemistry* 48, 5440–5445.
- [32] Aliverti, A., Curti, B. and Vanoni, M.A. (1999) Identifying and quantitating FAD and FMN in simple and in iron-sulfur-containing flavoproteins. *Methods Mol. Biol.* 131, 9–23.
- [33] Schmidt, D.M. and McCafferty, D.G. (2007) Trans-2-phenylcyclopropylamine is a mechanism-based inactivator of the histone demethylase LSD1. *Biochemistry* 46, 4408–4416.
- [34] Macheroux, P. (1999) UV-visible spectroscopy as a tool to study flavoproteins. *Methods Mol. Biol.* 131, 1–7.
- [35] Fraaije, M.W. and Mattevi, A. (2000) Flavoenzymes: diverse catalysts with recurrent features. *Trends Biochem. Sci.* 25, 126–132.

This document is confidential and is proprietary to the American Chemical Society and its authors. Do not copy or disclose without written permission. If you have received this item in error, notify the sender and delete all copies.

**Lysine-Specific Demethylase 1A (KDM1A/LSD1): Product Recognition and Kinetic Analysis of Full-Length Histones**

Journal:	<i>Biochemistry</i>
Manuscript ID	bi-2015-01135w
Manuscript Type:	Article
Date Submitted by the Author:	17-Oct-2015
Complete List of Authors:	Burg, Jonathan; Duke University, Department of Chemistry Gonzalez, Julie; Duke University Maksimchuk, Kenneth; Duke University, Department of Biochemistry McCafferty, Dewey; Duke University, Department of Chemistry

SCHOLARONE™  
Manuscripts

1  
2  
3  
4  
5  
6  
7  
8  
9  
10  
11  
12  
13  
14  
15  
16  
17  
18  
19  
20  
21  
22  
23  
24  
25  
26  
27  
28  
29  
30  
31  
32  
33  
34  
35  
36  
37  
38  
39  
40  
41  
42  
43  
44  
45  
46  
47  
48  
49  
50  
51  
52  
53  
54  
55  
56  
57  
58  
59  
60

# Lysine-Specific Demethylase 1A (KDM1A/LSD1): Product Recognition and Kinetic Analysis of Full-Length Histones

Jonathan M. Burg,<sup>†</sup> Julie J. Gonzalez,<sup>‡</sup> Kenneth R. Maksimchuk,<sup>⊥,§</sup> Dewey G.

McCafferty\*,<sup>†</sup>

<sup>†</sup>Department of Chemistry, B120 Levine Science Research Center, Box 90317, Duke  
University, Durham, North Carolina 27708, United States

<sup>‡</sup>Trinity College of Arts & Sciences, Duke University, Durham, North Carolina 27708,  
United States

<sup>⊥</sup>Department of Biochemistry, 255 Nanaline H. Duke, Box 3711, Duke University  
Medical Center, Durham, North Carolina 27710, United States

**ABBREVIATIONS**

1  
2  
3  
4  
5  
6  
7  
8  
9  
10  
11  
12  
13  
14  
15  
16  
17  
18  
19  
20  
21  
22  
23  
24  
25  
26  
27  
28  
29  
30  
31  
32  
33  
34  
35  
36  
37  
38  
39  
40  
41  
42  
43  
44  
45  
46  
47  
48  
49  
50  
51  
52  
53  
54  
55  
56  
57  
58  
59  
60

3,5-DCHBS, sodium 3,5-dichloro-2-hydroxybenzenesulfonate; 4-AAP, 4-aminoantipyrine; AOD, amine oxidase domain; CHAPS, 3-[(3-cholamidopropyl)dimethylammonio]-1-propanesulfonate; FAD, flavin adenine dinucleotide; HRP, horseradish peroxidase; IMAC, immobilized metal affinity chromatography; IPTG, isopropyl  $\beta$ -D-thiogalactoside; KDM1A, lysine-specific demethylase 1A; KDM1B, lysine-specific demethylase 1B; LB, lysogeny broth; LSD1, lysine-specific demethylase 1A; PMT, photomultiplier tube; PTM, posttranslational modification; RU, response units; SDS, sodium dodecyl sulfate; SWIRM, SWI3p, Rsc8p, and Moira; TB, Terrific Broth; THF, tetrahydrofolate; U, units

1  
2  
3 **ABSTRACT:** Lysine-specific demethylase 1A (KDM1A/LSD1) is a FAD-dependent  
4 enzyme that catalyzes the oxidative demethylation of histone H3K4me1/2 and  
5 H3K9me1/2 repressing and activating transcription, respectively. Although the active site  
6 is expanded compared to the greater amine oxidase superfamily, it is too sterically  
7 restricted to encompass the minimal 21-mer peptide substrate footprint. The remainder of  
8 the substrate/product is therefore expected to extend along the surface of KDM1A. We  
9 show that full-length histone H3 which lacks any posttranslational modifications is a  
10 tight-binding, competitive inhibitor of KDM1A demethylation activity with a  $K_i$  of  $18.9 \pm$   
11  $1.2$  nM; a value that is approximately 100-fold higher than the 21-mer peptide product.  
12 The relative H3 affinity is independent of preincubation time suggesting that H3 rapidly  
13 reaches equilibrium with KDM1A. Jump dilution experiments confirmed the increased  
14 binding affinity of full-length H3 was at least partially due to a slow off-rate ( $k_{\text{off}}$ ) of  $1.2 \times$   
15  $10^{-3} \text{ s}^{-1}$ , a half-life ( $t_{1/2}$ ) of 9.63 min, and residence time ( $\tau$ ) of 13.9 min. Independent  
16 affinity capture surface plasmon resonance experiments confirmed the tight-binding  
17 nature of the H3/KDM1A interaction, revealing a  $K_d$  of  $9.02 \pm 2.27$  nM, a  $k_{\text{on}}$  of  $9.26 \times$   
18  $10^4 \pm 1.5 \times 10^4 \text{ M}^{-1} \text{ s}^{-1}$  and a  $k_{\text{off}}$  of  $8.35 \times 10^{-4} \pm 3.4 \times 10^{-5} \text{ s}^{-1}$ . Additionally, no other core  
19 histones exhibited inhibition of KDM1A demethylation activity, which is consistent with  
20 H3 being the preferred histone substrate of KDM1A versus H2A, H2B, and H4. Together  
21 these data suggest that KDM1A likely contains a histone H3 secondary specificity  
22 element on the enzyme surface that contributes significantly to its recognition of  
23 substrates and products.  
24  
25  
26  
27  
28  
29  
30  
31  
32  
33  
34  
35  
36  
37  
38  
39  
40  
41  
42  
43  
44  
45  
46  
47  
48  
49  
50  
51  
52  
53  
54  
55  
56  
57  
58  
59  
60

1  
2  
3 Chromatin condensation and relaxation and the dynamic regulation of gene  
4 expression are regulated by posttranslational modifications (PTMs) of histone proteins by  
5 epigenetic enzyme complexes.<sup>1, 2</sup> Dysregulation of histone-modifying enzymes within  
6 these complexes underscores several disease pathologies, including cancers.<sup>3</sup> As such,  
7 this class of enzymes has become the subject of intense inquiry for their potential role as  
8 targets for therapeutic intervention. Among these PTMs is histone lysine methylation, a  
9 mark that is intimately linked to both transcriptional activation and repression.<sup>4</sup>

10  
11  
12  
13  
14  
15  
16  
17  
18  
19  
20 Although evidence of enzymatic demethylation of histones would arise with the  
21 work of Paik and Kim in 1973,<sup>5</sup> it would not be until almost four decades later that an  
22 enzyme directly responsible for this activity would be uncovered. The isolation and  
23 characterization of lysine-specific demethylase 1A (KDM1A also known as  
24 LSD1/AOF2/BHC110/KIAA0601/p110b) by Shi and coworkers provided direct evidence  
25 that histone lysine methylation was, in fact, a reversible mark.<sup>6</sup> KDM1A is a flavin-  
26 dependent amine oxidase that catalyzes the removal of methyl groups of mono- and  
27 dimethylated lysine residues at position 4 and 9 on histone H3 (H3K4me1/2 and  
28 H3K9me1/2, respectively).<sup>6-8</sup> From N- to C-terminus, KDM1A is composed of an  
29 unstructured region that contains the nuclear localization signal<sup>9, 10</sup> and three structured  
30 domains: a SWI3p, Rsc8p, and Moira (SWIRM) domain, an amine oxidase domain  
31 (AOD), and an unprecedented intervening domain within the AOD colloquially known as  
32 the tower (Figure 1A).<sup>11, 12</sup>

33  
34  
35  
36  
37  
38  
39  
40  
41  
42  
43  
44  
45  
46  
47  
48  
49  
50 More specifically, the tower domain KDM1A is composed of two antiparallel  $\alpha$ -  
51 helices (termed T $\alpha$ A and T $\alpha$ B) that form a coiled-coil and extend approximately 100 Å  
52 away from the AOD (Figure 1B).<sup>11, 12</sup> Functionally, this domain is the site of association  
53  
54  
55  
56  
57  
58  
59  
60

1  
2  
3 with the corepressor of the RE1-silencing transcription factor (CoREST also known as  
4 CoREST1/RCOR1/KIAA0071) as well as several homologous proteins (Figure 1B).<sup>12-15</sup>  
5  
6 Interestingly, CoREST endows KDM1A with the ability to demethylate nucleosomal  
7  
8 substrates as a non-catalytic domain donor with DNA binding ability bridging the gap  
9  
10 between KDM1A and its substrates.<sup>15-19</sup> On the other hand, the SWIRM domain of  
11  
12 KDM1A, which is found in multiple chromatin-associated proteins,<sup>20</sup> is a bundle of  $\alpha$ -  
13  
14 helices with a central helix that is joined by two smaller helix-turn-helix motifs (Figure  
15  
16 1B).<sup>11</sup> Moreover, consistent with other flavin-dependent oxidoreductases, the AOD of  
17  
18 KDM1A houses a non-covalently bound flavin adenine dinucleotide (FAD) cofactor and  
19  
20 can be further subdivided into an expanded Rossmann fold for cofactor binding and the  
21  
22 substrate-binding lobe (Figure 1B).<sup>12, 15</sup> Although, these characteristics group KDM1A  
23  
24 into the larger family of flavoenzymes, the structure of the AOD does contain unique  
25  
26 features due to the functional activity of the enzyme.  
27  
28  
29  
30  
31  
32  
33

34 As compared to other amine oxidases, KDM1A contains a more expansive  
35  
36 substrate-binding cavity ( $\sim 1,245 \text{ \AA}^3$ ) that is suggested to compliment its broad substrate  
37  
38 specificity, including non-histone proteins.<sup>12, 21</sup> Additionally, although KDM1A requires  
39  
40 a peptide substrate of at least 21 residues representing the N-terminal portion of histone  
41  
42 H3 for efficient catalysis,<sup>22</sup> the active site cavity is too sterically restricted to  
43  
44 accommodate this entire fragment.<sup>12</sup> In efforts to decode substrate specificity, several  
45  
46 groups have co-crystallized peptides with KDM1A that revealed two main  
47  
48 conformations.<sup>23-25</sup> Interestingly, the conformations result in the C-terminus of the  
49  
50 peptide exiting the active site in different orientations. Further confounding these results,  
51  
52  
53  
54  
55  
56  
57  
58  
59  
60  
Luka and coworkers recently solved a structure of KDM1A in complex with

1  
2  
3 tetrahydrofolate (THF) and suggested that the cofactor may sterically disrupt one of the  
4 binding conformations.<sup>26</sup> Prior to this finding, several groups have suggested that  
5 KDM1A substrates exit the active site and extend along a conspicuous surface groove  
6 along the SWIRM-AOD interface aiding in substrate binding and recognition.<sup>11, 15, 27, 28</sup>  
7  
8  
9

10  
11  
12 Consistent with this hypothesis, mutational analyses of residues that lie in this  
13 groove greatly reduce or abrogate the catalytic efficiency of KDM1A.<sup>11</sup> Additionally,  
14 Tochio and coworkers demonstrated that an isolated SWIRM domain of KDM1A is able  
15 to bind the N-terminal tail of histone H3 via surface plasmon resonance (SPR) studies.<sup>29</sup>  
16  
17  
18  
19  
20  
21  
22  
23  
24  
25  
26  
27  
28  
29  
30  
31  
32  
33  
34  
35  
36  
37  
38  
39  
40  
41  
42  
43  
44  
45  
46  
47  
48  
49  
50  
51  
52  
53  
54  
55  
56  
57  
58  
59  
60

Confounding these results, however, a 30-mer H3 peptide substrate showed no apparent  
change in catalytic efficiency when compared to a 21-mer.<sup>22</sup> Additionally, none of the  
structural studies listed above revealed electron density in the cleft along the SWIRM-  
AOD interface, raising the question as to whether this phenomenon exists and if so where  
the secondary binding site resides.

Herein we describe the kinetic analysis of full-length histone products against  
KDM1A as a preliminary investigation as to whether or not the enzyme recognizes  
additional residues of its products. We now show that histone H3 is a tight-binding,  
competitive inhibitor of KDM1A demethylation activity and has a 100-fold higher  
affinity as compared to the 21-mer peptide product. Additionally, the potency of H3  
inhibition is independent of preincubation time suggesting that the enzyme and product  
reach rapid equilibrium. Through jump dilution experiments, we illustrate that the  
increased affinity is at least partially due to the slow off-rate of the full-length product.  
Additionally, the tight-binding nature of the histone H3 product interaction was  
independently confirmed via SPR. As suspected, no other histone proteins inhibit

1  
2  
3 KDM1A demethylation activity. Together, these results suggest that KDM1A contains a  
4  
5 secondary histone H3 binding site on the enzyme surface that contributes significantly to  
6  
7 recognition of its histone H3 substrates and products. Additionally, our work further  
8  
9 validates the suggested role of KDM1A as a contributor to the stabilization of associated  
10  
11 multiprotein complexes within genetic loci.  
12  
13  
14  
15  
16

## 17 **EXPERIMENTAL PROCEDURES**

19  
20 **Reagents and Materials.** The clone of the *Homo sapiens* protein nΔ150 KDM1A  
21  
22 (UniProtKB accession no. O60341; residues 151-852) was codon optimized for  
23  
24 expression in *Escherichia coli* and synthesized by GenScript (Piscataway, NJ). The pDB-  
25  
26 HisGST expression vector was obtained from the DNASU Plasmid Repository. Buffer  
27  
28 salts were obtained from Sigma, EMD Millipore, and JT Baker. *Trans*-2-  
29  
30 Phenylcyclopropylamine hydrochloride salt (2-PCPA), 4-AAP, and 3,5-DCHBS were  
31  
32 obtained from Sigma. Protein purification was conducted using an ÄKTA FPLC  
33  
34 (Amersham Biosciences).  
35  
36  
37  
38  
39  
40

41  
42 **Expression and Purification of nΔ150 KDM1A.** The gene encoding nΔ150  
43  
44 KDM1A was subcloned into a pET-15b vector (Novagen) containing an N-terminal  
45  
46 6xHis-tag with an intervening thrombin cleavage site, utilizing NdeI and XhoI restriction  
47  
48 enzymes. The clone was expressed and purified as previously reported with minor  
49  
50 modifications (See Supporting Information for detailed procedure).<sup>13,30</sup> The final  
51  
52 concentration of KDM1A was routinely determined by UV absorption spectroscopy  
53  
54  
55  
56  
57  
58  
59  
60

1  
2  
3 using an extinction coefficient of  $10,790 \text{ M}^{-1}\text{cm}^{-1}$  at 458 nm, which was determined after  
4  
5 protein denaturation using 0.3% (w/v) SDS.<sup>22, 31</sup>  
6  
7  
8  
9

10 **Expression and Purification of His-GST-CoREST-C.** The gene encoding  
11 CoREST-C (CoREST1/RCOR1: UniProtKB accession no. Q9UKL0; residues 286-482)  
12 from *H. sapiens* was subcloned into a pDB-HisGST expression vector, containing an N-  
13 terminal 6xHis-tag and GST-tag with an intervening tobacco etch virus protease (TEV)  
14 cleavage site, utilizing NdeI and XhoI restriction sites. The clone was expressed and  
15 purified as previously reported with minor modifications.<sup>32</sup> Following IMAC, fractions  
16 containing His-GST-CoREST-C were extensively dialyzed against GST-PBS dialysis  
17 buffer (137 mM NaCl, 2.7 mM KCl, 10 mM Na<sub>2</sub>HPO<sub>4</sub>, 1.8 mM KH<sub>2</sub>PO<sub>4</sub> (pH 7.4), 5 mM  
18 βME) overnight in 3.5 kDa MWCO SnakeSkin dialysis tubing (Thermo Scientific) and  
19 applied at 0.1 mL/min to 10 mL Glutathione Sepharose 4 Fast Flow resin (GE  
20 Healthcare). The column was washed at 2.0 mL/min with 5 CV of GST-PBS dialysis  
21 buffer followed by 10 CV of TEV cleavage buffer (50 mM Tris-HCl (pH 7.8), 150 mM  
22 NaCl, and 1 mM DTT). GST-tag cleavage was performed by incubating column-bound  
23 protein in a 0.1 to 1 ratio of 7xHis TEV (S219V), prepared by previously described  
24 methods,<sup>33</sup> to column bound protein overnight. Eluted CoREST-C was pooled and  
25 supplemented with 5 mM imidazole and passed over IMAC resin equilibrated with 50  
26 mM Tris-HCl (pH 7.8), 150 mM NaCl, and 5 mM imidazole to remove TEV protease.  
27 Samples containing CoREST-C were pooled and concentrated using 5 kDa MWCO  
28 Vivaspin 20 centrifugal filters at  $2000 \times g$ . Samples were aliquoted, flash frozen in liquid  
29 N<sub>2</sub> and stored at  $-80^{\circ}\text{C}$ . This method routinely provides protein at > 90% purity as  
30  
31  
32  
33  
34  
35  
36  
37  
38  
39  
40  
41  
42  
43  
44  
45  
46  
47  
48  
49  
50  
51  
52  
53  
54  
55  
56  
57  
58  
59  
60

1  
2  
3 assessed by SDS-PAGE and with typical yields of 1.5 mg per liter of culture as  
4  
5 determined by Bradford method.  
6  
7  
8  
9

10 **Expression and Purification of His-GST-CoREST-Linker.** The coding  
11 sequence of the linker region of CoREST (residues 293-380) was extracted and amplified  
12  
13 by using PCR with a forward primer (5'-  
14 GCGCATATGGTCAAAAAGAAAACATAGC-3') and a reverse primer (5'-  
15 GCGCTCGAGTTAATTACATTTCTGAATGACC-3') under the following conditions:  
16  
17 an initial denaturation step for 2 min at 95°C, 30 cycles of denaturation for 30 sec at  
18  
19 95°C, annealing for 30 min over a gradient from 54 to 65°C, elongation for 1 min at  
20  
21 72°C, and a final elongation step for 10 min at 72°C. The primers were designed to  
22  
23 contain NdeI and XhoI restriction sites at the N- and C-termini, respectively, to allow for  
24  
25 facile ligation into pDB-HisGST expression vector. The resulting His-GST-CoREST-  
26  
27 Linker construct was expressed and purified as described above for His-GST-CoREST-C.  
28  
29  
30  
31  
32  
33  
34  
35  
36  
37  
38

39 **Purification of KDM1A/CoREST Complexes.** Purified CoREST constructs  
40 were mixed with KDM1A in a 1.5:1 molar ratio and allowed to incubate for 1 h on ice.  
41  
42 Incubated samples were then purified using a HiPrep 26/60 Sephacryl S-200 HR (GE  
43  
44 Healthcare) column equilibrated with 25 mM HEPES-Na (pH 7.4), 200 mM NaCl, 1 mM  
45  
46  $\beta$ ME and eluted at a flow rate of 0.7 mL/min. The elution peaks had retention volumes  
47  
48 that corresponded to the molecular weight of the complexes. Formation was further  
49  
50 verified by SDS-PAGE. Complexes were stored at -20°C in gel filtration buffer with a  
51  
52 final concentration of 40% glycerol.  
53  
54  
55  
56  
57  
58  
59  
60

1  
2  
3  
4  
5  
6 **Expression and Purification of Histone Proteins.** Expression and purification of  
7  
8 core histone proteins was conducted by combining two previously reported methods with  
9  
10 minor modifications (See Supporting Information for detailed procedure).<sup>34, 35</sup>  
11  
12

13  
14  
15 **Synthesis and Purification of Histone H3 Substrate and Product Peptides.** A  
16  
17 peptide corresponding to the first 21 amino acids of the N-terminal tail of histone H3 that  
18  
19 incorporated a dimethylated lysine at residue 4 (H3K4me<sup>2</sup><sup>1-21</sup>) was synthesized and  
20  
21 purified as previously described.<sup>30, 36</sup> The unmodified 21-mer histone H3 product peptide  
22  
23 (H3<sup>1-21</sup>) was synthesized and purified in a similar fashion.  
24  
25  
26  
27  
28

29 **Steady-State Kinetic Assays.** Steady-state kinetic assays employing continuous  
30  
31 fluorescence or absorbance-based methods for detection of enzymatic peroxide  
32  
33 production (Figure S1) were performed as previously described with slight modifications  
34  
35 (See Supporting Information for details; Figures S2 & S3).<sup>30, 36</sup>  
36  
37  
38

39 KDM1A tolerance for 3-[(3-cholamidopropyl)dimethylammonio]-1-  
40  
41 propanesulfonate (CHAPS) and dimethyl sulfoxide (DMSO) was assessed in order to  
42  
43 confirm usable range of additives (Figure S4). DMSO seemingly increases initial velocity  
44  
45 of KDM1A within 2-fold under 10% DMSO (v/v). CHAPS concentration for disruption  
46  
47 of non-specific aggregation affects was kept at 0.01% (w/v) in inhibitor analyses. For all  
48  
49 *IC*<sub>50</sub> titrations, unless otherwise noted, substrate concentration was held at or near the  
50  
51 apparent *K*<sub>M</sub> (*K*<sub>M</sub><sup>app</sup>) in order to ensure an equal population of the free enzyme and *ES*  
52  
53 complex was available for inhibitor interactions.<sup>37, 38</sup>  
54  
55  
56  
57  
58  
59  
60

1  
2  
3  
4  
5  
6 **Steady-State Kinetic Data Analysis.** Steady-state kinetic data were analyzed  
7  
8 using GraphPad Prism 6.0 (GraphPad Software, San Diego, CA) or Grafit 4.0 (Erithacus  
9 Software, London, UK). Briefly, the no enzyme control (n=3) was subtracted from all  
10 data sets. Data was then forced through the origin by subtraction of the initial time point  
11 and responses converted to concentration units of H<sub>2</sub>O<sub>2</sub> (μM). Initial velocities were  
12 calculated via linear regression and responses were limited to within 10% total product  
13 conversion. Initial velocities were then plotted versus substrate concentrations and fit to  
14 the Henri-Michaelis-Menten equation (eq 1)<sup>39</sup> utilizing non-linear regression analysis:  
15  
16  
17  
18  
19  
20  
21  
22  
23  
24  
25  
26

$$v_0 = \frac{V_{max}[S]}{K_m + [S]} \quad (1)$$

27  
28  
29  
30  
31

32 where  $v_0$  is the experimental initial velocity,  $[S]$  is the substrate concentration,  $V_{max}$  is the  
33 maximal velocity at the utilized enzyme concentration, and  $K_M$  is the substrate  
34 concentration at half maximal velocity.  
35  
36  
37

38  
39 Dose-response curves were prepared by comparing initial rate data at specified  
40 inhibitor concentrations to a no inhibitor control and fit directly to eq 2:  
41  
42  
43  
44  
45

$$\frac{v_i}{v_0} = \frac{1}{1 + ([I]/IC_{50})^h} \quad (2)$$

46  
47  
48  
49  
50

51 where  $v_0$  is the initial velocity of the control,  $v_i$  is the inhibited initial velocity,  $[I]$  is the  
52 inhibitor concentration,  $IC_{50}$  is the inhibitor concentration at which the rate of  
53  
54  
55  
56  
57  
58  
59  
60

demethylation is half that of the control, and  $h$  is the Hill coefficient of the curve (slope factor).

The  $K_i$  of reversible, competitive inhibitors was determined by a titration of inhibitor versus substrate followed by global fitting of the data to eq 3:

$$v_0 = \frac{V_{max}[S]}{K_m(1 + \frac{[I]}{K_i}) + [S]} \quad (3)$$

where  $K_i$  is the equilibrium inhibitory constant.

As a secondary determination of  $K_i$ , we used the Cheng-Prusoff relationship for competitive inhibition<sup>40</sup>:

$$IC_{50} = K_i \left( 1 + \frac{[S]}{K_m} \right) \quad (4)$$

where  $IC_{50}$  is the inhibitor concentration at which the rate of demethylation is half that of the control as defined above in eq 2.

In order to define the apparent  $K_i$  ( $K_i^{app}$ ) value of inhibitors that fall in the tight-binding regime (i.e.  $\leq 10[E]_T$ ), dose-response data was fit to the Morrison's quadratic equation for tight-binding inhibition<sup>41</sup>:

$$\frac{v_i}{v_0} = 1 - \frac{([E]_T + [I]_T + K_i^{app}) - \sqrt{([E]_T + [I]_T + K_i^{app})^2 - 4[E]_T[I]_T}}{2[E]_T} \quad (5)$$

1  
2  
3 where  $[I]_T$  is the total inhibitor concentration,  $K_i^{app}$  is the apparent equilibrium  
4 dissociation constant for the enzyme-inhibitor complex, and  $[E]_T$  is the total enzyme  
5 concentration.  
6  
7  
8  
9

10 As a secondary determination of  $K_i^{app}$ , data was transformed for analysis via a  
11 Henderson plot<sup>42</sup> and fit to the following linear expression:  
12  
13  
14

$$\frac{[I]}{1 - \frac{v_i}{v_0}} = K_i^{app} \left( \frac{v_0}{v_i} \right) + [E] \quad (6)$$

15  
16  
17  
18  
19  
20  
21

22  $IC_{50}$  dependence on enzyme concentration for confirmation of tight-binding nature  
23 of inhibitor and as an additional means to determine  $K_i^{app}$  was fit to the following  
24 equation:  
25  
26  
27  
28  
29  
30  
31

$$IC_{50} = K_i^{app} + m[E]_T \quad (7)$$

32  
33  
34  
35  
36

37 where  $m$  is the linear slope.

38 In order to determine the equilibrium inhibitory constant ( $K_i$ ) of tight-binding  
39 competitive inhibitors, data was fit to following equation:  
40  
41  
42  
43  
44  
45

$$IC_{50} = K_i \left( 1 + \frac{[S]}{K_m} \right) + \frac{1}{2}[E]_T \quad (8)$$

46  
47  
48  
49  
50

51 **Determination of Dissociation Rates of H3 from KDM1A.** Rates of  
52 dissociation for the H3/KDM1A binary complex were determined by monitoring the  
53 recovery of activity following a 1 h preincubation that included  $50 \times K_i^{app}$  of histone H3  
54  
55  
56  
57  
58  
59  
60

1  
2  
3 (3.0  $\mu\text{M}$ ) and  $100\times [E]$  (2.5  $\mu\text{M}$  KDM1A) to ensure saturation of enzyme<sup>43</sup> (Note: H3<sup>1-21</sup>  
4 and 2-PCPA were incubated at  $10\times IC_{50}$  since they do not display tight-binding  
5 characteristics; 50  $\mu\text{M}$  and 200  $\mu\text{M}$ , respectively). Preincubated samples were diluted  
6 100-fold into assay buffer containing  $5\times K_M$  of H3K4me2<sup>1-21</sup> peptide substrate (25  $\mu\text{M}$ ),  
7  
8 50  $\mu\text{M}$  Amplex Red, and 1 U/mL HRP. Product was monitored continuously using  
9 absorbance maximum at 572 nm for resorufin. Progress curve data was fit to eq 9 to  
10 generate  $k_{\text{obs}}$ :  
11  
12  
13  
14  
15  
16  
17  
18  
19

$$y = v_s t + \frac{v_i - v_s}{k_{\text{obs}}} (1 - e^{-k_{\text{obs}} t}) + \text{background} \quad (9)$$

20  
21  
22  
23  
24  
25  
26  
27  
28 where  $v_i$  and  $v_s$  represent the initial and steady-state velocities respectively,  $k_{\text{obs}}$  is the  
29 apparent first-order rate constant for the transition from  $v_i$  to  $v_s$  and  $t$  is time. Under the  
30 experimental conditions used,  $k_{\text{obs}}$  approximates the dissociation rate constant ( $k_{\text{off}}$ ) of the  
31 enzyme-inhibitor complex. The enzyme-inhibitor dissociation half-life ( $t_{1/2}$ ) was  
32 calculated using the formula  $t_{1/2} = 0.693/k_{\text{off}}$  and residence time ( $\tau$ ) was calculated using  
33 the equation  $\tau = 1/k_{\text{off}}$ .  
34  
35  
36  
37  
38  
39  
40  
41  
42  
43  
44

45 **Surface Plasmon Resonance (SPR) Measurements.** All SPR measurements  
46 were made using a BIAcore 3000 instrument, and data analyses were performed using  
47 BIAevaluation version 4.1 (BIAcore). An anti-histone H3 antibody (Abcam, ab1791) was  
48 immobilized [ $\bullet$ 3000 response units (RU)] on a research grade BIAcore CM5 chip using  
49 EDC-sNHS coupling chemistry with reagents obtained from BIAcore according to  
50 manufacturer's protocol. In a parallel flow cell, an anti-lysozyme antibody (Abcam,  
51  
52  
53  
54  
55  
56  
57  
58  
59  
60

1  
2  
3 ab2408) was immobilized [ $\bullet$ 2800 response RU]. During the screening experiments with  
4 degassed 50 mM sodium phosphate (pH 7.4) and 1 mM DTT as a running buffer, H3 and  
5 lysozyme were injected over immobilized antibodies in respective flow cells for 2 min at  
6 a flow rate of 30  $\mu$ L/min and washed with running buffer until sensograms equilibrated.  
7  
8 KDM1A was then injected for 2 min at a flow rate of 30  $\mu$ L/min to  
9 monitor the binding interaction. The surfaces were regenerated via injection of 10  $\mu$ L of  
10 glycine (pH 2.0) at a flow rate of 50  $\mu$ L/min. The response from the KDM1A-lysozyme-  
11 anti-lysozyme antibody surface was used to subtract out the background (nonspecific)  
12 signal. The  $K_d$  value of the H3/KDM1A interaction was measured via injection of  
13 KDM1A for 2 min at various concentrations ranging from 5.0 to 50.0 nM. Global curve  
14 fitting to the 1:1 Langmuir binding model was used to determine the association ( $k_{on}$ ) and  
15 dissociation ( $k_{off}$ ) rates and the apparent equilibrium dissociation constant ( $K_d$ ).  
16  
17  
18  
19  
20  
21  
22  
23  
24  
25  
26  
27  
28  
29  
30  
31  
32  
33  
34

## 35 RESULTS

36  
37  
38  
39 **CoREST (CoREST1/RCOR1) Does Not Alter the Catalytic Efficiency of**  
40 **KDM1A Toward Minimal Peptide Substrates.** KDM1A requires a minimal substrate  
41 corresponding to the first 21 residues of the N-terminal histone H3 tail for efficient  
42 demethylation activity.<sup>22</sup> Although the enzyme itself is sufficient for demethylation of  
43 peptide and histone substrates; activity toward nucleosomes *in vitro* is regulated by its  
44 interaction with CoREST, the minimal portion of which contains the linker and SANT2  
45 domain or possibly the SANT1 domain.<sup>15, 16, 18</sup> As such, we wanted to evaluate KDM1A  
46 activity toward a peptide substrate in the presence and absence of various CoREST  
47  
48  
49  
50  
51  
52  
53  
54  
55  
56  
57  
58  
59  
60

1  
2  
3 constructs to determine the degree to which the partner influenced its catalytic activity  
4 and/or affinity for its substrates. Kinetic parameters and representative data for KDM1A  
5 activity in the presence of equimolar CoREST are listed in Table 1. Of the complexes  
6 tested, KDM1A/CoREST-Linker (residues 293-380) and KDM1A/CoREST-C (residues  
7 286-452), showed only a very modest 1.5-fold increase in the initial velocity as compared  
8 to KDM1A. Despite this enhanced velocity, the complexes maintained nearly identical  
9 catalytic efficiencies because of a proportional rise in the apparent  $K_M$ . We should note  
10 that our derived kinetic values are in reasonable agreement with previously reported  
11 values with and without CoREST.<sup>13, 22, 23, 30</sup>

12  
13  
14  
15  
16  
17  
18  
19  
20  
21  
22  
23  
24  
25  
26  
27 **H3<sup>1-21</sup> is a Competitive Inhibitor of KDM1A Demethylation Activity.** In order  
28 to provide a basis for comparison for full-length products, we first reconfirmed the  
29 inhibition modality and potency of the peptide products of the enzymatic reaction (Figure  
30 S5). The unmodified peptide product representing the first 21 residues of histone H3  
31 (H3<sup>1-21</sup>) has previously been reported to be a competitive inhibitor of KDM1A activity  
32 with a  $K_i$  of  $1.8 \pm 0.6 \mu\text{M}$ .<sup>22</sup> In order to eliminate any potential deleterious non-specific  
33 aggregation effects, we utilized 0.01% (w/v) CHAPS in our assay buffers.<sup>44</sup> Dose-  
34 response curves of H3<sup>1-21</sup> showed an average  $IC_{50}$  of  $4.84 \pm 0.16 \mu\text{M}$  for KDM1A.  
35 Potency and mechanism of inhibition of H3<sup>1-21</sup> toward KDM1A was determined through  
36 a double titration of inhibitor ( $[I]$  that gives 30% to 75% activity as determined by eq 2)  
37 versus the substrate followed by global fitting of the data. The data were fit to models of  
38 competitive, uncompetitive, and non-competitive inhibition and were best described by a  
39 competitive model, as determined by  $F$ -test analysis. The double titration revealed a  $K_i$  of  
40  
41  
42  
43  
44  
45  
46  
47  
48  
49  
50  
51  
52  
53  
54  
55  
56  
57  
58  
59  
60

1  
2  
3 1.77 ± 0.08 μM. Subsequent reciprocal transformation and Lineweaver-Burk plot  
4  
5  
6 analysis of the data also fit the pattern to competitive inhibition, resulting in a series of  
7  
8  
9 nested lines intersecting at a single  $y$ -intercept. Additionally, a secondary plot of apparent  
10  
11  $K_M$  versus  $[I]$  also revealed a  $K_i$  of 1.84 ± 0.14 μM, while the Cheng-Prusoff relationship  
12  
13 for competitive inhibition yielded a value of 2.07 ± 0.07 μM.<sup>40</sup> In our hands, the  
14  
15 competitive nature of the product peptide and potency is nearly identical to that  
16  
17  
18 previously reported.  
19

20  
21  
22  
23 **The H3/KDM1A Interaction Reaches Rapid Equilibrium.** With the relative  
24  
25 affinity and competitive nature of the unmodified peptide product reassessed, we looked  
26  
27 to investigate the full-length H3 product (H3<sup>1-135</sup>). As an initial test of potency, we  
28  
29 assessed the dose-response of H3 inhibition of KDM1A-mediated demethylation of a  
30  
31 peptide substrate. The initial rates as a function of H3 do not appear to be curvilinear in  
32  
33 nature and are best fit by linear regression (Figure 2A). This suggests that the degree of  
34  
35 inhibition at a fixed concentration of H3 does not vary over time and the interaction is not  
36  
37 slow binding in nature. However, in some cases the establishment of the enzyme-  
38  
39 inhibitor equilibrium is much slower than the course of the assay.  
40  
41  
42

43  
44 In order to assess this potential explanation for the increase in observed binding  
45  
46 affinity, we preincubated KDM1A with H3 for specified times and then initiated the  
47  
48 assay. We observed no significant change in the  $IC_{50}$  as a function of time even with long  
49  
50 preincubation times of up to an hour. Analysis of the dose-response curves resulted in an  
51  
52 average  $IC_{50}$  of 153.3 ± 26.0 nM ( $[E]_T = 175$  nM) (Figure 2B), a value within the  
53  
54 theoretical tight-binding limit of the assay. As there was no change in the average  $IC_{50}$  as  
55  
56  
57  
58  
59  
60

1  
2  
3 a function of time, and the initial velocities as a function of  $[I]$  appear linear, we suggest  
4  
5 that H3 and KDM1A reach rapid equilibrium under the assay parameters utilized.  
6  
7  
8 However, one cannot rule out that the time-dependent transition occurs at a rate that is  
9  
10 faster than the detection limits of the assay used.  
11

12  
13 We should note that as controls we tested the activity of HRP in the presence of  
14  
15 increasing concentrations of full-length histone H3. Hydrogen peroxide (2.5  $\mu\text{M}$ ) and  
16  
17 HRP (1 U/mL) were set at fixed concentrations and titrated against H3. In this assay,  
18  
19 HRP retained all of its activity even at the highest concentrations tested (Figure S6A).  
20  
21 Additionally, H3 was tested for its ability to both quench resorufin derived fluorescence  
22  
23 and absorbance as well as quinoneimine dye derived absorbance (Figure S6B-C) In this  
24  
25 assay, peroxide was titrated against fixed HRP and H3 to establish standard curves of  
26  
27 responses versus peroxide concentration. Even at the highest concentrations of H3 tested,  
28  
29 these assays showed no statistical difference between standard curves prepared in the  
30  
31 presence and absence of H3. These controls strongly suggest that the inhibitory activity  
32  
33 realized in the demethylation assays were solely due to the H3/KDM1A interaction.  
34  
35  
36  
37  
38  
39  
40

41 **Full-Length Histone H3 is a Tight-Binding, Competitive Inhibitor of**  
42 **KDM1A.** As noted above, the average  $IC_{50}$  of full-length H3 toward KDM1A, appears to  
43  
44 be within the theoretical tight-binding limit (i.e  $\leq 10$ -fold  $[E]_T$ ). Therefore, in order to  
45  
46 assess the apparent affinity of H3 toward KDM1A we first conducted a titration of H3 at  
47  
48 a starting point of 30-fold  $[E]_T$  in a 1.5-fold dilution series.<sup>45</sup> Data were fit to the  
49  
50 Morrison quadratic equation for concentration-response data for tight-binding inhibitors  
51  
52 (eq 5) resulting in a  $K_i^{\text{app}}$  of  $59.1 \pm 5.95$  nM (Figure 3A). Data were additionally analyzed  
53  
54  
55  
56  
57  
58  
59  
60

1  
2  
3 via Henderson plot revealing a  $K_i^{\text{app}}$  of  $103.4 \pm 4.47$  nM that was consistent with the  
4  
5 tight-binding nature of the H3 interaction (Figure S7).<sup>42</sup>  
6  
7

8 One of the hallmarks of tight-binding ligands is the dependence of  $IC_{50}$  on  
9 enzyme concentration (eq 7).<sup>46</sup> Therefore, in order to further confirm the tight-binding  
10 nature of the full-length H3 we assessed the effect of enzyme concentration on  $IC_{50}$ .  
11 Here, enzyme at differential concentrations was titrated against histone H3 with a fixed  
12 concentration of peptide substrate held at the apparent  $K_M$  (Figure 3B). Linear regression  
13 of the data resulted in a  $K_i^{\text{app}}$  of  $61.2 \pm 5.78$  nM. This analysis again confirmed the tight-  
14 binding nature of the H3/KDM1A interaction that leads to complications when assessing  
15 ligand modality.  
16  
17  
18  
19  
20  
21  
22  
23  
24  
25  
26

27 Since the potency of H3 is near the concentration of KDM1A used in the assays;  
28 standard mechanism of inhibition through double titration of inhibitor followed by global  
29 fitting of the data is precluded. Instead, the  $IC_{50}$  determined at several substrates  
30 concentrations were plotted against the  $[S]/K_M$  ratio (0.156 to  $10 \times K_M$ ) (Figure 3C). The  
31 data were fit to models of competitive, uncompetitive, and non-competitive inhibition  
32 and were best fit by a competitive model as determined by  $F$ -test analysis. A  $K_i$  of  $18.9 \pm$   
33  $1.2$  nM was observed. This  $K_i$  is nearly a 100-fold increase in binding affinity towards the  
34 free enzyme as compared to the peptide product described above.  
35  
36  
37  
38  
39  
40  
41  
42  
43  
44  
45

46 In order to determine if the binding affinity of  $H3^{1-135}$  was either primarily  
47 electrostatic or hydrophobic in nature, an  $IC_{50}$  shift assay was completed with increasing  
48 NaCl concentrations. At higher ionic strength, the potency of  $H3^{1-135}$  toward KDM1A in  
49 the demethylation assay decreased (Figure 3D). Based on this data, we suggest that the  
50 interaction of  $H3^{1-135}$  with KDM1A is likely to be mostly electrostatic in nature. It is  
51  
52  
53  
54  
55  
56  
57  
58  
59  
60

1  
2  
3 interesting to note that KDM1A showed negligible activity over background at 300 mM  
4 NaCl. Therefore, as a control experiment, we repeated the titration of H3<sup>1-135</sup> against HRP  
5 in the presence of H<sub>2</sub>O<sub>2</sub> and 300 mM NaCl and activity was unaffected (data not shown).  
6  
7  
8 We can therefore conclude that the binding of KDM1A to the peptide substrate  
9  
10 H3K4me1/2<sup>1-21</sup> is also electrostatic in nature, which was also postulated by Forneris and  
11  
12 coworkers.<sup>22</sup>  
13  
14  
15  
16  
17  
18  
19

20 **Histone H3/KDM1A Binary Complex has an Observable Residence Time.** To  
21 confirm reversibility of inhibition and to determine the off-rate ( $k_{\text{off}}$ ) of full-length H3  
22 binding, rapid dilution experiments were conducted where enzyme and inhibitor were  
23 preincubated for 1 h. The enzyme/inhibitor complex was then diluted 100-fold into assay  
24 buffer containing the peptide substrate, coupling enzyme, and chromophore. Reaction  
25 progress curve data show that KDM1A activity is slowly recovered over time ( $t_{1/2} = 9.63$   
26 min) (Figure 4). In control experiments using the H3 product peptide (H3<sup>1-21</sup>), the  
27 progress curve appears linear, as there is no distinguishable delay in the recovery of  
28 activity (Figure S8). Additionally,  $t_{1/2}$  was unable to be defined by the data, suggesting  
29 that this interaction is rapidly reversible (Table 2). We also used 2-PCPA as a  
30 mechanism-based irreversible inhibitor control,<sup>36</sup> in the presence of which KDM1A did  
31 not recover activity as expected (Figure 4). The jump dilution experiment confirms the  
32 long residence time and reversibility of the H3/KDM1A interaction.  
33  
34  
35  
36  
37  
38  
39  
40  
41  
42  
43  
44  
45  
46  
47  
48  
49  
50

51  
52  
53 **Surface Plasmon Resonance (SPR) Measurements.** In order to confirm the  
54 tight-binding interaction between KDM1A and full-length H3 independent of catalysis,  
55  
56  
57  
58  
59  
60

1  
2  
3 we turned to SPR measurements. Here, an antibody specific to the histone H3 C-terminus  
4 was covalently immobilized on the chip surface as the capturing antibody to which H3  
5 was immobilized. This experimental set-up allowed subsequent analysis of the  
6 H3/KDM1A binding interaction (Figure 5A). As is shown in Figure 5B, the increase in  
7 response units over time represents the amount of KDM1A bound to the antibody-  
8 immobilized histone H3. This response is proportional to the association rate constant  
9 ( $k_{\text{on}}$ ) of  $9.26 \times 10^4 \pm 1.5 \times 10^4 \text{ M}^{-1}\text{s}^{-1}$ . After the association of KDM1A and immobilized  
10 H3, additional buffer was injected over the flow cell to dissociate the bound enzyme. This  
11 analysis yielded a dissociation rate constant ( $k_{\text{off}}$ ) of  $8.35 \times 10^{-4} \pm 3.4 \times 10^{-5} \text{ s}^{-1}$ . These  
12 calculated rate constants result in an equilibrium dissociation constant ( $K_{\text{d}}$ ) of  $9.02 \pm 2.27$   
13 nM that is within approximately 2-fold of that calculated in the continuous assay. This  
14 technique independently confirmed that the interaction between KDM1A and H3 has a  $K_{\text{d}}$   
15 in the low nanomolar, tight-binding range and is suggestive of a 1:1 stoichiometry.  
16 Additionally, the off-rate determined from this experiment is in good agreement with the  
17 results of the rapid dilution experiment. We also suggest that the presence of DTT in the  
18 running buffers strongly precludes the formation of disulfide bonds as a contributing  
19 factor of the tight-binding nature of the H3/KDM1A interaction.  
20  
21  
22  
23  
24  
25  
26  
27  
28  
29  
30  
31  
32  
33  
34  
35  
36  
37  
38  
39  
40  
41  
42  
43  
44  
45  
46  
47

48 **Additional Core Histone Proteins have no Effect on KDM1A.** Several groups  
49 have illustrated that KDM1A catalyzes the oxidative demethylation of histone  
50 H3K4me1/2 and H3K9me1/2 as well as non-histone substrates.<sup>6-8, 21</sup> Despite a broad  
51 substrate specificity profile, the demethylase has never been reported to recognize PTMs  
52 on the additional core histone proteins. In order to confirm this observation in terms of  
53  
54  
55  
56  
57  
58  
59  
60

1  
2  
3 inhibition of demethylation activity, dose-response titrations were completed for each of  
4  
5 the other core histone proteins, H2A, H2B and H4, against KDM1A. Consistent with  
6  
7 these reports, none of the other core histone proteins inhibited KDM1A activity (Figure  
8  
9 S9). We can safely conclude that the demethylase specifically recognizes histone H3 and  
10  
11 is not negatively regulated by the other core histones. However, this analysis does not  
12  
13 prove that KDM1A does not contain surface recognition elements that bind these other  
14  
15 core histones.  
16  
17  
18  
19

## 20 21 22 **DISCUSSION**

23  
24 Many groups have suggested that the substrates and products of KDM1A exit the  
25  
26 expanded yet restricted active site pocket and interact with a secondary binding site on  
27  
28 the enzyme surface.<sup>11, 15, 27, 28</sup> This secondary surface element is expected to that facilitate  
29  
30 substrate/product binding and recognition. To assess this hypothesis, we investigated the  
31  
32 ability of unmodified, full-length histone proteins to inhibit KDM1A dependent  
33  
34 demethylation activity. We chose longer, “native-like” products in order to determine  
35  
36 whether or not the enzyme could potentially recognize a larger portion of these species,  
37  
38 thereby increasing the apparent binding affinity. Before we began this study we chose to  
39  
40 assess whether or not differential CoREST constructs (CoREST1/RCOR1) altered  
41  
42 KDM1A catalytic efficiency toward peptide substrates.  
43  
44  
45  
46  
47

48 Using various truncated CoREST constructs, we observed no statistical difference  
49  
50 in catalytic efficiency suggesting that this binding partner doesn't control activity toward  
51  
52 the minimal substrate footprint. This result supports the idea that KDM1A catalytic  
53  
54 activity is modular in nature, as it often exists as a member of multiprotein complexes  
55  
56  
57  
58  
59  
60

1  
2  
3 that dictate function.<sup>19</sup> We should note that KDM1A catalytic efficiency and substrate  
4 specificity might be further altered if chromatin or nucleosomes are utilized as  
5 substrates.<sup>22</sup> In fact, Tan and coworkers recently illustrated that the KDM1A/CoREST-C  
6 complex has greater than a 25-fold increase in catalytic efficiency when using site-  
7 specifically methylated nucleosomes with extranucleosomal DNA as substrates; a  
8 phenomenon driven by  $K_M^{app}$ .<sup>19</sup> Despite this evidence, there appears to be further  
9 confounding aspects to the regulation of KDM1A activity. For example, CoREST  
10 paralogues (CoREST2/RCOR2 and CoREST3/RCOR3) were recently shown to alter  
11 KDM1A activity toward nucleosomal substrates as assessed by their DNA binding ability  
12 and also affected catalytic efficiency toward peptide substrates.<sup>17, 47, 48</sup> Since we are  
13 utilizing the minimal peptide substrate (H3K4me2<sup>1-21</sup>) in these studies, and inhibitor  
14 potency seems to be unaffected by the presence of CoREST *in vitro*,<sup>23, 49</sup> we moved  
15 forward with our investigation using isolated KDM1A.  
16  
17  
18  
19  
20  
21  
22  
23  
24  
25  
26  
27  
28  
29  
30  
31  
32  
33

34 In line with our hypothesis, initial dose-response analysis of full-length H3 versus  
35 KDM1A demethylation activity suggested that the interaction was in the theoretical tight-  
36 binding limit of the assay (i.e.  $IC_{50} \leq 10\text{-fold } [E]_T$ ). If we consider the basic definition of  
37 the equilibrium dissociation constant for competitive inhibitors, where  $K_i = k_{off}/k_{on}$ , it is  
38 easy to see that affinity is driven by either rapid association of the binary *EI* complex or a  
39 slow rate of release of the ligand from the target enzyme.<sup>50</sup> In order to assess the onset of  
40 inhibition we examined the initial rate data upon assay initiation. These initial rates  
41 appeared linear suggesting that H3 and KDM1A reach rapid equilibrium under the  
42 specified assay conditions. Additional support for this observation came from  
43 preincubation of H3 with KDM1A. Even with extended incubation times of up to 1 h the  
44  
45  
46  
47  
48  
49  
50  
51  
52  
53  
54  
55  
56  
57  
58  
59  
60

1  
2  
3 average  $IC_{50}$  did not change significantly. In order to next assign the modality of full-  
4  
5 length H3, we next determined the  $IC_{50}$  of H3 at a wide range of substrate  
6  
7 concentrations.<sup>50</sup>  
8  
9

10 Our data support that the binding of full-length histone H3 to KDM1A is  
11  
12 competitive in nature and displayed nearly a 100-fold increase in binding affinity ( $K_i$  of  
13  
14  $18.9 \pm 1.2$  nM) as compared to the 21-mer product peptide. This value of magnitude  
15  
16 increase strongly suggests some form of additional product recognition with the full-  
17  
18 length histone and time-dependence of the binding interaction. We therefore looked to  
19  
20 investigate the source of this increase in observed binding affinity as low  $K_i$  values  
21  
22 typical of tight-binding inhibitors are driven mainly by very slow rates of complex  
23  
24 dissociation (i.e. low values of  $k_{off}$ ) and by relation large target residence times.<sup>50</sup>  
25  
26  
27  
28

29 We note that the increase in binding affinity of the H3/KDM1A interaction may  
30  
31 be at least be partially attributed to the long residence time, as the  $t_{1/2}$  of the interaction  
32  
33 was determined to be 9.63 min with a  $k_{off}$  of  $1.2 \times 10^{-3} \text{ s}^{-1}$ . Additionally, we independently  
34  
35 confirmed the tight-binding nature of the interaction and slow rate of dissociation of the  
36  
37 binary complex with SPR experiments in which histone H3 was immobilized to the chip  
38  
39 surface via interaction with a C-terminal specific antibody. Importantly, our assessment  
40  
41 that increasing ionic strength results in an increase in relative  $IC_{50}$  suggests that the  
42  
43 interaction of full-length histone H3 with both the flavin-containing active site and  
44  
45 secondary exo-site is electrostatic in nature. Notably, there are several regions on the  
46  
47 surface of KDM1A that are electronegative in nature and could thereby provide the  
48  
49 secondary binding site for histone H3.  
50  
51  
52  
53  
54  
55  
56  
57  
58  
59  
60

1  
2  
3  
4 Consistent with our proposal of a secondary binding site on the enzyme surface of  
5  
6 KDM1A, the paralog KDM1B contains such a site that was identified through  
7  
8 crystallographic efforts.<sup>51</sup> Additionally, we envision that this secondary binding site may  
9  
10 play a role in the “stick-and-catch” model recently proposed by Mattevi and coworkers.<sup>17</sup>  
11  
12 Here, KDM1A can probe a nucleosomal substrate using both its active site and secondary  
13  
14 recognition element and lock the complex into a competent binding mode. On the other  
15  
16 hand, after demethylation the secondary binding site is expected to contribute to the  
17  
18 stability of the nucleosome/demethylase complex. Importantly, KDM1A can remain  
19  
20 bound to genetic loci on time scales that are in line with large-scale chromatin  
21  
22 rearrangement.<sup>2</sup> Upon formation of this stable product complex, KDM1A can ‘lie in wait’  
23  
24 and serve as a docking element for protein, transcription factor, or repressor recruitment  
25  
26 as first suggested by Forneris and coworkers.<sup>22, 52</sup> These proteins can then cause  
27  
28 concomitant gene expression or repression or facilitate the dissociation of KDM1A from  
29  
30 the product complex. The role of KDM1A as a docking module is also consistent with the  
31  
32 observation that demethylation activity at specific estrogen responsive elements (EREs)  
33  
34 is required for ER $\alpha$  recruitment and concomitant target gene expression.<sup>53, 54</sup> Our  
35  
36 observations of an increased binding affinity for full-length products and target residence  
37  
38 time not only have implications in the role of KDM1A as a docking element, but also the  
39  
40 kinetic mechanism of the enzyme.  
41  
42  
43  
44  
45  
46  
47

48  
49 Due to the time scale of dissociation of the H3/KDM1A binary complex, we also  
50  
51 suspect that the overall demethylation reaction *in vivo* and *in vitro* may be either partially  
52  
53 or wholly rate-limited by product release with full-length histones or nucleosomes  
54  
55 (Scheme 1). In this model, the rate of product release,  $k_3$ , is much smaller than the rate of  
56  
57  
58  
59  
60

1  
2  
3 catalysis and product rebinding ( $k_2$  and  $k_{-3}$ , respectively) resulting in an *EP* binary  
4 complex with an observable half-life. Well in line with this hypothesis, there was more  
5 than a 5-fold reduction in  $k_{\text{cat}}^{\text{app}}$  values observed when nucleosomal substrates were  
6 utilized.<sup>19</sup> Additionally, the observation that KDM1A completely demethylates p53  
7 (K370) *in vitro* but only removes a single methyl mark when this activity is probed in cell  
8 culture further supports our claim. Together, our and others' results suggest that the  
9 product dissociation rate of KDM1A may be “tuned” by several factors including  
10 substrate, binding partners, or splice variations to the enzyme itself.  
11  
12  
13  
14  
15  
16  
17  
18  
19  
20  
21

22 In summary, our kinetic study has verified the tight-binding interaction between  
23 full-length histone H3 and KDM1A suggesting the existence of secondary binding site on  
24 the demethylase surface. The contact between the H3/KDM1A binary complex likely  
25 occurs through an extensive interaction interface with broad implications for enzyme  
26 function and control. As the complex also has a measurable residence time, the presence  
27 of KDM1A on specific genetic loci, may be further investigated in order to provide  
28 insights into the order of partner protein recruitment, complex nucleation, or dissociation.  
29  
30  
31  
32  
33  
34  
35  
36  
37  
38  
39  
40

## 41 **ACKNOWLEDGEMENTS**

42  
43 The authors gratefully acknowledge the help of Nate Nicely and Charles W. Pemble IV  
44 in the Duke Human Vaccine Institute X-ray Crystallography Shared Resource for their  
45 assistance with protein purification and preparation. We also thank Professor Karolin  
46 Luger from Colorado State University for providing expression plasmids of *X. laevis* core  
47 histones. SPR measurement services were kindly provided by the Duke Human Vaccine  
48 Institute Biomolecular Interaction Analysis Facility under the direction of Dr. S. Munir  
49  
50  
51  
52  
53  
54  
55  
56  
57  
58  
59  
60

1  
2  
3 Alam. We also thank Jennifer E. Link and members of the McCafferty laboratory for  
4  
5 their thoughtful insight during the preparation of the manuscript.  
6  
7  
8  
9

## 10 ASSOCIATED CONTENT

### 11 Supporting Information

12  
13 The Supporting Information is available free of charge on the ACS Publications website.  
14  
15 A detailed description of Materials and Methods and Figures S1–S9.  
16  
17  
18  
19

## 20 REFERENCES

- 21  
22  
23 1. Bannister, A. J., and Kouzarides, T. (2011) Regulation of chromatin by histone  
24 modifications, *Cell research* 21, 381-395.  
25  
26 2. Voss, T. C., and Hager, G. L. (2014) Dynamic regulation of transcriptional states by  
27 chromatin and transcription factors, *Nature reviews. Genetics* 15, 69-81.  
28  
29 3. Butler, J. S., Koutelou, E., Schibler, A. C., and Dent, S. Y. (2012) Histone-modifying  
30 enzymes: regulators of developmental decisions and drivers of human disease,  
31 *Epigenomics* 4, 163-177.  
32  
33 4. Gozani, O. S., Y. (2014) Histone Methylation in Chromatin Signaling, In  
34 *Fundamentals of Chromatin* (Workman, J. L. A., S.M., Ed.), pp 213-256,  
35 Springer New York.  
36  
37 5. Paik, W. K., and Kim, S. (1973) Enzymatic demethylation of calf thymus histones,  
38 *Biochemical and biophysical research communications* 51, 781-788.  
39  
40 6. Shi, Y., Lan, F., Matson, C., Mulligan, P., Whetstine, J. R., Cole, P. A., Casero, R. A.,  
41 and Shi, Y. (2004) Histone demethylation mediated by the nuclear amine oxidase  
42 homolog LSD1, *Cell* 119, 941-953.  
43  
44 7. Metzger, E., Wissmann, M., Yin, N., Muller, J. M., Schneider, R., Peters, A. H.,  
45 Gunther, T., Buettner, R., and Schule, R. (2005) LSD1 demethylates repressive  
46 histone marks to promote androgen-receptor-dependent transcription, *Nature* 437,  
47 436-439.  
48  
49 8. Laurent, B., Ruitu, L., Murn, J., Hempel, K., Ferrao, R., Xiang, Y., Liu, S., Garcia, B.  
50 A., Wu, H., Wu, F., Steen, H., and Shi, Y. (2015) A specific LSD1/KDM1A  
51 isoform regulates neuronal differentiation through H3K9 demethylation,  
52 *Molecular cell* 57, 957-970.  
53  
54 9. Kubicek, S., and Jenuwein, T. (2004) A crack in histone lysine methylation, *Cell* 119,  
55 903-906.  
56  
57 10. Jin, Y., Kim, T. Y., Kim, M. S., Kim, M. A., Park, S. H., and Jang, Y. K. (2014)  
58 Nuclear import of human histone lysine-specific demethylase LSD1, *Journal of*  
59 *biochemistry* 156, 305-313.  
60

11. Stavropoulos, P., Blobel, G., and Hoelz, A. (2006) Crystal structure and mechanism of human lysine-specific demethylase-1, *Nature structural & molecular biology* 13, 626-632.
12. Chen, Y., Yang, Y., Wang, F., Wan, K., Yamane, K., Zhang, Y., and Lei, M. (2006) Crystal structure of human histone lysine-specific demethylase 1 (LSD1), *Proceedings of the National Academy of Sciences of the United States of America* 103, 13956-13961.
13. Hwang, S., Schmitt, A. A., Luteran, A. E., Toone, E. J., and McCafferty, D. G. (2011) Thermodynamic characterization of the binding interaction between the histone demethylase LSD1/KDM1 and CoREST, *Biochemistry* 50, 546-557.
14. Wang, Y., Zhang, H., Chen, Y., Sun, Y., Yang, F., Yu, W., Liang, J., Sun, L., Yang, X., Shi, L., Li, R., Li, Y., Zhang, Y., Li, Q., Yi, X., and Shang, Y. (2009) LSD1 is a subunit of the NuRD complex and targets the metastasis programs in breast cancer, *Cell* 138, 660-672.
15. Yang, M., Gocke, C. B., Luo, X., Borek, D., Tomchick, D. R., Machius, M., Otwinowski, Z., and Yu, H. (2006) Structural basis for CoREST-dependent demethylation of nucleosomes by the human LSD1 histone demethylase, *Molecular cell* 23, 377-387.
16. Shi, Y. J., Matson, C., Lan, F., Iwase, S., Baba, T., and Shi, Y. (2005) Regulation of LSD1 histone demethylase activity by its associated factors, *Molecular cell* 19, 857-864.
17. Pilotto, S., Speranzini, V., Tortorici, M., Durand, D., Fish, A., Valente, S., Forneris, F., Mai, A., Sixma, T. K., Vachette, P., and Mattevi, A. (2015) Interplay among nucleosomal DNA, histone tails, and corepressor CoREST underlies LSD1-mediated H3 demethylation, *Proceedings of the National Academy of Sciences of the United States of America* 112, 2752-2757.
18. Lee, M. G., Wynder, C., Cooch, N., and Shiekhhattar, R. (2005) An essential role for CoREST in nucleosomal histone 3 lysine 4 demethylation, *Nature* 437, 432-435.
19. Kim, S. A., Chatterjee, N., Jennings, M. J., Bartholomew, B., and Tan, S. (2015) Extranucleosomal DNA enhances the activity of the LSD1/CoREST histone demethylase complex, *Nucleic acids research* 43, 4868-4880.
20. Da, G., Lenkart, J., Zhao, K., Shiekhhattar, R., Cairns, B. R., and Marmorstein, R. (2006) Structure and function of the SWIRM domain, a conserved protein module found in chromatin regulatory complexes, *Proceedings of the National Academy of Sciences of the United States of America* 103, 2057-2062.
21. Burg, J. M., Link, J. E., Morgan, B. S., Heller, F. J., Hargrove, A. E., and McCafferty, D. G. (2015) KDM1 class flavin-dependent protein lysine demethylases, *Biopolymers* 104, 213-246.
22. Forneris, F., Binda, C., Vanoni, M. A., Battaglioli, E., and Mattevi, A. (2005) Human histone demethylase LSD1 reads the histone code, *The Journal of biological chemistry* 280, 41360-41365.
23. Forneris, F., Binda, C., Adamo, A., Battaglioli, E., and Mattevi, A. (2007) Structural basis of LSD1-CoREST selectivity in histone H3 recognition, *The Journal of biological chemistry* 282, 20070-20074.

- 1
  - 2
  - 3
  - 4
  - 5
  - 6
  - 7
  - 8
  - 9
  - 10
  - 11
  - 12
  - 13
  - 14
  - 15
  - 16
  - 17
  - 18
  - 19
  - 20
  - 21
  - 22
  - 23
  - 24
  - 25
  - 26
  - 27
  - 28
  - 29
  - 30
  - 31
  - 32
  - 33
  - 34
  - 35
  - 36
  - 37
  - 38
  - 39
  - 40
  - 41
  - 42
  - 43
  - 44
  - 45
  - 46
  - 47
  - 48
  - 49
  - 50
  - 51
  - 52
  - 53
  - 54
  - 55
  - 56
  - 57
  - 58
  - 59
  - 60
24. Baron, R., Binda, C., Tortorici, M., McCammon, J. A., and Mattevi, A. (2011) Molecular mimicry and ligand recognition in binding and catalysis by the histone demethylase LSD1-CoREST complex, *Structure* *19*, 212-220.
25. Yang, M., Culhane, J. C., Szewczuk, L. M., Gocke, C. B., Brautigam, C. A., Tomchick, D. R., Machius, M., Cole, P. A., and Yu, H. (2007) Structural basis of histone demethylation by LSD1 revealed by suicide inactivation, *Nature structural & molecular biology* *14*, 535-539.
26. Luka, Z., Pakhomova, S., Loukachevitch, L. V., Calcutt, M. W., Newcomer, M. E., and Wagner, C. (2014) Crystal structure of the histone lysine specific demethylase LSD1 complexed with tetrahydrofolate, *Protein science : a publication of the Protein Society* *23*, 993-998.
27. Culhane, J. C., and Cole, P. A. (2007) LSD1 and the chemistry of histone demethylation, *Current opinion in chemical biology* *11*, 561-568.
28. Hou, H., and Yu, H. (2010) Structural insights into histone lysine demethylation, *Current opinion in structural biology* *20*, 739-748.
29. Tochio, N., Umehara, T., Koshiha, S., Inoue, M., Yabuki, T., Aoki, M., Seki, E., Watanabe, S., Tomo, Y., Hanada, M., Ikari, M., Sato, M., Terada, T., Nagase, T., Ohara, O., Shirouzu, M., Tanaka, A., Kigawa, T., and Yokoyama, S. (2006) Solution structure of the SWIRM domain of human histone demethylase LSD1, *Structure* *14*, 457-468.
30. Gaweska, H., Henderson Pozzi, M., Schmidt, D. M., McCafferty, D. G., and Fitzpatrick, P. F. (2009) Use of pH and kinetic isotope effects to establish chemistry as rate-limiting in oxidation of a peptide substrate by LSD1, *Biochemistry* *48*, 5440-5445.
31. Aliverti, A., Curti, B., and Vanoni, M. A. (1999) Identifying and quantitating FAD and FMN in simple and in iron-sulfur-containing flavoproteins, *Methods in molecular biology (Clifton, N.J.)* *131*, 9-23.
32. Burg, J. M., Makhoul, A. T., Pemble, C. W. t., Link, J. E., Heller, F. J., and McCafferty, D. G. (2015) A rationally-designed chimeric KDM1A/KDM1B histone demethylase tower domain deletion mutant retaining enzymatic activity, *FEBS letters* *589*, 2340-2346.
33. Tropea, J. E., Cherry, S., and Waugh, D. S. (2009) Expression and purification of soluble His(6)-tagged TEV protease, *Methods in molecular biology (Clifton, N.J.)* *498*, 297-307.
34. Loyola, A., He, S., Oh, S., McCafferty, D. G., and Reinberg, D. (2004) Techniques used to study transcription on chromatin templates, *Methods in enzymology* *377*, 474-499.
35. Luger, K., Rechsteiner, T. J., Flaus, A. J., Waye, M. M., and Richmond, T. J. (1997) Characterization of nucleosome core particles containing histone proteins made in bacteria, *Journal of molecular biology* *272*, 301-311.
36. Schmidt, D. M., and McCafferty, D. G. (2007) trans-2-Phenylcyclopropylamine is a mechanism-based inactivator of the histone demethylase LSD1, *Biochemistry* *46*, 4408-4416.
37. Copeland, R. A. (2003) Mechanistic considerations in high-throughput screening, *Analytical biochemistry* *320*, 1-12.

- 1  
2  
3  
4  
5  
6  
7  
8  
9  
10  
11  
12  
13  
14  
15  
16  
17  
18  
19  
20  
21  
22  
23  
24  
25  
26  
27  
28  
29  
30  
31  
32  
33  
34  
35  
36  
37  
38  
39  
40  
41  
42  
43  
44  
45  
46  
47  
48  
49  
50  
51  
52  
53  
54  
55  
56  
57  
58  
59  
60
38. Acker, M. G., and Auld, D. S. (2014) Considerations for the design and reporting of enzyme assays in high-throughput screening applications, *Perspectives in Science I*, 56-73.
  39. Michaelis, L., Menten, M. L., Johnson, K. A., and Goody, R. S. (2011) The original Michaelis constant: translation of the 1913 Michaelis-Menten paper, *Biochemistry* 50, 8264-8269.
  40. Cheng, Y., and Prusoff, W. H. (1973) Relationship between the inhibition constant (K<sub>I</sub>) and the concentration of inhibitor which causes 50 per cent inhibition (I<sub>50</sub>) of an enzymatic reaction, *Biochemical pharmacology* 22, 3099-3108.
  41. Morrison, J. F. (1969) Kinetics of the reversible inhibition of enzyme-catalysed reactions by tight-binding inhibitors, *Biochimica et biophysica acta* 185, 269-286.
  42. Henderson, P. J. (1972) A linear equation that describes the steady-state kinetics of enzymes and subcellular particles interacting with tightly bound inhibitors, *The Biochemical journal* 127, 321-333.
  43. Copeland, R. A., Basavapathruni, A., Moyer, M., and Scott, M. P. (2011) Impact of enzyme concentration and residence time on apparent activity recovery in jump dilution analysis, *Analytical biochemistry* 416, 206-210.
  44. Feng, B. Y., Simeonov, A., Jadhav, A., Babaoglu, K., Inglese, J., Shoichet, B. K., and Austin, C. P. (2007) A high-throughput screen for aggregation-based inhibition in a large compound library, *Journal of medicinal chemistry* 50, 2385-2390.
  45. Murphy, D. J. (2004) Determination of accurate K<sub>I</sub> values for tight-binding enzyme inhibitors: an in silico study of experimental error and assay design, *Analytical biochemistry* 327, 61-67.
  46. Straus, O. H., and Goldstein, A. (1943) ZONE BEHAVIOR OF ENZYMES : ILLUSTRATED BY THE EFFECT OF DISSOCIATION CONSTANT AND DILUTION ON THE SYSTEM CHOLINESTERASE-PHYSOSTIGMINE, *The Journal of general physiology* 26, 559-585.
  47. Upadhyay, G., Chowdhury, A. H., Vaidyanathan, B., Kim, D., and Saleque, S. (2014) Antagonistic actions of Rcor proteins regulate LSD1 activity and cellular differentiation, *Proceedings of the National Academy of Sciences of the United States of America* 111, 8071-8076.
  48. Barrios, A. P., Gomez, A. V., Saez, J. E., Ciossani, G., Toffolo, E., Battaglioli, E., Mattevi, A., and Andres, M. E. (2014) Differential properties of transcriptional complexes formed by the CoREST family, *Molecular and cellular biology* 34, 2760-2770.
  49. Mould, D. P., McGonagle, A. E., Wiseman, D. H., Williams, E. L., and Jordan, A. M. (2015) Reversible inhibitors of LSD1 as therapeutic agents in acute myeloid leukemia: clinical significance and progress to date, *Medicinal research reviews* 35, 586-618.
  50. Copeland, R. A. (2005) Evaluation of enzyme inhibitors in drug discovery. A guide for medicinal chemists and pharmacologists, *Methods of biochemical analysis* 46, 1-265.
  51. Chen, F., Yang, H., Dong, Z., Fang, J., Wang, P., Zhu, T., Gong, W., Fang, R., Shi, Y. G., Li, Z., and Xu, Y. (2013) Structural insight into substrate recognition by histone demethylase LSD2/KDM1b, *Cell research* 23, 306-309.

- 1  
2  
3  
4 52. Forneris, F., Binda, C., Dall'Aglio, A., Fraaije, M. W., Battaglioli, E., and Mattevi, A.  
5 (2006) A highly specific mechanism of histone H3-K4 recognition by histone  
6 demethylase LSD1, *The Journal of biological chemistry* 281, 35289-35295.  
7 53. Pollock, J. A., Larrea, M. D., Jasper, J. S., McDonnell, D. P., and McCafferty, D. G.  
8 (2012) Lysine-specific histone demethylase 1 inhibitors control breast cancer  
9 proliferation in ERalpha-dependent and -independent manners, *ACS chemical*  
10 *biology* 7, 1221-1231.  
11 54. Garcia-Bassets, I., Kwon, Y. S., Telese, F., Prefontaine, G. G., Hutt, K. R., Cheng, C.  
12 S., Ju, B. G., Ohgi, K. A., Wang, J., Escoubet-Lozach, L., Rose, D. W., Glass, C.  
13 K., Fu, X. D., and Rosenfeld, M. G. (2007) Histone methylation-dependent  
14 mechanisms impose ligand dependency for gene activation by nuclear receptors,  
15 *Cell* 128, 505-518.  
16  
17  
18  
19  
20  
21  
22  
23  
24  
25  
26  
27  
28  
29  
30  
31  
32  
33  
34  
35  
36  
37  
38  
39  
40  
41  
42  
43  
44  
45  
46  
47  
48  
49  
50  
51  
52  
53  
54  
55  
56  
57  
58  
59  
60

## TABLES

**Table 1.** Representative steady-state kinetic parameters of KDM1A and differential KDM1A/CoREST complexes using an H3K4me2<sup>1-21</sup> peptide substrate.

	$K_M^{\text{app}}$ ( $\mu\text{M}$ )	$k_{\text{cat}}^{\text{app}}$ ( $\text{min}^{-1}$ )	$k_{\text{cat}}^{\text{app}}/K_M^{\text{app}}$ ( $\mu\text{M}^{-1} \text{min}^{-1}$ )
n $\Delta$ 150 KDM1A <sup>a</sup>	4.46 $\pm$ 0.27	6.00 $\pm$ 0.07	1.35 $\pm$ 0.25
n $\Delta$ 150 KDM1A/CoREST-linker <sup>a</sup>	8.89 $\pm$ 0.65	9.42 $\pm$ 0.10	1.06 $\pm$ 0.37
n $\Delta$ 150 KDM1A/CoREST-C <sup>a</sup>	8.14 $\pm$ 0.52	9.54 $\pm$ 0.09	1.17 $\pm$ 0.30

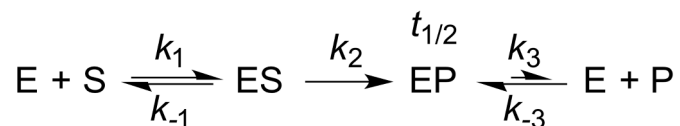
<sup>a</sup>In 50 mM HEPES-Na (pH 7.5), 125  $\mu\text{M}$  4-AAP, 1.0 mM 3,5 DCHBS, 300 nM [E], & 1 U/mL HRP at 25°C in air saturated buffer; peptide titrated from 50  $\mu\text{M}$  to 0 in 2-fold dilution series (n=3).

**Table 2.** Inhibition constants for full-length histones and histone peptides against KDM1A.

Entry	$IC_{50}$ (nM)	$K_i$ (nM)	$k_{off}$ (s <sup>-1</sup> )	residence time ( $\tau$ ) (min)	half-life ( $t_{1/2}$ ) (min)
H3 <sup>1-21</sup>	4840	1770	ND	ND	ND
H3	153.3	18.9	$1.2 \times 10^{-3}$	13.9	9.63
H4	N/A	-	-	-	-
H2A	N/A	-	-	-	-
H2B	N/A	-	-	-	-

N/A = not applicable; entry did not effectively inhibit KDM1A.  $IC_{50}$  values were determined at 5.0  $\mu$ M ( $\sim K_M^{app}$ ) and 175 nM KDM1A. ND = not determined, inhibition was rapidly reversible. Residence time was calculated with the formula;  $\tau = 1/k_{off}$ , assuming that the dilution is large enough that the rate of compound rebounding is assumed insignificant. Half-life was calculated with the formula;  $t_{1/2} = 0.693/k_{off}$ .

## SCHEMES



**Scheme 1.** Overview of simplified model of KDM1A substrate turnover and product release. Here  $k_3 \ll k_{-3}$  and  $k_2$  and the  $EP$  binary complex would therefore have an observable half-life. This model suggests that the rate-limiting step of catalysis may in some cases be the rate of product release.

**FIGURE LEGENDS**

**Figure 1.** Domain and structural overview of KDM1A and CoREST. (A) Domain maps of KDM1A and CoREST1. KDM1A: SWIRM domain is shown in green, AOD is shown in blue, and tower domain is shown in magenta. CoREST: Linker is shown in orange and SANT2 is shown in cyan. The ELM1 and SANT1 domains are shown in gray due to the lack structural information. (B) Structural overview of KDM1A in complex with CoREST-C (residues 286-482). Coloring scheme follows that of the domain maps above, FAD is denoted in yellow, and N and C-termini are labeled (PDB 2IW5).

**Figure 2.** Investigation of time-dependence of inhibition of full-length histone H3 against KDM1A as monitored in fluorescence-based HRP coupled assay. (A) Linear fit of the initial velocity of KDM1A in the presence of increasing concentrations of histone H3 with no preincubation prior to assay initiation and H3K4me2<sup>1-21</sup> substrate held at apparent  $K_M$ . (B) Investigation of  $IC_{50}$  values with preincubation of KDM1A in the presence of full-length H3 prior to assay initiation into substrate solution show no apparent time-dependence with an average of  $153.3 \pm 26.0$  nM ( $[E]_T = 175$  nM).

**Figure 3.** Inhibition profiling of full-length histone H3 against KDM1A as monitored in fluorescence-based HRP coupled assay reveals the tight-binding nature of the interaction. (A) Concentration-response plot of H3 (1.5-fold dilution series from 30-fold  $[E]_T$ ) against KDM1A fit to Morrison's equation revealing a  $K_i^{app}$  of  $59.1 \pm 5.95$  nM. (B) Plot of  $IC_{50}$  as a function of  $[E]_T$  measured over a range of concentrations from 88.9 to 400 nM

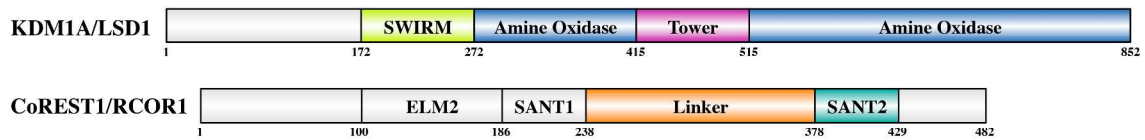
1  
2  
3 KDM1A generating a  $K_i^{\text{app}}$  of  $61.2 \pm 5.78$  nM. (C) Plot of  $IC_{50}$  as a function of  $[S]/K_M$   
4  
5 over a range of concentrations from 0.156 to  $10.0 \times K_M$  is best fit to a competitive model  
6  
7  
8 generating a  $K_i$  of  $18.9 \pm 1.2$  nM. (D) Plot of  $IC_{50}$  as a function of NaCl concentration  
9  
10 from 0 to 150 mM suggests that the H3/KDM1A interaction is ionic in nature.  
11  
12  
13  
14

15 **Figure 4.** The H3/KDM1A binary complex has an observable residence time. 2.5  $\mu\text{M}$  of  
16  
17 KDM1A and 3.0  $\mu\text{M}$  H3 ( $50 \times K_i^{\text{app}}$ ) or 200  $\mu\text{M}$  2-PCPA ( $10 \times IC_{50}$ ) were incubated for 1  
18  
19 h followed by 100-fold dilution into assay buffered containing 25  $\mu\text{M}$  peptide substrate,  
20  
21 50  $\mu\text{M}$  Amplex Red, 1 U/mL HRP. The recovery of enzyme activity was monitored over  
22  
23 time by monitoring resorufin-derived absorbance at 572 nm. Histone H3's inhibition of  
24  
25 KDM1A is slowly reversible with an off rate of  $1.2 \times 10^{-3} \text{ s}^{-1}$  as compared to 2-PCPA in  
26  
27 which the activity was not recovered.  
28  
29  
30  
31  
32  
33  
34

35 **Figure 5.** Surface plasmon resonance experiments independently confirm the tight-  
36  
37 binding nature of the H3/KDM1A interaction. (A) Diagram of the experimental set-up in  
38  
39 which anti-H3 antibody was covalently immobilized to chip surface in order to capture  
40  
41 histone H3. KDM1A was subsequently injected over chip surface to monitor binding. (B)  
42  
43 Response curves obtained during and after injection of KDM1A over anti-body  
44  
45 immobilized H3 chip surface. Global curve fitting of sensograms reveal an association  
46  
47 rate constant ( $k_{\text{on}}$ ) of  $9.26 \times 10^4 \pm 1.5 \times 10^4 \text{ M}^{-1}\text{s}^{-1}$  and dissociation rate constant ( $k_{\text{off}}$ ) of  
48  
49  $8.35 \times 10^{-4} \pm 3.4 \times 10^{-5} \text{ s}^{-1}$  and were used to calculate a dissociation constant ( $K_d$ ) of  $9.02$   
50  
51  $\pm 2.27$  nM.  
52  
53  
54  
55  
56  
57  
58  
59  
60

## FIGURES

A



B

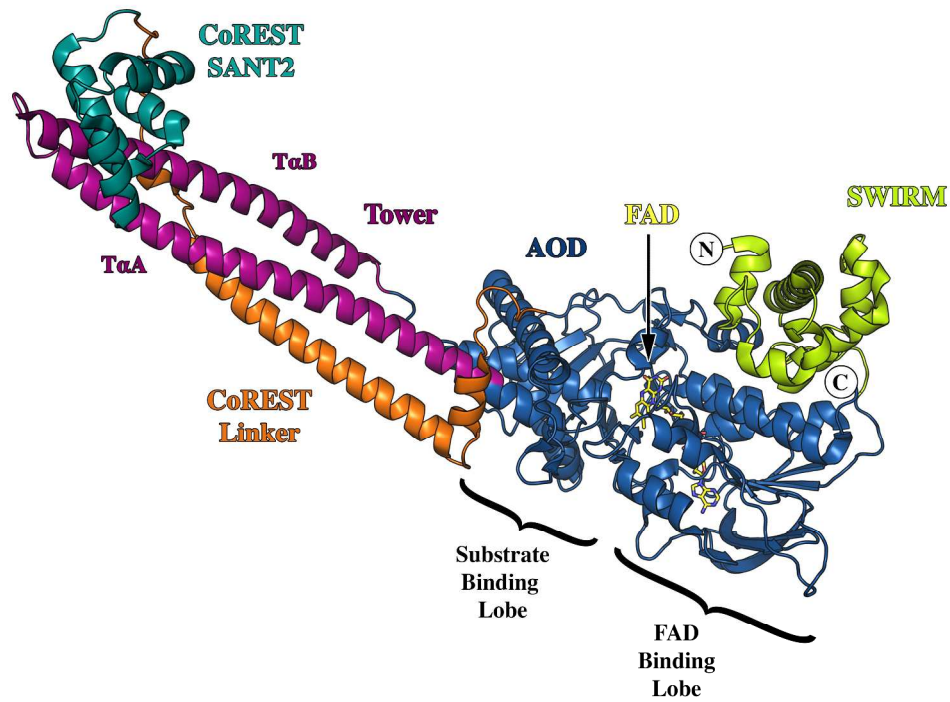


Figure 1

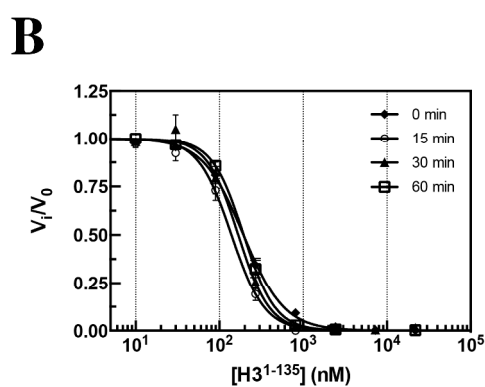
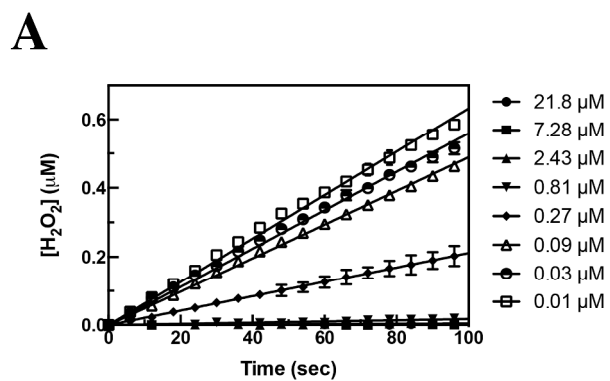


Figure 2

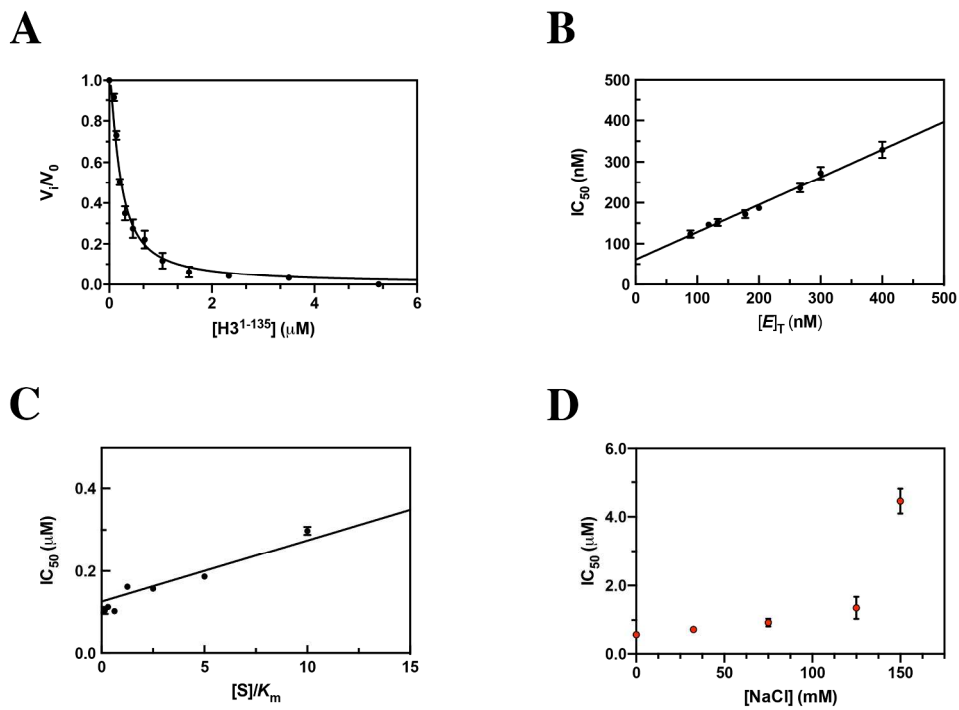


Figure 3

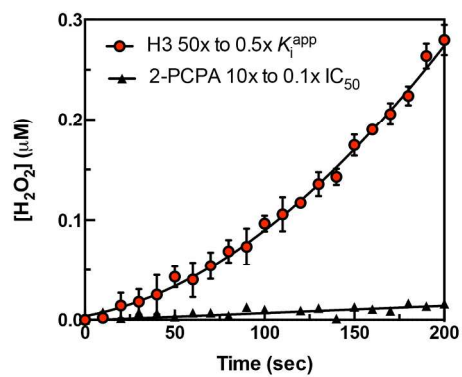


Figure 4

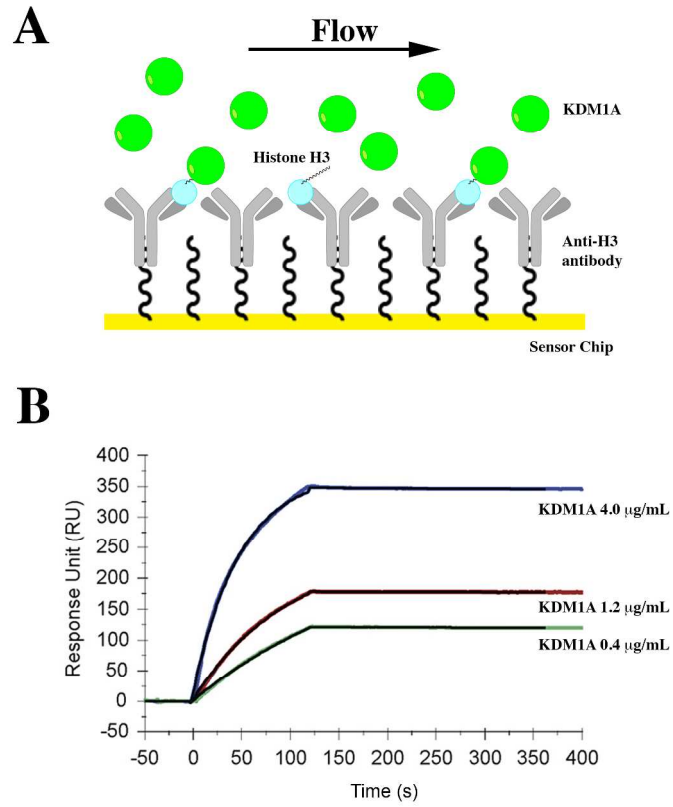
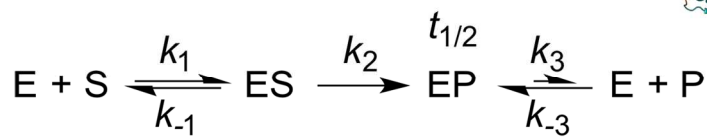
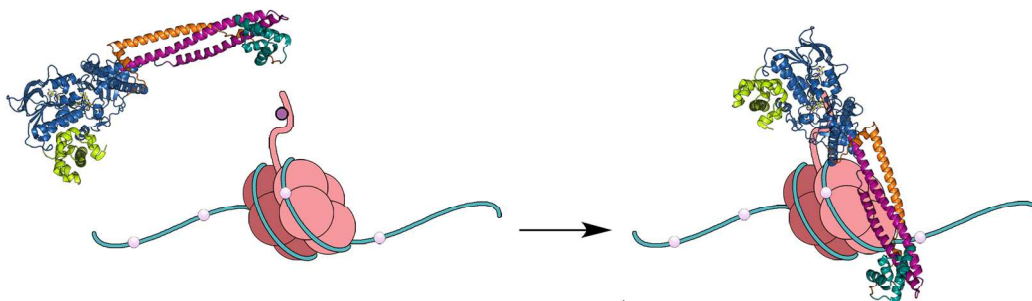


Figure 5

## GRAPHIC FOR THE TABLE OF CONTENTS



**AUTHOR INFORMATION****Corresponding Author**

\*Address: Department of Chemistry, Duke University, B120 Levine Science Research Center, Box 90346, 450 Research Drive, Durham, NC 27708-0346. Telephone: (919) 660-1516. Email: dewey.mccafferty@duke.edu

**Present Address**

§K.R.M.: Department of Chemical and Biomolecular Engineering, 2109 Partners II, North Carolina State University, Raleigh, NC 27606, United States

**Author Contributions**

J.M.B. and D.G.M. conceived this study. J.M.B. designed and performed experiments, analyzed data, and wrote the manuscript. J.J.G. performed experiments. K.R.M. designed experiments. J.J.G. and K.R.M. helped analyze the data and revised the manuscript. D.G.M. designed the research, analyzed the data, revised the manuscript, and supervised all aspects of this study.

**Funding**

This work was kindly supported by U.S. DoD CDMRP Grant W81XWH-13-1-0400 to D.G.M., National Institutes of Health Predoctoral Training Grant T32-GM008487-19 in Structural Biology and Biophysics to J.M.B., and National Science Foundation Predoctoral Graduate Research Fellowship NSF GRFP 2011121201 to K.R.M.

1  
2  
3  
4  
5  
6 **Notes**  
7

8 The authors declare no competing financial interest.  
9  
10  
11  
12  
13  
14  
15  
16  
17  
18  
19  
20  
21  
22  
23  
24  
25  
26  
27  
28  
29  
30  
31  
32  
33  
34  
35  
36  
37  
38  
39  
40  
41  
42  
43  
44  
45  
46  
47  
48  
49  
50  
51  
52  
53  
54  
55  
56  
57  
58  
59  
60